# CHARACTERISATION AND APPLICATIONS OF $CO_2$-EXPANDED SOLVENTS

Thesis submitted for the degree of

**Doctor of Philosophy**

at the University of Leicester

by

**Reena Mistry MChem (Hull)**

Department of Chemistry

University of Leicester

**May 2008**

# CHARACTERISATION AND APPLICATIONS OF $CO_2$-EXPANDED SOLVENTS

**REENA MISTRY**

UNIVERSITY OF LEICESTER

2008

## ABSTRACT

The use of $CO_2$ as an alternative to traditional organic solvents has been an extensive area of research over the last several decades with research focusing mainly on supercritical applications. Gas eXpanded Liquids (GXLs) combine the advantages of liquid $CO_2$ and co-solvents. Much like its supercritical counterpart, the solvent power of GXLs can be tuned by varying the liquid phase concentration as a function of pressure. Determination of solvent-solute interactions is key to the understanding of solvent properties in liquids and expanded solvents.

Spectroscopic measurements of a range of binary mixtures of organic solvent with carbon dioxide have been recorded to calculate solvatochromic parameters for gas expanded liquids. Data obtained for gas expanded solvents showed a significant change in local polarity upon addition of $CO_2$, modifying the properties of traditional organic solvents. Protic solvents were found to behave anomalously to conventional aprotic solvents.

Density, relative permittivity, and $CO_2$ solubility at 25 $^{\circ}$C and 50 bar pressure for a range of $CO_2$-expanded solvents are reported for the first time. The dissolution of $CO_2$ into liquid organic solvents to generate expanded liquids has resulted in significant changes in bulk solvent properties. Collation of relative permittivity data and solvatochromism data of the expanded liquids has given an insight into the structural changes occurring in the local and bulk regions of the solvent, resulting in the occurrence of preferential solvation. Variation in these solvent properties are understood by the determination of molar free volumes which was correlated with the Hildebrand solubility parameter showing that the expansion of molecular solvents is controlled by the thermodynamics of cavity formation.

A range of applications have been probed using gas expanded liquids as replacement solvents. One of the most prominent advantages of GXLs for chemical synthesis is their adjustable solvating power. Areas such as biphasic chemistry, selective reactions, solubility, and phase behaviour studies have been explored. It was found that in each application the $CO_2$ expanded solvent had a varied 'role'.

**ACKNOWLEDGEMENTS**

Firstly, a big thank you goes out to my supervisor, Prof. Andrew Abbott, for being a constant source of ideas, advice, and endless enthusiasm during my time at Leicester. The interdisciplinary and team-orientated atmosphere that he has created within our lab group has provided a great learning environment.

I would like to thank my committee members Prof. Eric Hope and Dr. Alison Stuart and also Dr Karl Ryder and Dr Katy for their interest and support in my work.

A special mention goes to Dr Donna Palmer for introducing me to 'Mr Evil Rig'. I still haven't quite managed to put him all back together again!

'Cheers big ears!' goes to Rob, Jose, Dan, Kiran, James, and John for their ideas and support in the lab, especially when I first started. I would like to give a special thanks to members of the Abbott group and Fluorine group (past and present) for their support, discussion, and friendship in the past few years. Many thanks also go to 'mum' of the group (Dr Emma) without whom I would have been stuck in a group full of boys! Yuk!

I would also like to thank Keith Wilkinson, John Weale, and Carl Schieferstein for making/fixing/modifying almost everything that I used. My innocent 'it wasn't me' never quite got me out of trouble for breaking things!

Finally, I must gratefully acknowledge the love and support of my parents, my sister Dina, and my brother Anil, I love you all lots xXx. I thank them for instilling in me a love of learning and education, the confidence to dream big, and the perseverance to follow through.

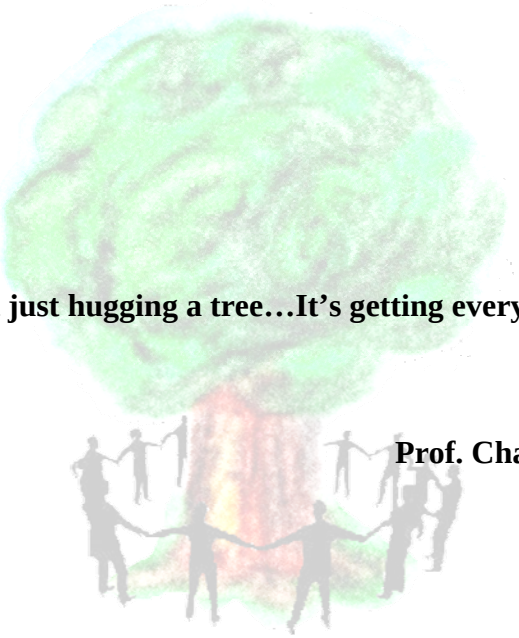

**“Sustainable is not just hugging a tree…It’s getting everyone to hug a tree”**

**Prof. Charles A. Eckert (2007)**

# CONTENTS

# LIST OF FIGURES

# LIST OF TABLES

# LIST OF ABBREVIATIONS

| | |
|---|---|
| ASES | aerosol solvent extraction systems |
| BzBr | benzyl bromide |
| BzCl | benzyl chloride |
| CFC | chlorofluorocarbons |
| $CO_2$ | carbon dioxide |
| CXL | carbon dioxide expanded liquid |
| DELOS | depressurisation of an expanded liquid organic |
| DDM | diazodiphenylmethane |
| EOS | equation of state |
| EPA | Environmental Protection Agency |
| $E_T$ | Energy of transition |
| GAS | gas-antisolvent |
| GC | gas chromatography |
| GXL | gas-expanded liquid |
| HBA | hydrogen bond acceptor |
| HBD | hydrogen bond donor |
| HFC | hydrofluorocarbons |
| HFC 32 | difluoromethane |
| IR | infrared |
| LSER | linear solvation energy relationship |
| MS | mass spectrometry |
| NHB | non-hydrogen bonding |
| OATS | organic-aqueous tunable solvents |
| PCA | precipitation with compressed anti-solvents |
| PERC | perchloroethylene |
| PGSS | particles from a gas gaturated solution |
| PR | Peng-Robinson |
| PTFE | polytetrafluoroethylene |
| RESS | rapid expansion of a supercritical solution |
| RK | Redlich-Kwong |
| sc | supercritical |
| SCA | supercritical alcoholysis |
| SCF | supercritical fluid |
| SEDS | solution enhanced dispersion by supercritical fluids |
| SFE | supercritical fluid extraction |
| SPPE | polarisability/dipolarity effect of the solvent |
| SRK | Soave-Redlich-Kwong |
| TOF | Turnover frequency |
| UV-Vis | ultraviolet-visible |

# CHAPTER 1

# INTRODUCTION

---



---

## 1.1 Introduction

Solvents, defined as substances able to dissolve or solvate other substances, are commonly used in industrialised and laboratory processes and are often requisite for many applications such as cleaning, coatings, synthetic chemistry, and separations.[1] Millions of tonnes of solvent waste is released into the environment annually, either as volatile emissions or with aqueous discharge streams.[2] Many of these solvents are known to disrupt our ecosystems by causative depletion of the ozone layer and by contributing to reactions that form tropospheric smog. In addition, some solvents are carcinogenic, neurotoxins, or can cause sterility in those individuals frequently exposed to them. Although controlled use of these solvents would be acceptable from both an environmental and health point of view, such operations are not simple to achieve, and alternative 'cleaner' solvents are currently being sought to curtail the problems inherent with the release of solvents into the environment. Green applications are not simply limited to replacing hazardous solvents with more environmentally benign alternatives, but also the adherence to three main factors:

- Environmental aspect – Monitored as the product of the amount of waste effluent produced and its toxicity.
- Chemical selectivity – The efficiency of a process, and its ability to be atom economic[3] using a minimum of reagents, and reducing by-product formation or the need for further purification procedures.
- Economical viability – Be designed to be energy efficient minimising both environmental and economic impacts, and on consideration of the above two factors be commercially feasible.

## 1.2 Solvent Classification

Classification of solvents is becoming more complex as the diversity of such reaction media increases. A general method is to classify them according to their physical properties. Fundamental properties include melting and boiling points, density, dipole moment, viscosity, dielectric constant, conductivity, and cohesive pressure. The importance of each property changes with the desired application.

Solvents are usually employed as a means of increasing reaction rates by dispersing reactant molecules and increasing the collision frequency. Current problems with traditional solvents include the inefficiencies associated with their

recovery and reuse. The search for alternative reaction mediums should concentrate on environmental impact as well as efficient recycling procedures. Many solvents have a diverse spectrum of physical properties, and so a range of alternatives would have to be able to cover these varying characteristics. The list below shows the acceptability of solvents in terms of their safety and environmental impact.[4]

| | | |
|---|---|---|
| Most acceptable | - | *None (rarely possible)* |
| | - | *Water* |
| | - | *Oxygenated (alcohols, ethers, ketones & esters)* |
| | - | *Aliphatic Hydrocarbons* |
| | - | *Aromatic Hydrocarbons* |
| | - | *Dipolar Aprotic* |
| | - | *Chlorinated (DCM)* |
| | - | *Ozone Depleters (CFC's)* |
| Least acceptable | - | *Toxic & Carcinogenic ($CCl_4$ & Benzene)* |

In June 2003, Global Safety and Environmental Affairs (GSEA) were given the responsibility of developing appropriate protocols and assessment methods for a pilot program at multinational companies. Based on this pilot program, a formal Safety, Health & Environment (SHE) assessment program was fully implemented in 2005. The main objective of the program is to monitor SHE risks associated with SHE programs set-up by employers and the potential impacts to the safety and health of employees and surrounding communities as well as the potential impact to the local environment. Two of the key factors assessed include hazards associated with manufacturing processes and the hazardous characteristics of materials used. The impending impact on human health and the environment and recycling costs associated with the use of solvent are important considerations. $CO_2$ is a good example of a solvent which can be excluded from the requirement of high recovery. For these reasons, the use of $CO_2$ as an alternative to traditional organic solvents has been an extensive area of research over the last several decades. This chapter looks into the use of environmentally benign solvents for use as alternative reaction media, concentrating more specifically on $CO_2$ based systems.

### 1.3 Carbon Dioxide as a Solvent

One of the major problems associated with the use of $CO_2$ is its classification as a greenhouse gas. However, its use as a solvent is not viewed as damaging as it is collected from the atmosphere, converted for use as a liquid or in gaseous form, and then returned back to the atmosphere. Thus, the net concentration of $CO_2$ remains unchanged.

#### 1.3.1 Supercritical Fluids (SCF)

A supercritical fluid (SCF) is defined as a substance above its critical temperature ($T_c$) and pressure ($P_c$). The critical point corresponds to the highest temperature and pressure at which the substance can exist as a liquid and vapour at equilibrium. An example of this is shown in the phase diagram below, Figure 1.1.

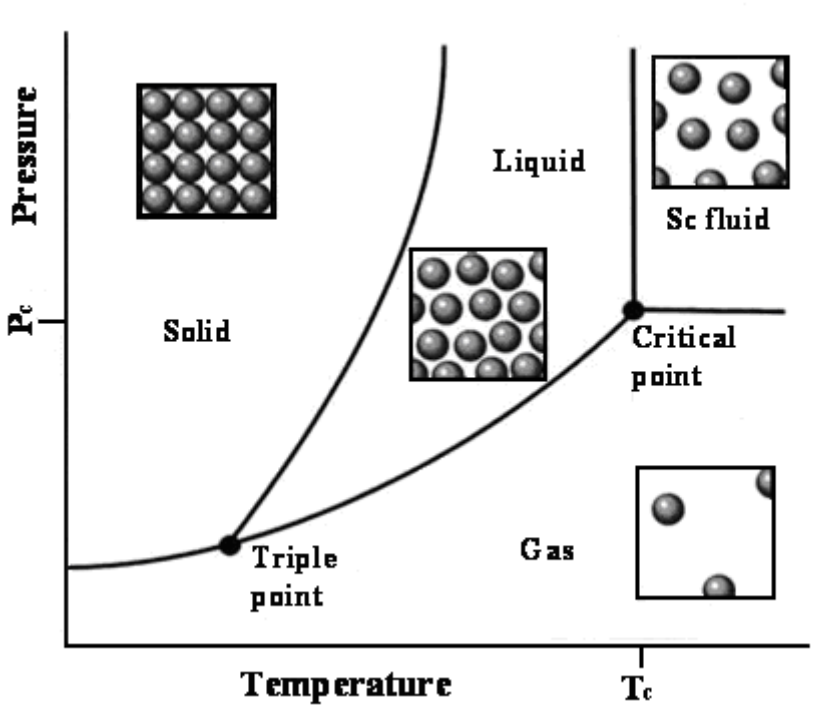


***Figure 1.1*** *A typical pressure-temperature phase diagram showing the supercritical phase region*

The phase lines show where two phases coexist, and the triple point represents the coexistence of the solid, liquid and gas phases. As the boiling curve is extended, increasing both temperature and pressure, the density of the liquid decreases due to thermal expansion, but the density of the gas increases as a result of pressure increase. Similarly to a gas, a supercritical fluid occupies the total volume available to it, and so

lacks the meniscus that would be present in a liquid.[5] The point at which the densities of the equilibrium liquid phase and the saturated gas phases become equal is called the critical point and thus beyond here the substance is said to be in a supercritical form. Density changes significantly with increasing pressure, and properties that directly relate to density have pressure dependence in supercritical (sc) media. This can be seen in Figure 1.2.

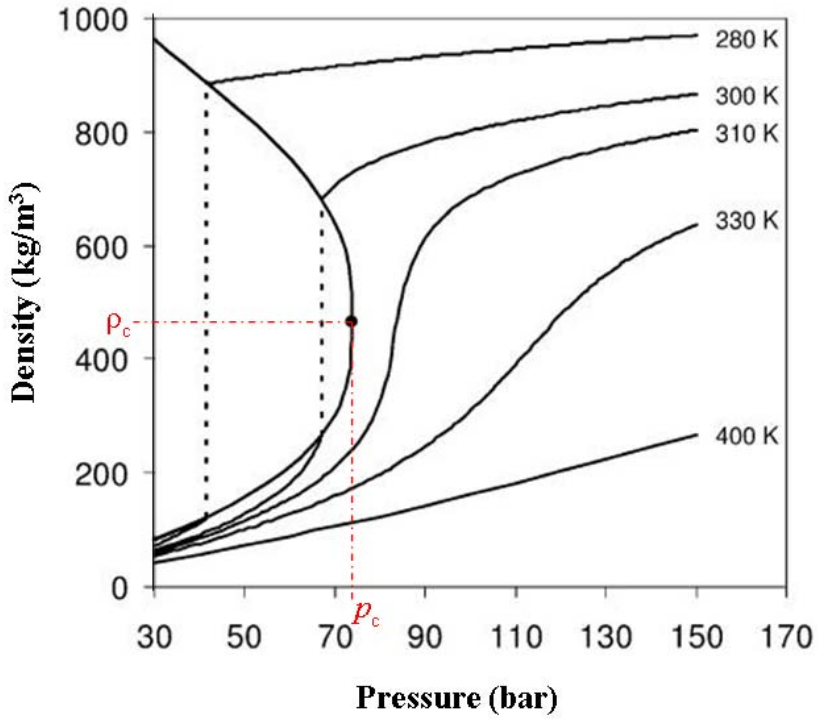


***Figure 1.2*** *Density of $CO_2$ as a function of pressure at different temperatures (solid lines) and at the vapour-liquid equilibrium line (dashed lines)*[6]

Supercritical fluids are attractive solvents because they have a useful combination of physical properties, such as gas-like diffusivity and viscosity, zero surface tension, and liquid-like solvation and densities. This can lead to higher reaction rates in SCFs, relative to those of liquid solvents for reactions which are mass transfer limited. Solvent power can be "tuned" by adjusting temperature and pressure to create a more suitable solvent for the desired application. Hence, this can be a useful tool, as not only does it allow for selective separation of the solvent from the solute, but it may also be possible to enable the facile separation of product from reactant.

As a reaction solvent SCFs have been used widely for heterogeneous,[7-12] homogeneous[13-18] and bio-catalytic[19] applications with the most common use being for supercritical fluid extraction (SFE).[20] Supercritical and near-critical fluids have been investigated as green solvents for the last two decades. Many of the physical properties of SCFs are intermediate between those of gases and liquids. Some of these properties are compared in Table 1.1.

***Table 1.1*** *Comparison of thermo-physical properties of gases liquids and SCFs*[21]

| **Property** | **Gas** | **SCF** | **Liquid** |
|---|---|---|---|
| **Density (g cm$^{-3)}$** | $10^{-3}$ | 0.3-0.8 | 1 |
| **Viscosity (g cm$^{-1}$ s$^{-1}$)** | $10^{-2}$ | 0.03-0.1 | 1 |
| **Diffusivity (cm$^2$ s$^{-1}$)** | 0.1 | $10^{-4}$ | $10^{-5}$ |

Table 1.1 shows that the properties of a supercritical fluid are intermediate between that of a gas and a liquid. Supercritical carbon dioxide ($scCO_2$) has received the most attention for use as a reaction medium due to its relatively low critical parameters (31.1 °C, 73.8 bar), its environmentally benign nature and its low cost. The limitations of these processes are solubilities that are significantly less than in liquid solvents and high capital costs associated with process equipment. The limited solubilities of most compounds seen in SCFs have led to their modification by the use of cosolvents such as methanol and acetone.

Traditionally, solvents are selected to have dielectric properties that help maximise solubility of the reagents and/or catalyst and also improve the rate of the desired reaction. Supercritical systems with added cosolvents still have the benefits of improved mass transfer and ease of solvent removal, but also have a wider range of solvent power.[22] Many current uses of SCFs include bettering reactions,[23] extraction and separation techniques and conventional catalysis.[13, 24-27] Baiker[12] and Jessop[5] compare uses for supercritical solvents in homogeneous and heterogeneous catalysis respectively. There are also reports of supercritical fluids in combination with ionic liquids as reaction media.[28, 29]

The main disadvantage associated with these systems is the resultant increase in the critical pressure of the mixture from adding cosolvent, and this has limiting effects on processing variables. Also, due to the relative expense of maintaining reaction conditions compared to other traditional solvents and the difficulty in scaling up high pressure reaction vessels to industrial scales, supercritical media are regarded more relevant to high value synthesis and extraction processes.

### 1.3.2 Liquid $CO_2$

$CO_2$ in the liquid state offers many of the same benefits as $scCO_2$ but at lower pressure. The distinct advantages of operating at lower pressures can significantly reduce capital and operating costs, as the pressure rating of equipment will be a lot less. One of the best-known commercial uses for liquid $CO_2$ is its use as an alternative solvent in the dry cleaning industry.[30] On its own, liquid $CO_2$ is not strong enough to solubilise all types of compounds on soiled fabrics, but when combined with the use of specialised surfactants it performs more efficiently. Most commercial processes employ perchloroethylene (PERC). The Environmental Protection Agency (EPA) classified PERC as both a groundwater contaminant and a potential human health hazard. It was found that inhaling PERC for short periods of time could adversely affect the central nervous system. Micell Technologies made $CO_2$ surfactant technology available commercially. The Micareô system was a commercially available washing machine that utilised $CO_2$ and a $CO_2$ surfactant, thereby eliminating the need for PERC.[31]

More recently, BOC have developed a new precision cleaning process for the removal of micron and submicron particulates and contaminated organics using liquid $CO_2$.[32] The *Eco-Snow* system operates by expanding liquid $CO_2$ through a specially designed nozzle which generates a fast-moving stream of solid $CO_2$ particles and $CO_2$ gas as shown in Figure 1.3. When directed at a contaminated surface the process of momentum transfer results in the displacement of particulates away from the surface. Since the particulates are detached from the surface, solid $CO_2$ undergoes sublimation and the contaminants are then swept away in the $CO_2$ gas stream.

***Figure 1.3*** *The spray nozzle is specially designed to suit the $CO_2$ cleaning requirements of the application. The employment of an inimitable double filtering system takes away all particulates from the $CO_2$ before the formation of $CO_2$ 'snow'. Cleaning performances are optimised by the use of various nozzle designs which provide specific spray characteristics*

### 1.3.3 Gas eXpanded Liquids (GXLs)

Gas expanded liquids are quite simply liquids 'expanded' with a gaseous cosolvent. A GXL is a mixture of pure gas and an organic solvent at pressure and temperature conditions which are below that of the critical point of the mixture. Operating conditions exceeding the critical point result in formation of a cosolvent-modified supercritical fluid. Similar to its sc counterpart, the solvent power of GXLs can be "tuned" by varying the liquid phase concentration as a function of pressure. The dissolved gas can modify the physical properties of the liquid or solvent, making it less viscous and thereby enhancing its mass transport properties. As pressure increases, $CO_2$ concentration increases and solvent power is lowered as shown in Figure 1.4.

The operating pressures for gas expanded systems are typically between three to eight MPa, hence much lower than the pressures required for reaching the supercritical phase. This gives GXLs a practical advantage over comparable supercritical systems in terms of specialised equipment and the outlay associated with them. In terms of solvent power and transportability when compared to gases and liquids, GXLs express more liquid-like characteristics than supercritical fluids.

Gas expanded liquids have shown to have great potential for tunability when the possible combinations of solvent, expanding gas, and/or cosolvent are taken into

consideration. Depending on the nature of the solvent media and the gas used, gas expansion has been shown to either increase solubility (to induce miscibility more specifically for biphasic systems) or decrease solubility (for applications in crystallisation, extraction or separation). Although $CO_2$ is the most common gas used for expansion, other compressed gases are also capable of acting as an expanding medium such as ethane, and nitrous oxide. The use of different gases can also have an effect on the 'expansion' process and also the solvent-solute interactions taking place within the expanded mixture.[33]

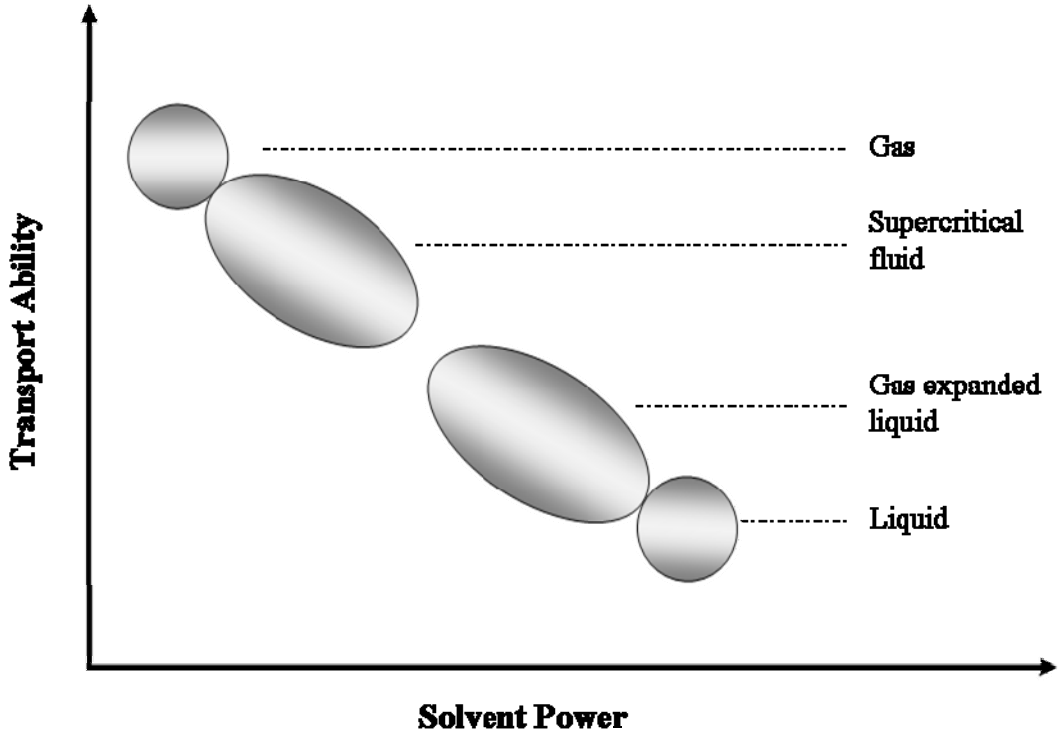


***Figure 1.4*** *Solvent power versus transport ability for gases, supercritical fluids, gas expanded liquids, and liquids. GXLs are 'hybrid' solvents exhibiting properties intermediate between those of gaseous and liquid solvents*

## 1.4 Applications of Compressed $CO_2$

It is recognised that dense carbon dioxide, both in supercritical or subcritical form, can be tailor-made for use in a variety of applications, in particularly $CO_2$-expanded liquids, by fine-tuning its thermodynamic and transport properties. One of the biggest applications of the use of compressed $CO_2$ is for the micronisation of chemical substances which has led to the optimisation of many different methods for particle formation.

### 1.4.1 Particle Formation

One of the biggest applications for the use of compressed gases is for inducing crystallisation. Conventional techniques for particle reduction include mechanical processing such as crushing, grinding and milling, freeze-drying and spray drying. These techniques are usually quite successful and simple to apply but can lead to high local temperatures. Numerous processes for fine powder generation using high pressure have been developed, and the specific properties of dense gases allow for the production of fine dispersed solids even for those substances with high viscosities, low melting points, or waxy consistencies. Crystallisation methods at both supercritical and subcritical (gas expanded) conditions have been studied widely and can be classified into three main groups depending on the solvating behaviour of the compressed fluid.[34]

- **Rapid Expansion of a Supercritical Solution**

  The crystallisation technique called Rapid Expansion of a Supercritical Solution (RESS) uses a compressed fluid as a solvent. RESS involves the dissolution of the solute of interest in a pure compressed fluid, generally under supercritical conditions.[35-38] Figure 1.5 shows the schematic for the process, rapid expansion of the solution through a small orifice to atmospheric pressure produces a dramatic decrease in the density and solvation power of the SCF, resulting in a greater extent of solute supersaturation and subsequent nucleation and growth of monodisperse particles.[39]

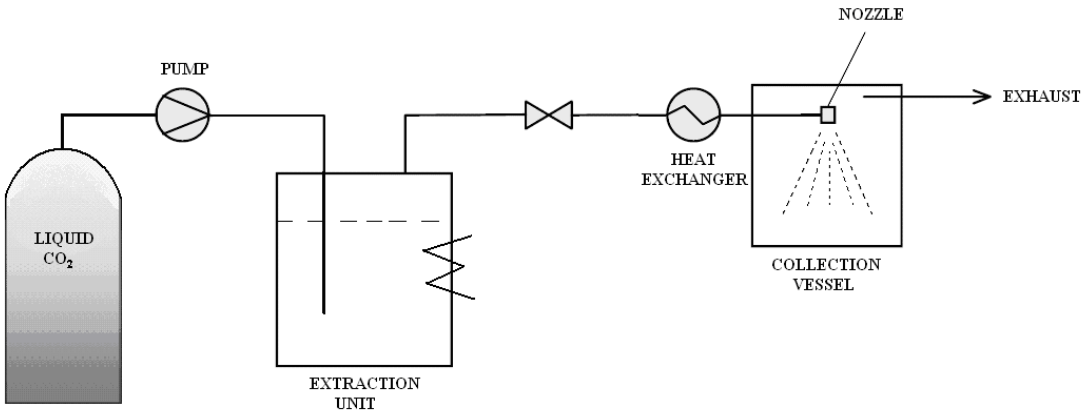


***Figure 1.5*** *Process of Rapid Expansion of a Supercritical Solution*

RESS processing parameters that influence supersaturation and the rate of nucleation can be specified in order to generate particles which are quite different in size and morphology in comparison to the original starting material. Beneficial characteristics of the RESS technique include; the production of very fine particles, controllable particle size distribution, and also RESS products are generated with little or no residual solvent. Disadvantages of this method include the high ratios of gas/substrate required due to the limited miscibility of the substance, and the high pressures (and sometimes temperatures) required when operating under supercritical conditions.

One of the first comprehensive studies into RESS was carried out by Krukonis *et al.*[40] They used supercritical $CO_2$ to produce fine powders from a wide range of materials including dyes, polymers, organic materials and pharmaceuticals. Chang and Randolph reported the precipitation of β-carotene from ethylene.[36] They researched expansion into gelatinised solutions and found that this decreased the degree of agglomeration. It was also concluded that cosolvents may be used whilst still maintaining a single solvent phase after expansion. Use of a cosolvent improved the solubility of β-carotene, however at high co-solvent concentrations the system was no longer monophasic, and particle sizes were more widely distributed. Mathematical models have been derived by a number of research groups to predict particle sizes for organic compounds. [41-43] Comprehension of the mechanisms behind their growth and formation has led to the establishment of a good agreement between experimental and theoretical models.

- **Gas Anti-Solvent Crystallisation**

Gas Anti-Solvent (GAS) recrystallisation makes use of a gas as an anti-solvent for implementing precipitation of a solid dissolved in an organic liquid. The solute of interest is dissolved in an organic solvent to form a solution. The solute is then precipitated from this solution in two alternative ways. In the first method, called gas anti-solvent (GAS) crystallisation, a batch of the liquid solution is expanded several-fold by mixing it with the compressed liquid. This expansion produces a solvating power decrease of the mixture, which becomes supersaturated and then the solute precipitates as micron- or nano-sized particles.[40, 44-49]

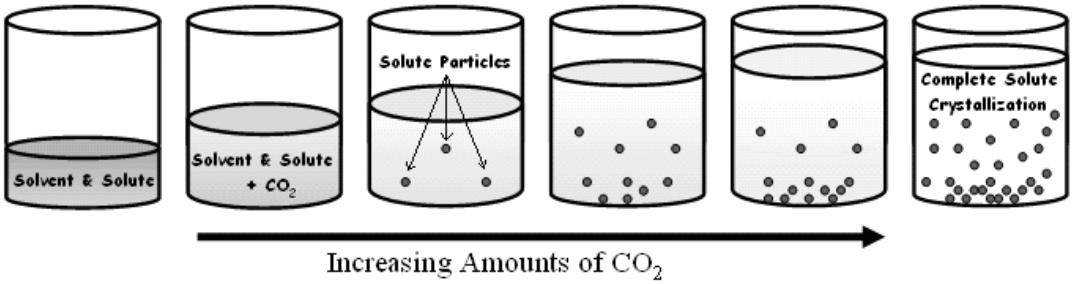


***Figure 1.6*** *The GAS process – Liquid solvent is expanded with $CO_2$ gas, volume expansion of the solvent is observed as the solution becomes saturated. Solvent power decreases and the solute precipitates out*

The GAS system can nucleate the crystals homogeneously throughout the solution. This influences uniform nucleation unlike in traditional systems where cooling is employed to supersaturate the system to induce nucleation and growth of crystals. Unfortunately, problems have occurred, such as selective nucleation at cooler surfaces resulting in non-uniform crystals being produced.[50] GAS technology has had great success as it relies on the fact that $CO_2$ is not the extracting solvent but instead a highly soluble solute that forces other solutes out of solution.[51-53] Examples include the separation of organic compounds such as acids[54] and β-carotene from solution.[55] A distinct advantage of the GAS process is that the rate of pressurisation can be tightly controlled, leading to a high level of control over the rate of crystallisation and particle characteristics. McLeod *et al.*[48] employed the tunable properties of gas expanded organic solvents in order to induce size-selective precipitation and separation of ligand-stabilised metal

nanoparticle dispersions as a function of $CO_2$ pressure. Solvent strength was manipulated through successive $CO_2$ pressurisation to stimulate sequential precipitation of progressively smaller particles. The design of novel apparatus enabled the separation of polydisperse silver nanoparticles into different fractions of uniform sizes by controlling the pressure of the expanding gas.

A similar technique is the precipitation with compressed anti-solvents (PCA). PCA involves the use of a nozzle to spray fine droplets of organic solution into the compressed fluid. In this process, the gas diffuses into the sprayed solvent resulting in expansion of the solvent reducing its solvating ability, and forcing the solute to precipitate or crystallise out.[56, 57] Optimisation of this process has been carried out for various process requirements. A technique involving continuous flow of the solution and the anti-solvent, is referred to as aerosol solvent extraction systems (ASES)[58] In ASES, the solvent is not only expanded but is in fact completely dissolved into the expanding gas. Hanna and York[59, 60] developed a process whereby concurrent feeding of the expanding gas and a solution of solute in an organic solvent through a nozzle produced finer particles than in the conventional PCA or ASES processes. This process became known as Solution Enhanced Dispersion by Supercritical fluids, or SEDS.

- **Particles from a Gas Saturated Solution**

  As a relatively new process for the production and fractionation of fine particles by the use of compressed gases - Particles from a Gas Saturated Solution (PGSS)[61] differs from the aforementioned techniques as it involves the use of a compressed fluid as a solute as opposed to a solvent. PGSS entails the solubilisation, at a given pressure and temperature, of a compressed gas in a neat liquid substance to be crystallised giving rise to a gas saturated solution. As a result of the Joule-Thompson effect and/or evaporation and volume expansion of the gas a sudden temperature drop of the solution below the melting point of the solvent is observed. Once the solution is allowed to homogenise and reach equilibrium, it is expanded to atmospheric conditions; the compressed fluid evaporates resulting in the rapid cooling of the solution which leads to crystallisation of the solvent. As cooling is induced almost instantly, homogeneous nucleation is observed. A separate expansion chamber collects the powder produced, and the compressed fluid may be recycled if necessary.[62]

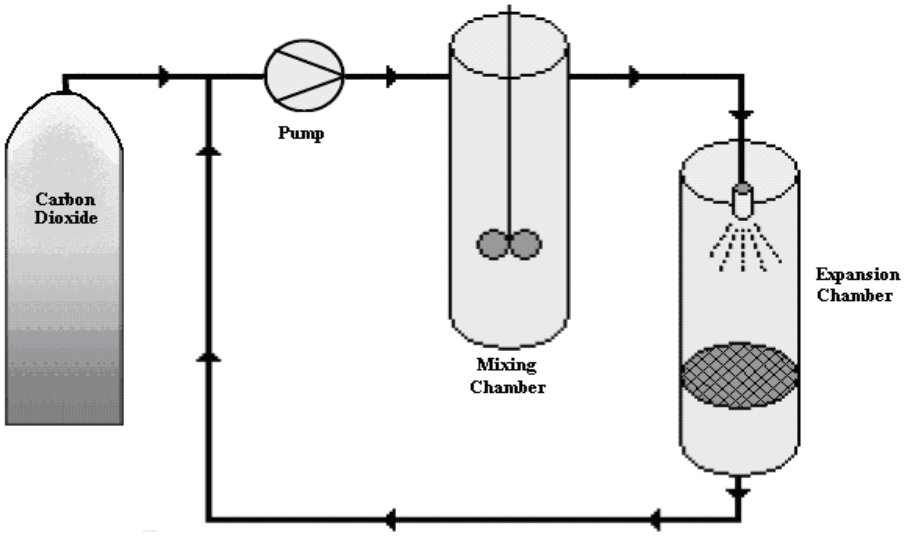


***Figure 1.7*** *Schematic of PGSS process*

Particle morphology and size, as well as the residual solvent content of the resulting powder can be influenced by the choice of process parameters like pre-expansion pressure and temperature, post-expansion temperature and the specific mass flow ratio.

- **Depressurisation of an Expanded Liquid Organic Solution (DELOS)**

The depressurisation of an expanded liquid organic solution (DELOS) is a relatively new crystallisation technique that uses a compressed fluid such as $CO_2$ as a cosolvent for the production of micron-sized particles. This process stands out from other high pressure crystallisation techniques as the compressed gas acts as a cosolvent which has complete miscibility with the organic solution of the solute to be crystallised for set temperature and pressure parameters.[63] The DELOS process works optimally for organic solutes in organic solvents and has been shown to be useful for pharmaceuticals and polymers for which traditional methods of micro/nanoparticle formation are rendered ineffective due to physical and chemical limitations.[64] The method by which DELOS crystallisation functions is a quick and significant (homogeneous) temperature reduction experienced by the solution comprising of a compressed fluid similar to that observed by the PGSS process when the system is depressurised. This fast drop in temperature simultaneously results in a reduction in the saturation limit causing crystallisation

of particles from the solution. The DELOS process is a three-step system as illustrated in Figure 1.8.

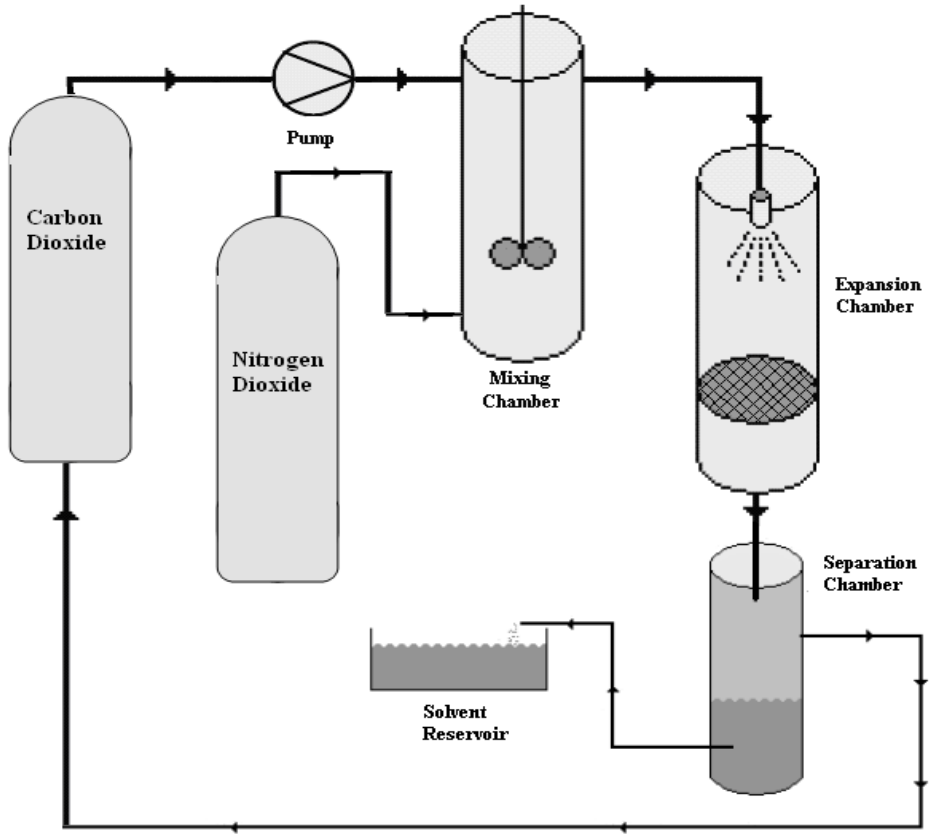


***Figure 1.8*** *DELOS Process – Firstly, a solute is dissolved into an organic solvent and heated to the desired temperature. A pre-heated compressed fluid is then added to the solution and used to achieve the operating pressure. As the solution is allowed to equilibrate it is expanded through a one-way valve into a collection chamber to atmospheric pressure*

Crystallisation through this process is dependent on a large temperature drop, the yield can be maximised by increasing the amount of compressed gas used. However, too much compressed gas can also pose a problem, and in cases where the limit is exceeded the GAS crystallisation process can result. It is therefore feasible to vary significantly particle size characteristics allowing for the production of either micro- or macro-sized particles depending on the specific combination of process parameters such as the type of compressed gas used, the rate of expansion, and the solute concentration.

There are various methods of processing materials using expanded fluids. The choice of method depends largely on the solubility of the material of interest in the expanding gas. Table 1.2 summarises the operating parameters of the most common methods of particle formation.

***Table 1.2*** *Summary of particle formation applications of $CO_2$*

| | **RESS** | **GAS** | **PGSS** | **DELOS** |
|---|---|---|---|---|
| **Amount of Gas Required** | High | Medium | Low | Low |
| **Operating Pressure** | High | Medium | Medium | Medium |
| **Role of Gas** | Solvent | Anti-Solvent | Solute | Cosolvent |
| **Use of Organic solvent** | × | ✓ | ✓ | ✓ |
| **Driving Force** | Pressure | Solubility | Temperature | Temperature |
| **Length of Procedure** | 2 step | 3 step | 2 step | 3 step |

### 1.4.2 Reaction Chemistry

Researchers have studied extensively the use of carbon dioxide expanded liquids (CXL) as replacement solvents. A few of these reactions have been outlined below, however literature reviews are available for further examples and a more in-depth discussion.[65-67]

- **Biphasic Reactions in GXLs**

  Phase Transfer Catalysis (PTC) is a widely used technique for conducting reactions between two or more reagents in two or more phases when the reaction is inhibited, as the reactants cannot simply react together. For this reason, a phase transfer agent is added to transfer one of the reagents to a site where it can conveniently and rapidly react with the other reagent. The use of CXLs has been adopted to facilitate the dispersion of phase transfer catalysts into the aqueous phase in liquid-liquid extraction systems by reducing the polarity of the organic phase. A significant alteration in the distribution of catalyst can be achieved on pressurisation with $CO_2$ such that even in dilute organic solutions they can undergo selective separation requiring just a small fraction of the water needed in traditional aqueous extractions. It has also been noted[68] that GXLs under moderate

$CO_2$ pressure have a much greater solvent power towards nonpolar substances whilst still maintaining most green benefits of $CO_2$.

As a subset of GXLs, Organic Aqueous Tunable Solvents (OATS) are of particular significance since they are a type of mixed solvent with both organic and aqueous qualities that can be phase separated with the addition of $CO_2$. At ambient conditions the mixed solvents are in a single homogeneous phase and can dissolve both salts and organic substrates. Introduction of $CO_2$ into the system results in $CO_2$ preferentially dissolving in the organic component of the mixed solvent resulting in phase separation. When biphasic conditions are employed, the salts remain in the aqueous phase and the organic substrate in the expanded organic phase.

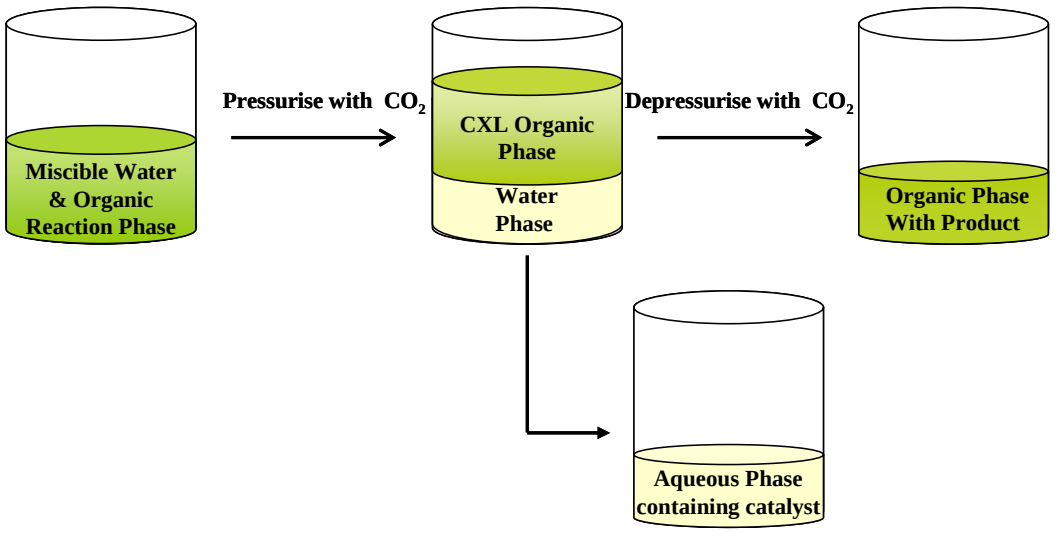


*Figure 1.9 The OATS system – The catalysed reaction is carried out in a homogeneous phase containing both organic and aqueous components. On reaction completion the system is pressurised resulting in phase separation. The aqueous phase is decanted off along with the dissolved catalyst, and the remaining expanded organic phase is depressurised to leave solvent and the reaction product*

A biphasic system may not seem ideal for catalysis applications since the substrate reactivity will be dramatically reduced by its low solubility in the aqueous phase. However, in the absence of $CO_2$ pressure, it is the model system for performing homogeneous catalysis and in the presence of $CO_2$ pressure, efficient product recovery and facile catalyst recycle are achievable.

Another well-established area of research is the use of partially fluorinated solvents such as hydrofluorocarbons (HFCs) to replace chlorofluorocarbons (CFCs) in various applications.[69, 70] HFCs are more advantageous due to their chemical stability and reduced environmental impact in relation to their CFC counterparts. The dissolution of $CO_2$ has been shown to act as a "phase switch" to make immiscible fluorinated and organic solvent systems into a homogeneous solution for homogeneous catalysts.[71] Similarly to organic solvents, expanding fluorinated solvent systems with moderate pressures of $CO_2$ has shown the potential to combine the tunability of GXLs and the $CO_2$-phillic properties of fluorinated solvents.[72]

- **Formation of acidic species**

Dissolution of $CO_2$ in water results in a reduction in pH of the solution even though $CO_2$ has limited solubility in water. An increase in the applied pressure results in little change in the solution properties.[73] Eckert and colleagues have shown that alcohols behave analogously to water.[74] They have reported that $CO_2$ is able to act as both reactant and solvent for reactions in GXLs such as the formation of alkylcarbonic acid on expansion of methanol with $CO_2$.

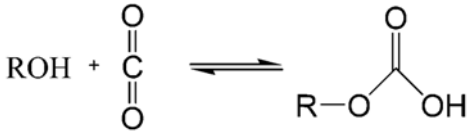


***Figure 1.10*** *Formation of Alkyl carbonic acid*

The Eckert group monitored the formation of such acids in $CO_2$ expanded alcohols by using a reactive probe, diazodiphenylmethane (DDM) to trap the acid species. Reichardt's dye was used as a solvatochromic probe that responds to solvent polarity. Relative reaction rates of the alcohols with this probe molecule were measured by observing the disappearance of the UV-Vis absorption band for DDM (525 nm) in order to determine the relative strengths of the corresponding alkylcarbonic acid. Reaction profiles were found to exhibit pseudo first order kinetics with respect to DDM, and were in the range 0.5-3.5 x $10^{-5}$ $s^{-1}$ which is comparable to the acid strength of supercritical $CO_2/H_2O$ systems. Reaction rates were found to be more pronounced in high short-chain alcohols such as methanol,

and to a lesser extent rates were lower in the high molecular weight, branched alcohols like *t*-butanol.[75]

Methylcarbonic acid can be formed reversibly (Figure 1.10) *in-situ* for applications in catalysis and it does not require neutralisation, or exhibit problems with waste disposal. Examples of the use of this and similar weakly acidic GXLs are the catalysed acetal formation[76] and the hydrolysis reaction of β-pinene to form terpineol,[77] this process conventionally requires strong acid catalysts and long reaction times. Peroxycarbonic acids have also been used to catalyse the epoxidation of cyclohexene.[78] The work of Nolen *et al.* was based on the formation of a peroxycarbonic acid species on reaction of $H_2O_2$ with $CO_2$. This oxidant was shown to facilitate olefin epoxidations. Standard methods for this process generally have a biphasic nature, and so the homogeneous system generated on pressurisation with $CO_2$ offers rate advantages stemming from mass transport improvements, and ease of separation after depressurisation. It was thought that peroxycarbonic acid acted as the catalyst, resulting from the peroxide/$CO_2$ reaction analogous to water/$CO_2$ to form carbonic acid, although such a species was not isolated.

- **Catalysed Reactions**

**Oxidations**

Busch *et al.* have carried out extensive research using GXLs to study greener routes for catalyst systems in high profile reactions such as olefin epoxidation and functional group oxidation.[79] They have reported the promising effects of using CXLs for the development of catalytic oxidation processes which are environmentally acceptable, highly selective, and yet economical. Use of a CXL was found to expand solvent volume considerably without resulting in precipitation of substrate, catalyst, or oxidant from the reaction mixture. This allows for the reaction to be carried out in a completely homogeneous $CO_2$ expanded mixture, with relatively moderate operating pressure (between 50 to 90 bars), yet still maintaining a high mole fraction of $CO_2$ (typically between 65 and 80 %) in the system. They investigated the homogeneous catalytic oxidation of 2,6-di-*tert*-butylphenol (DTPB) by Co(salen) at various reaction temperatures. The structure of the ligand in shown in Figure 1.11, and the reaction scheme is outlined in Figure 1.12.

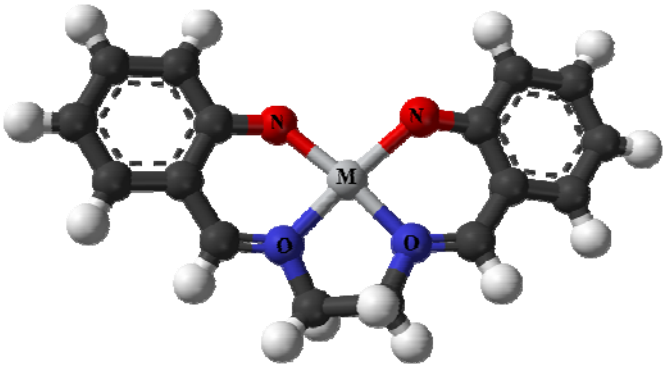


***Figure 1.11*** *Salen ligand with 'M' as the metal centre. Salen is an abbreviated contraction for salicylic aldehyde and ethylene diamine which are the precursors to the ligand*

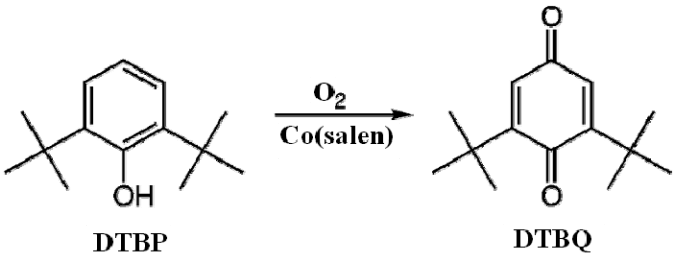


***Figure 1.12*** *Catalytic oxidation of 2,6-di-tert-butylphenol with Co(salen)*

The reaction was monitored and compared in $scCO_2$, $CO_2$ expanded acetonitrile, and neat liquid solvent. Turnover frequencies for the acetonitrile expanded system were between one and two orders of magnitude larger than for the supercritical reaction (carried out at 207 bar). Reaction advantages included the higher miscibility of oxygen in the expanded fluids compared to neat organic solvents, and also the use of unmodified transition metal catalysts for enhancing solubilities. It was suggested that the improved turnover frequencies (TOFs) observed in the expanded solvent may be accredited to the ability of the polar solvent to stabilise the polar transition state, thus reducing the energy of activation and increasing the reaction rate. Both selectivity and turnover frequencies were lowest in the neat acetonitrile at ambient pressure. The authors concluded that CXLs can be shown to complement $scCO_2$ as suitable reaction media by increasing the range of catalyst and solvent combinations for which oxidations can

be performed. The associated environmental and safety advantages are also noteworthy. The use of GXLs significantly reduces the amount of organic solvent required, and allows the ability to operate at much lower pressures than those utilised by supercritical fluids, and more importantly the possibility to eradicate the formation of potentially explosive mixtures in the presence of oxidants, thereby making such catalytic oxidations inherently safer when carried out in GXLs.

**Hydrogenations**

Hydrogenation reactions are mostly performed in three-phase (gas-liquid-solid) or biphasic (gas-solid) reactors. The additional step of $H_2$ transport across the gas/liquid interface unfortunately makes three-phase hydrogenation reactions susceptible to mass transfer limitations.[80] Supercritical $CO_2$ has been acknowledged as an alternative reaction medium.[12, 81, 82] $scCO_2$ has been shown to have high solubility of $H_2$ with $CO_2$ and also acts as a very good solvent for the dissolution of many small organic molecules yet still maintaining its characteristic supercritical phase. Unfortunately, the operating conditions required to achieve this supercritical phase are not suited to some particular hydrogenation processes.[83, 84]

GXLs make an even better alternative. As mentioned previously, compressed $CO_2$ when expanded observes lower viscosity and higher diffusion coefficients than its unexpanded equivalent. $H_2$ has even been reported to have enhanced solubility in CXLs at certain operating conditions.[83, 85] Devetta's group[85] researched the selective hydrogenation of an unsaturated ketone in biphasic conditions. The $CO_2$-expanded ketone showed a marked improvement in the rate of hydrogenation in comparison to that of the unswollen ketone.

$CO_2$-expanded liquids have also been used to form protecting groups for reaction intermediates. In $CO_2$-expanded THF, $CO_2$ reacts with primary amines to form solid carbamic acids and/or ammonium carbamates.[86]

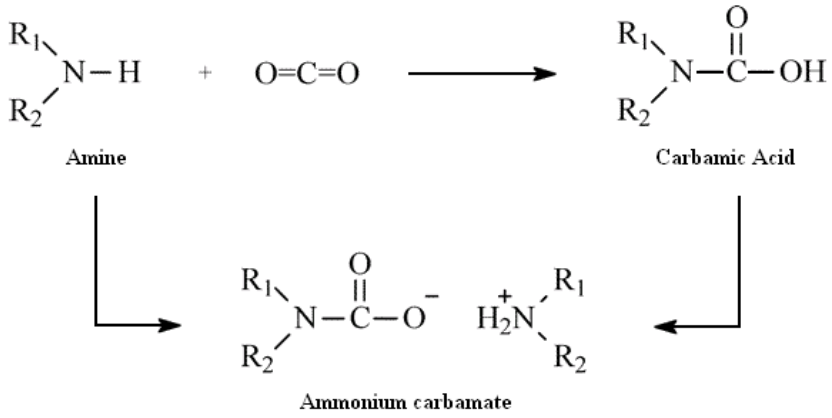


***Figure 1.13*** *Reaction scheme for the formation of carbamic acid*

The formation of ammonium carbamates blocked nucleophilic attack and encouraged selective formation of primary amines with a $NaBH_4$ catalyst. Overall, use of this solvent system resulted in a change in the product distribution and also reduced formation of substituted by-products. The effectiveness of the carbamate group was comparable to current chemical protecting groups in use for these reactions when carried out under ambient pressure conditions. Homogeneous hydrogenation for the formation of primary amines from nitriles has been shown to be facilitated by $CO_2$ expanded THF.[86] The $CO_2$ forms the carbamate salt as shown in Figure 1.12 above, this insoluble salt can be easily removed by a simple filtration process and then reconverted back to the amine by heating.

**Hydroformylations**

Hydroformylation is the simultaneous addition of carbon monoxide and hydrogen across a carbon-carbon double bond of an alkene to produce linear and branched aldehydes. There is an ever increasing need to continue research for more efficient metal catalysts, improve selectivity, reduce the formation of by-products and employ milder and environmentally acceptable conditions.[87] Subramaniam's group have reported the homogeneous hydroformylation of 1-octene using an unmodified rhodium catalyst $[Rh(acac)(CO)_2]$ in $CO_2$-expanded solvents using mild conditions of ~40 bar, and 60 $^oC$.[88] TOFs were reported to be in the order of 300 $h^{-1}$ and high selectivity towards the linear aldehyde (~90%), which was significantly higher than those obtained in either neat acetone or $scCO_2$. In CXLs

lower temperatures were found to favour selectivity towards the aldehyde, and increasing the concentration of $H_2$ in the system improved reaction rates.

Jessop and coworkers have studied the effective solvent free hydroformylation of 2-vinylnaphthalene catalysed by $RhH(CO)(PPh_3)_3$ as shown in Figure 1.13.[89] Without $CO_2$, the melting point of the reaction mixture is 65 $^oC$ (that of 2-vinylnaphthalene) which then decreases after partial conversion is achieved, and finally increases again up towards the melting point of the final product as the reaction approaches completion. Use of a CXL enabled the reaction to start off more quickly, and reach completion more rapidly.

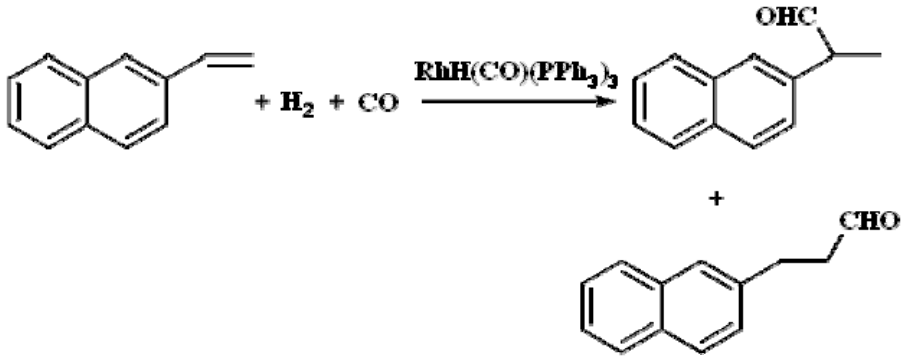


***Figure 1.14*** *Hydroformylation of 2-vinylnaphthalene catalysed by $RhH(CO)(PPh_3)_3$*

### 1.4.3 Transport Properties

A modified version of the Stokes-Einstein equation[90] has been used by the Eckert group to determine the diffusion coefficients of benzene in $CO_2$-expanded methanol and estimate the viscosity of each expanded fluid. A linear viscosity variation was observed between the pure component values at conditions of 50 °C and 150 bar. Methanol showed a decrease in viscosity when expanded, the degree to which it reduced was dependent on the amount of $CO_2$ dissolved.

Laird *et al.*[91] have presented a molecular simulation study estimating the translational and rotational diffusion constants of liquid mixtures formed by acetonitrile and $CO_2$ as a function of pressure at constant temperature (298 K).[92] They reported that the translational and rotational diffusion rates increase with $CO_2$ mole fraction for both acetonitrile and $CO_2$ components, and that modifying the amount of

$CO_2$ in the mixture allows tunability of transport rates by a factor of three to four. In the mixture, there is a large tendency toward increasing the translational diffusion of acetonitrile as the mole fraction of $CO_2$ in the expanded solvent increases. Rotational constants exhibit an opposing trend.

Shukla *et al.* have reported the use of molecular dynamic simulations to compute self-diffusion coefficients of methanol and acetone in their $CO_2$ expanded form.[93] The simulations allowed them to probe local solvation and transport effects. GXLs showed local density enhancements comparable to those seen in supercritical fluids, but to a lesser extent. A common trend of enhancement in solvent diffusivity with $CO_2$ addition was produced however; experimental values for diffusion coefficients were not in complete agreement with computed values.

## 1.5 Project Outline

The chemical industry is under increasing demands to replace traditional organic solvents with more benign alternatives that have lower toxicity and pose less threat to the environment. Various legislation has banned the use of many solvents already due to environmental concerns. Companies are also beginning to phase out the use of solvents that were once mainstays of formulation chemistry in order to reduce the costs of regulatory compliance. With only a few key 'green' solvents remaining, one alternative is to take advantage of the use of solvent mixtures. In recent years it has been highlighted that GXLs can be used as alternative solvents combining the advantages of using compressed $CO_2$ and liquid organic solvents. These mixed systems can be tuned by simply varying the relative amount of each component in the mixture allowing an entire spectrum of solvent properties. These solvents can be found to replace undesirable pure solvents, but in most cases, the mixture composition can surpass the capability of the pure component that it is replacing. CXLs are formed by mixing nontoxic, nonflammable carbon dioxide with a traditional organic solvent. The expanded solvent greatly reduces the potential for forming explosive vapours and possesses tunable properties desirable as a medium for performing catalytic reactions. Moreover, CXLs have shown to reduce the volume of organic solvent required (in some cases by up to 80 vol %) and thereby reduce emissions of organic vapours into the atmosphere.

Earlier work in the area of GXLs has concentrated mostly on synthetic applications and computational studies on the cybotactic region of these solvents. The work presented here reports the determination of fundamental physical parameters which are key to understanding the change in behaviour of organic solvents when they are expanded with $CO_2$ at 50 bar pressure at room temperature. Chapter Three investigates the use of a spectroscopic method of probing the local environment around a solute (cybotactic region), measuring the effect of $CO_2$ on solvent polarity when expanded at moderate pressure. Solvent polarisability/dipolarity and hydrogen bond donor characteristics have been measured to show that a new spectrum of solvent polarities is achievable.

In the second part of this research bulk solvent polarity is measured using a dielectrometry technique reported previously.[26, 94] This is the first reported study of relative permittivity measurements for GXLs, and $CO_2$ mole fraction solubility measurements using data obtained from the dielectrometry method. To understand the changes observed in $CO_2$ solubilities, the density of the expanded solvents was measured, and the free volume for each solvent system was calculated to give a better understanding of the 'packing' ability for different GXLs.

The final part of this study is a brief examination into application areas where liquid and supercritical solvents are currently used. Biphasic reaction chemistry, selectivity, solubility and phase behaviour have all been probed as potential applications for gas expanded solvents.

## 1.6 References


1. Grayson M, *Industrial Solvents*, Wiley and Sons, New York, 1983.
2. P. T. Anastas, C. A. Farris, American Chemical Society. Division of Environmental Chemistry. and American Chemical Society. Meeting, *Benign by Design: Alternative Synthetic Design for Pollution Prevention*, American Chemical Society, Washington, DC, 1994.
3. P. T. Anastas and J. C. Warner, *Green chemistry : theory and practice*, Oxford University Press, Oxford [England] ; New York, 1998.
4. D. J. Adams, P. J. Dyson and S. J. Tavener, *Chemistry in Alternative Reaction Media*, John Wiley & Sons Ltd, West Sussex, 2004.
5. W. Leitner and P. G. Jessop, *Chemical synthesis using supercritical fluids*, Wiley-VCH, Weinheim ; New York, 1999.
6. R. Span and W. Wagner, *Journal of Physical and Chemical Reference Data*, 1996, **25**, 1509-1596.
7. A. Kruse and H. Vogel, *Chemie Ingenieur Technik*, 2008, **80**, 567-572.
8. J. Li, Z. Qin, G. Wang, D. Mei and J. Wang, *Shiyou Huagong*, 2007, **36**, 1083-1092.
9. A. Kruse and H. Vogel, *Chemie Ingenieur Technik*, 2007, **79**, 707-720.
10. S. Pereda, S. B. Bottini and E. A. Brignole, *Applied Catalysis, A: General*, 2005, **281**, 129-137.
11. J.-D. Grunwaldt, R. Wandeler and A. Baiker, *Catalysis Reviews - Science and Engineering*, 2003, **45**, 1-96.
12. A. Baiker, *Chemical Reviews*, 1999, **99**, 453-473.
13. P. G. Jessop, T. Ikariya and R. Noyori, *Chemical Reviews*, 1999, **99**, 475-493.
14. P. G. Jessop, *Journal of Supercritical Fluids*, 2006, **38**, 211-231.
15. C. M. Gordon and W. Leitner, *Multiphase Homogeneous Catalysis*, 2005, **2**, 644-658.
16. L.-h. Wang, Y.-m. Wang and H. Liu, *Gongye Cuihua*, 2004, **12**, 1-4.
17. T. R. Early, A. B. Holmes, J. k. Lee, E. Quaranta and L. M. Stamp, *Carbon Dioxide Recovery and Utilization*, 2003, 149-168.
18. P. G. Jessop, *Yuki Gosei Kagaku Kyokaishi*, 2003, **61**, 484-488.
19. P. Pellerin, *Perfum Flavor*, 1991, **16**, 37-39.

20. A. J. Mesiano, E. J. Beckman and A. J. Russell, *Chemical Reviews*, 1999, **99**, 623-633.
21. R. S. Oakes, A. A. Clifford and C. M. Rayner, *Journal of the Chemical Society-Perkin Transactions 1*, 2001, 917-941.
22. D. L. Tomasko, B. L. Knutson, F. Pouillot, C. L. Liotta and C. A. Eckert, *Journal of Physical Chemistry*, 1993, **97**, 11823-11834.
23. M. Caravati, *Journal of Catalysis*, 2006, **240**, 126-136.
24. A. K. Chaudhary, S. V. Kamat, E. J. Beckman, D. Nurok, R. M. Kleyle, P. Hajdu and A. J. Russell, *Journal of the American Chemical Society*, 1996, **118**, 12891-12901.
25. Y. Ikushima, N. Saito and T. Yokoyama, *Chemistry Letters*, 1993, 109-112.
26. A. P. Abbott, S. Corr, N. E. Durling and E. G. Hope, *Journal of Chemical and Engineering Data*, 2002, **47**, 900-905.
27. A. P. Abbott, S. Corr, N. E. Durling and E. G. Hope, *Journal of Physical Chemistry B*, 2004, **108**, 4922-4926.
28. J. Lu, C. L. Liotta and C. A. Eckert, *Abstracts of Papers of the American Chemical Society*, 2002, **224**, U624-U624.
29. J. Lu, C. L. Liotta and C. A. Eckert, *Journal of Physical Chemistry A*, 2003, **107**, 3995-4000.
30. T. J. Romack, D. F. Cauble and J. B. McClain, *Dry Cleaning system Using Densified Carbon Dioxide and a Silicone Surfactant Adjunct.* , U.S., 2000.
31. S. H. Jureller, J. L. Kerschner and D. S. Murphy, *Dry Cleaning Methods and Carbon-Dioxide-Based Compositions*, U.S., 1999.
32. J. Burgess, *Spectrochimica Acta Part A - Molecular and Biomolecular Spectroscopy*, 1989, **45**, 159-161.
33. C. A. Thomas, R. J. Bonilla, Y. Huang and P. G. Jessop, *Canadian Journal of Chemistry*, 2001, **79**, 719.
34. I. Kikic, M. Lora and A. Bertucco, *Industrial Engineering Chemical Research*, 1997, **36**, 5507.
35. J. W. Tom and P. G. Debenedetti, *Biotechnology Progress*, 1991, **7**, 403-411.
36. C. J. Chang and A. D. Randolph, *American Institute of Chemical Engineers Journal*, 1989, **35**, 1876-1882.
37. R. S. Mohamed, P. G. Debenedetti and R. K. Prudhomme, *American Institute of Chemical Engineers Journal*, 1989, **35**, 325-328.

38. D. W. Matson, R. C. Petersen and R. D. Smith, *Journal of Materials Science*, 1987, **22**, 1919-1928.
39. S. D. Yeo and E. Kiran, *Journal of Supercritical Fluids*, 2005, **34**, 287-308.
40. P. M. Gallagher, M. P. Coffey, V. J. Krukonis and N. Klasutis, *Acs Symposium Series*, 1989, **406**, 334-354.
41. G. R. Shaub, J. F. Brennecke and M. J. McCready, *Journal of Supercritical Fluids*, 1995, **8**, 318-328.
42. B. Helfgen, M. Turk and K. Schaber, *Journal of Supercritical Fluids*, 2003, **26**, 225-242.
43. P. G. Debenedetti, J. W. Tom, X. Kwauk and S. D. Yeo, *Fluid Phase Equilibria*, 1993, **82**, 311-321.
44. S. D. Yeo, G. B. Lim, P. G. Debenedetti and H. Bernstein, *Biotechnology and Bioengineering*, 1993, **41**, 341-346.
45. T. W. Randolph, A. D. Randolph, M. Mebes and S. Yeung, *Biotechnology Progress*, 1993, **9**, 429-435.
46. E. Reverchon and G. Della Porta, *Pure and Applied Chemistry*, 2001, **73**, 1293-1297.
47. M. Anand, M. C. McLeod, P. W. Bell and C. B. Roberts, *Journal of Physical Chemistry B*, 2005, **109**, 22852-22859.
48. M. C. McLeod, M. Anand, C. L. Kitchens and C. B. Roberts, *Nano Letters*, 2005, **5**, 461-465.
49. M. C. McLeod, C. L. Kitchens and C. B. Roberts, *Langmuir*, 2005, **21**, 2414-2418.
50. N. Elvassore, T. Parton, A. Bertucco and V. Di Noto, *American Institute of Chemical Engineers Journal*, 2003, **49**, 859-868.
51. F. Fusaro, M. Hanchen, M. Mazzotti, G. Muhrer and B. Subramaniam, *Industrial & Engineering Chemistry Research*, 2005, **44**, 1502-1509.
52. F. Fusaro, M. Mazzotti and G. Muhrer, *Crystal Growth & Design*, 2004, **4**, 881-889.
53. A. Bertucco, M. Lora and I. Kikic, *American Institute of Chemical Engineers Journal*, 1998, **44**, 2149-2158.
54. A. Shishikura, K. Kanamori, H. Takahashi and H. Kinbara, *Journal of Agricultural and Food Chemistry*, 1994, **42**, 1993-1997.

55. C. M. J. Chang, A. D. Randolph and N. E. Craft, *Biotechnology Progress*, 1991, **7**, 275-278.

56. D. J. Dixon and K. P. Johnston, *Journal of Applied Polymer Science*, 1993, **50**, 1929-1942.

57. S. Mawson, M. Z. Yates, M. L. Oneill and K. P. Johnston, *Langmuir*, 1997, **13**, 1519-1528.

58. J. Bleich and B. W. Muller, *Journal of Microencapsulation*, 1996, **13**, 131-139.

59. B. Y. Shekunov, M. Hanna and P. York, *Journal of Crystal Growth*, 1999, **198**, 1345-1351.

60. B. Y. Shekunov, M. Hanna and P. York, *Journal of Crystal Growth*, 1999, **199**, 1345-1351.

61. Knez, *E. Weidner, Z. Knez, Z. Novak, PGSS (Particles from Gas saturated Solutions) a new process for powder generation, in: G. Brunner, M. Perrut (Eds.), Proceedings of the Third International Symposium on Supercritical Fluids, Strasbourg, France 1994, vol. 3, IBSN 2-905-267-23-8, p 229.*

62. T. Wendt, *Chemie Ingenieur Technik*, 2007, **79**, 287-295.

63. N. Ventosa, S. Sala, J. Veciana, J. Torres and J. Llibre, *Crystal Growth & Design*, 2001, **1**, 299-303.

64. N. Ventosa, S. Sala and J. Veciana, *Journal of Supercritical Fluids*, 2003, **26**, 33-45.

65. B. Subramaniam and M. A. McHugh, *Industrial & Engineering Chemistry Process Design and Development*, 1986, **25**, 1-12.

66. C. A. Eckert, B. L. Knutson and P. G. Debenedetti, *Nature*, 1996, **383**, 313-318.

67. P. G. Jessop and B. Subramaniam, *Chemical Reviews*, 2007, **107**, 2666-2694.

68. C. M. J. Chang, K. L. Chiu and C. Y. Day, *Journal of Supercritical Fluids*, 1998, **12**, 223-237.

69. A. Sekiya and S. Misaki, *Journal of Fluorine Chemistry*, 2000, **101**, 215-221.

70. N. Takada, R. Tamai, H. Yamamoto, A. Sekiya, N. Tsukida and H. Takeyasu, *Journal of Cellular Plastics*, 1999, **35**, 389-+.

71. K. N. West, J. P. Hallett, R. S. Jones, D. Bush, C. L. Liotta and C. A. Eckert, *Industrial & Engineering Chemistry Research*, 2004, **43**, 4827-4832.

72. Y. W. Kho, D. C. Conrad and B. L. Knutson, *Fluid Phase Equilibria*, 2003, **206**, 179-193.

73. K. L. Toews, R. M. Shroll, C. M. Wai and N. G. Smart, *Analytical Chemistry*, 1995, **67**, 4040-4043.

74. K. N. West, C. Wheeler, J. P. McCarney, K. N. Griffith, D. Bush, C. L. Liotta and C. A. Eckert, *Journal of Physical Chemistry A*, 2001, **105**, 3947-3948.

75. R. R. Weikel, J. P. Hallett, C. L. Liotta and C. A. Eckert, *Topics in Catalysis*, 2006, **37**, 75-80.

76. X. F. Xie, C. L. Liotta and C. A. Eckert, *Industrial & Engineering Chemistry Research*, 2004, **43**, 2605-2609.

77. T. S. Chamblee, R. R. Weikel, S. A. Nolen, C. L. Liotta and C. A. Eckert, *Green Chemistry*, 2004, **6**, 382-386.

78. S. A. Nolen, J. Lu, J. S. Brown, P. Pollet, B. C. Eason, K. N. Griffith, R. Glaser, D. Bush, D. R. Lamb, C. L. Liotta, C. A. Eckert, G. F. Thiele and K. A. Bartels, *Industrial & Engineering Chemistry Research*, 2002, **41**, 316-323.

79. G. Musie, M. Wei, B. Subramaniam and D. H. Busch, *Coordination Chemistry Reviews*, 2001, **219**, 789-820.

80. G. W. Roberts, *The Influence of Mass and Heat Transfer on the Performance of Heterogeneous Catalysts in Gas/Liquid/ Solid System* Academic Press, New York, 1976.

81. M. Freemantle, *Chemical & Engineering News*, 2001, **79**, 30-34.

82. E. J. Beckman, *Journal of Supercritical Fluids*, 2004, **28**, 121-191.

83. D. W. Xu, R. G. Carbonell, D. J. Kiserow and G. W. Roberts, *Industrial & Engineering Chemistry Research*, 2005, **44**, 6164-6170.

84. L. Devetta, P. Canu, A. Bertucco and K. Steiner, *Chemical Engineering Science*, 1997, **52**, 4163-4169.

85. L. Devetta, A. Giovanzana, P. Canu, A. Bertucco and B. J. Minder, *Catalysis Today*, 1999, **48**, 337-345.

86. X. F. Xie, C. L. Liotta and C. A. Eckert, *Industrial & Engineering Chemistry Research*, 2004, **43**, 7907-7911.

87. J. K. Huang, S. Serron and S. P. Nolan, *Organometallics*, 1998, **17**, 4004-4008.

88. H. Jin and B. Subramaniam, *Chemical Engineering Science*, 2004, **59**, 4887-4893.

89. P. Jessop, D. C. Wynne, S. DeHaai and D. Nakawatase, *Chemical Communications*, 2000, 693-694.

90. G. F. Woerlee, *Industrial & Engineering Chemistry Research*, 2001, **40**, 465-469.

91. Y. Houndonougbo, K. Kuczera, B. Subramaniam and B. B. Laird, *Molecular Simulation*, 2007, **33**, 861-869.

92. Y. Houndonougbo, H. Jin, B. Rajagopalan, K. Wong, K. Kuczera, B. Subramaniam and B. Laird, *Journal of Physical Chemistry B*, 2006, **110**, 13195-13202.

93. C. L. Shukla, J. P. Hallett, A. V. Popov, R. Hernandez, C. L. Liotta and C. A. Eckert, *Journal of Physical Chemistry B*, 2006, **110**, 24101-24111.

94. A. P. Abbott, C. A. Eardley and R. Tooth, *Journal of Chemical and Engineering Data*, 1999, **44**, 112-115.

# CHAPTER 2

# EXPERIMENTAL

---



---

## 2.1 Materials

### 2.1.1 Solvents

The solvents used in this work are shown in Table 2.1. All solvents were used as received, and the commercial source and purity of each is shown.

***Table 2.1*** *Source and purity of materials used*

| Solvents | Abbreviation | Source | Purity (%) |
|---|---|---|---|
| Carbon Dioxide | $CO_2$ | BOC gases | >99.5% |
| Cyclohexane | C.Hex | Fisher | >99.9% |
| Diethyl Ether | Ether | Fisher | >99% |
| Dichloromethane | DCM | Fisher | >99% |
| Toluene | Tol | Fisher | >99% |
| Tetrahydrofuran | THF | Fisher | >99% |
| Acetone | Acet | Fisher | >99% |
| Acetonitrile | MeCN | Fisher | >99.9 |
| Dimethylformamide | DMF | Fisher | >99% |
| Dimethyl Sulfoxide | DMSO | Lancaster | >99% |
| Methanol | MeOH | Fisher | >99% |
| Ethanol | EtOH | Fisher | >99.9% |
| 1-Propanol | Prop1 | Fisher | >99% |
| 2-Propanol | Prop2 | Fisher | >99% |
| Butanol | BuOH | Fisher | >99% |
| *tert*-Butanol | *t*-BuOH | Aldrich | >99.5% |

### 2.1.2 Solutes

The solutes employed in this work and their purity, molecular mass and source are shown in Table 2.2. Each solute was used as received.

***Table 2.2*** *Solutes investigated in this work*

| Solutes | Molecular Mass (g $mol^{-1}$) | Melting Point (°C) | Source | Purity (%) |
|---|---|---|---|---|
| Naphthalene | 128.17 | 80-82 | Fisons | 98 |
| *p*-toluic Acid | 136.15 | 180-182 | Aldrich | 98 |
| *o*-hydroxybenzoic acid | 138.13 | 158-160 | Fisons | 97 |

### 2.1.3 Solvatochromic Probes

The solvatochromic dyes Phenol Blue [Eastman chemicals, 97 %], Nile Red [Aldrich, 99 %], $E_T(30)$ [Aldrich, 95 %], and $E_T(33)$ [Fluka, 99 %] were used as received. Dye concentrations were maintained between $10^{-5}$ to $10^{-6}$ mol $dm^{-3}$, such that solute-solute interactions could be ignored.

### 2.1.4 Reagents & Catalysts

The reactants used for the phase transfer work were benzyl chloride (Aldrich), benzyl bromide [Aldrich], potassium bromide [Aldrich], and potassium chloride [Aldrich]. The phase transfer catalysts, tetrabutylammonium chloride, and tetrabutylammonium bromide were both obtained from Aldrich (>99.9%). The calibration standard biphenyl was also obtained from Sigma-Aldrich. Liquid withdrawal carbon dioxide was supplied by BOC gases. The reagents used in the biodiesel reaction are shown in Table 2.3.

***Table 2.3*** *Source, Formula, and purity of reagents used for esterification work.*

| Name | Origin | Formula | Purity |
|---|---|---|---|
| Ethyl caprate | Aldrich | $CH_3(CH_2)_8COOEt$ | 99 % |
| Soybean oil | Aldrich | $CH_2OCHOCH_2O$(complex long-chain ester)$_3$ | Unknown |
| Sunflower oil | Aldrich | $CH_2OCHOCH_2O$(complex long-chain ester)$_3$ | Unknown |
| Rapeseed oil | Aldrich | $CH_2OCHOCH_2O$(complex long-chain ester)$_3$ | Unknown |
| Sodium hydroxide | Aldrich | NaOH | 99 % |
| Potassium hydroxide | Aldrich | KOH | 99 % |
| Glycerol | Fisher | $CH_2OHCHOHCH_2OH$ | 98 % |

## 2.2 Instrumentation

### 2.2.1 General Apparatus

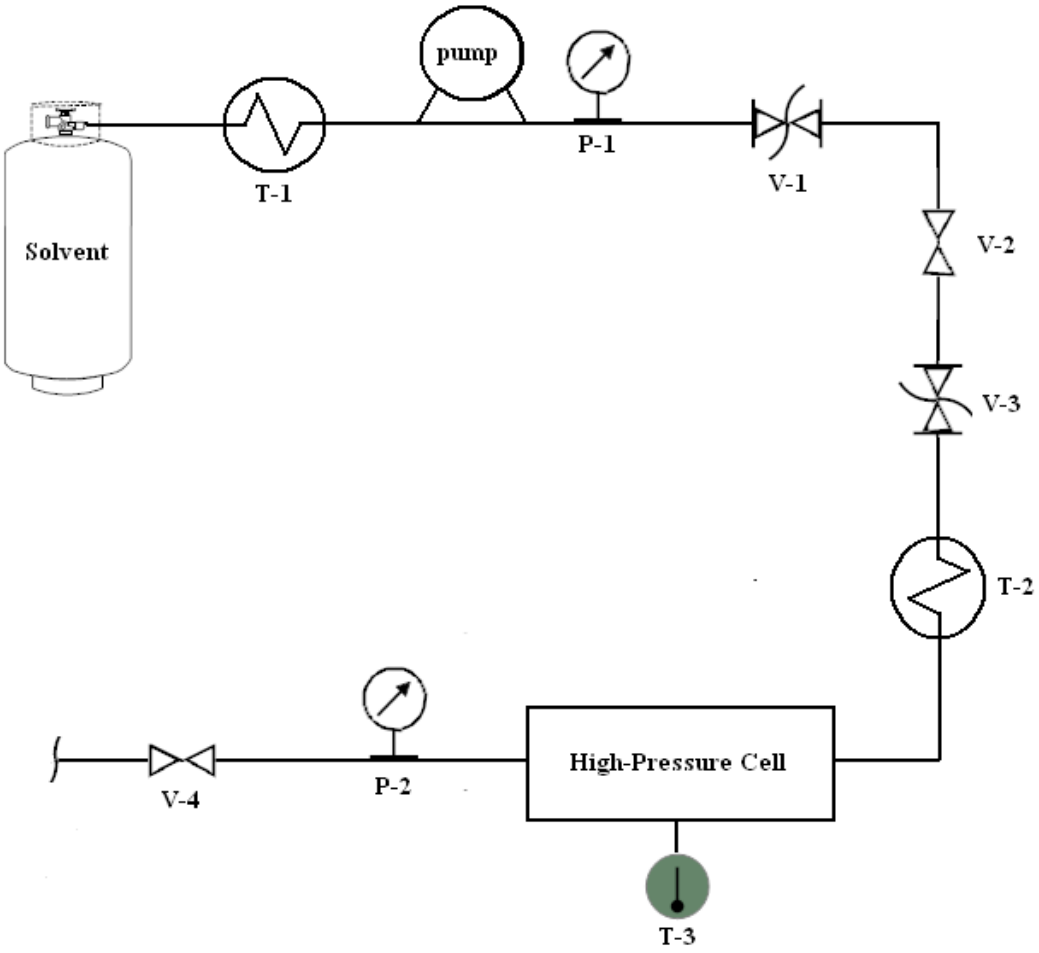


***Figure 2.1*** *Schematic diagram of high pressure equipment*

***Symbols***

- ***T-1 Cooler***
- ***T-2 Heater***
- ***T-3 Temperature Monitor***
- ***P-1 Pump Pressure Gauge***
- ***P-2 Cell Pressure Gauge***
- ***V-1 Safety Burst Disc***
- ***V-2 One-way Valve***
- ***V-3 Safety Burst Disc***
- ***V-4 One-way Valve to Exhaust***

The high pressure apparatus used for this study is shown schematically in Figure 2.1. Pressure was applied using a model P50-series piston controlled pump (Thar Technologies Inc.; Pittsburg, PA) and was monitored (±2 bar) using a Swagelok manometer. The temperature of the cell was measured using an iron/constantan thermocouple, the tip of which was in contact with the solvent close to the centre of the cell. This was held at a given value (± 0.5 K) using a CAL-9300 controlled heater. A picture of the apparatus is shown in Figure 2.2 below.

***Figure 2.2*** *The High-pressure apparatus*

### 2.2.2 High Pressure Optical Cell

A Shimadzu Model UV-1601 Spectrophotometer was used to measure the solvatochromic shift of the different indicator dyes in the visible absorbance spectrum. The optical high-pressure cell is shown in Figure 2.3. This cell was constructed from 316 stainless steel with 1 cm thick sapphire windows. The gas seals were made from Teflon. The cell path length was 6 cm and the cell volume was 70 $cm^3$. Light was fed into and out of the high-pressure cell by fibre-optic cables (Hellma, Müllheim, FRG) fitted with a 662 QX prism adapter.

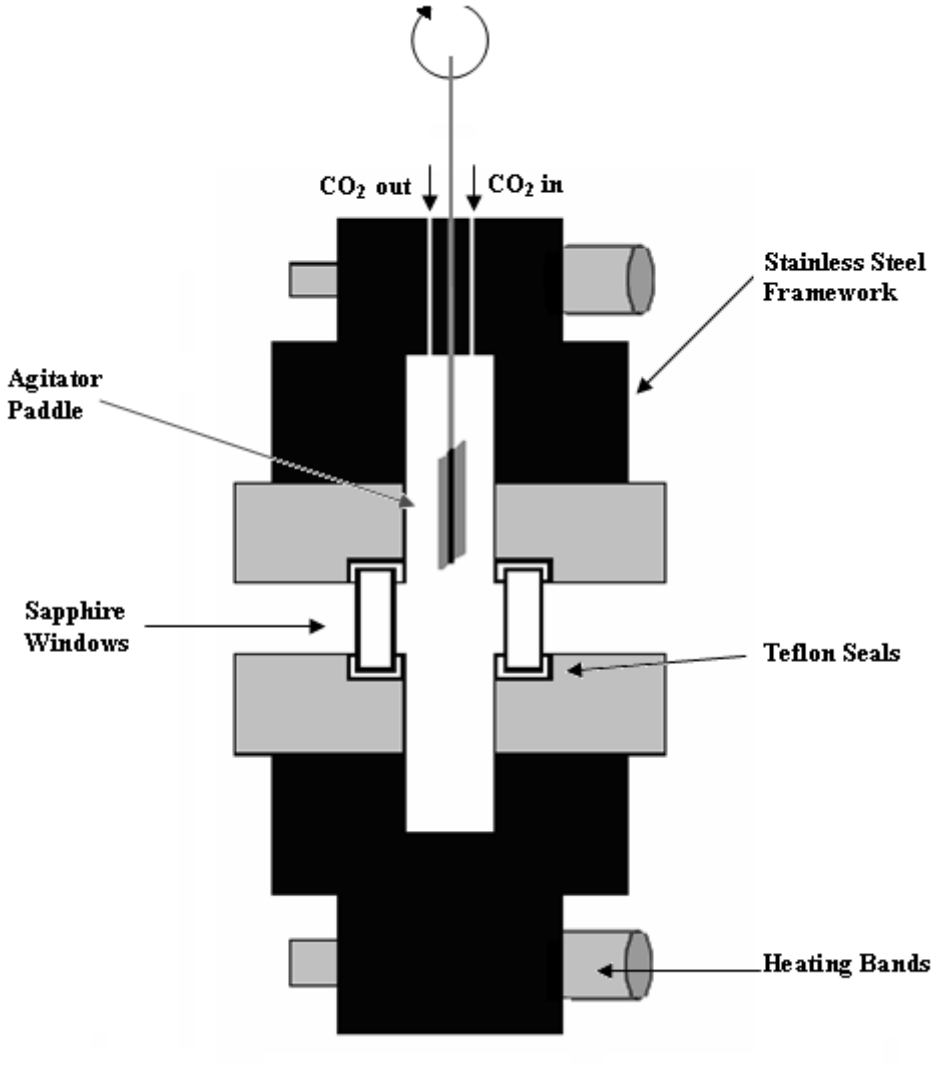


***Figure 2.3*** *The high-pressure optical view cell for use with an on-line UV-Vis spectrometer*

### 2.2.3 Dielectrometry Apparatus

A schematic of the high pressure apparatus is shown in Figure 2.4. The reaction vessel was constructed from 316 stainless steel and was rated to 1.5 kbar. The internal volume of the cell, lined with a layer of Teflon (1 mm thick), was 24.7 $cm^3$. An O-ring covered in Teflon was used to provide a high-pressure seal between the head and base of the cell and the electrical feedthroughs (RS Components Ltd.) employed were sealed with Swagelok fittings. Prior to each experiment the cell was purged with the appropriate gas. The pressure was then applied using a model 10-500 pump (Hydraulic Engineering Corp.; Los Angeles, CA) driven by compressed air and retained at a given value (± 2 bar) using a UCC type PGE 1001.600 manometer. The temperature of the cell was measured using an iron/constantan thermocouple, the tip of which was in contact with the solvent close to the centre of the cell. This was held at a given value (± 0.5 K) using a CAL 9900 controlled heater.

The cell consists of two rectangular stainless steel plates, (attached to the electrical feedthroughs) with an area of 6.6 $cm^2$, held 1 mm apart by Teflon spacers as shown in the enlargement in Figure 2.5.

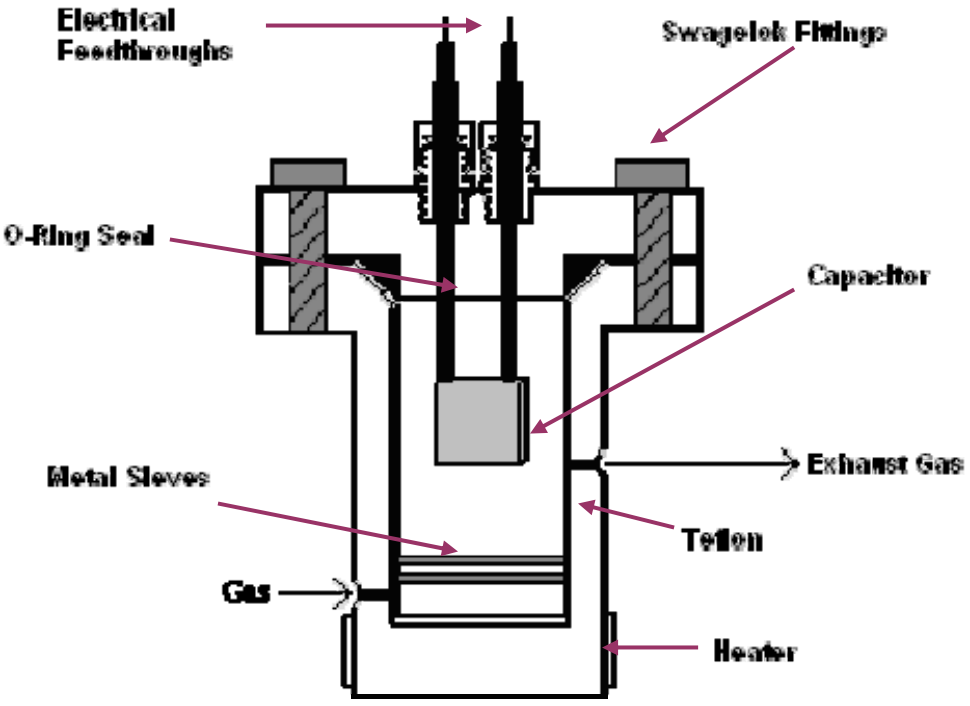


***Figure 2.4*** *The capacitance reaction vessel*

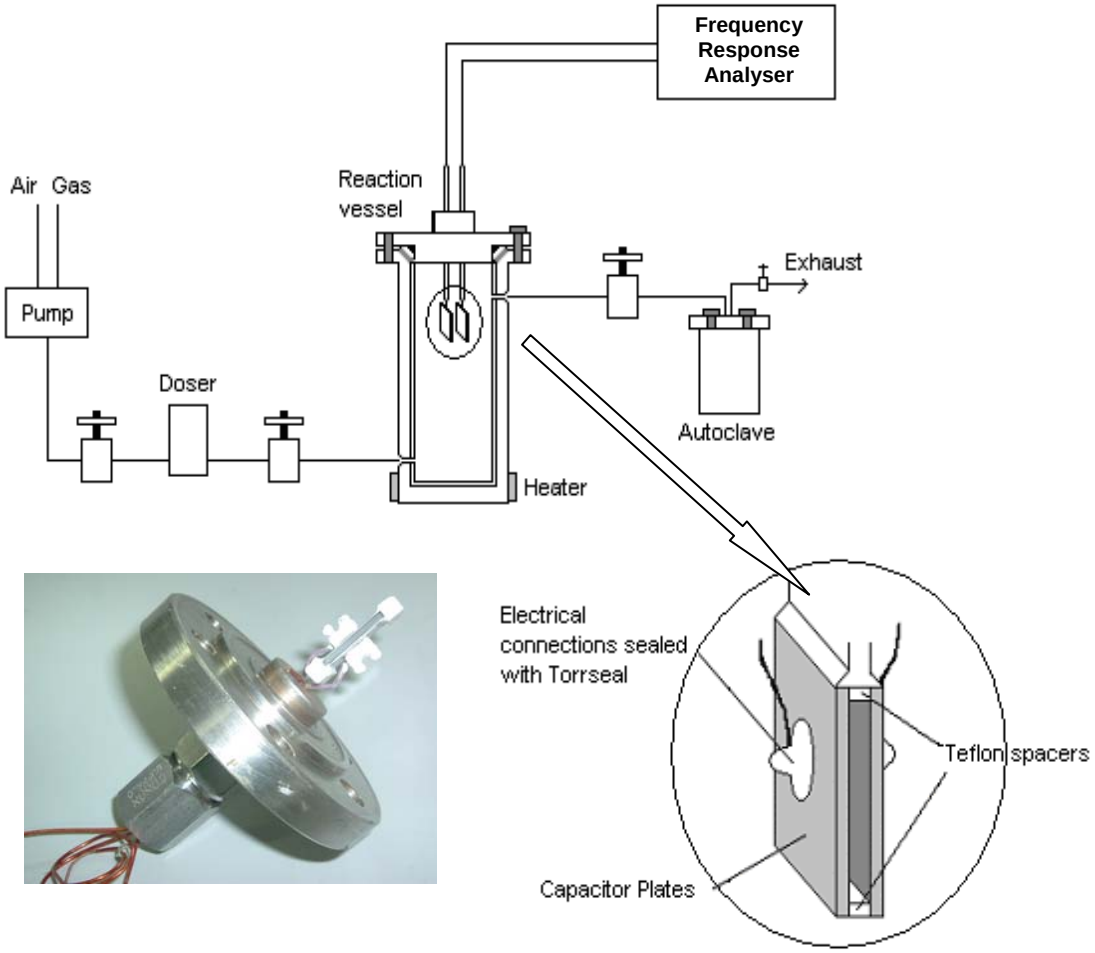


***Figure 2.5*** *The parallel plate capacitor used for dielectrometry studies*

### 2.2.4 Density Apparatus

The density of liquid solvents (at ambient pressure and temperature) and gas expanded solvents (room temperature and 50 bar $CO_2$) was determined using an Anton Paar DMA 512P densitometer and an Anton Paar mPDS 1000 evaluation unit designed to make measurements at both atmospheric and high pressures. The densitometer consists of a vibrating U-tube constructed from stainless steel with a volume of just a few $cm^3$ (occupied by the sample). The principle of the unit is based on the evaluation of the natural frequency of the electronic excitement of a tuning fork. A schematic diagram of the apparatus in shown in Figure 2.6. The sample is placed inside a double steel-walled cylinder sealed at both ends, and the whole unit is thermostatted using an oil flow system which regulates the temperature to within one quarter of a degree. The electronic part of the unit involves a system which excites the tuning fork at constant amplitude and a frequency meter which records the time corresponding to a fixed number of periods.

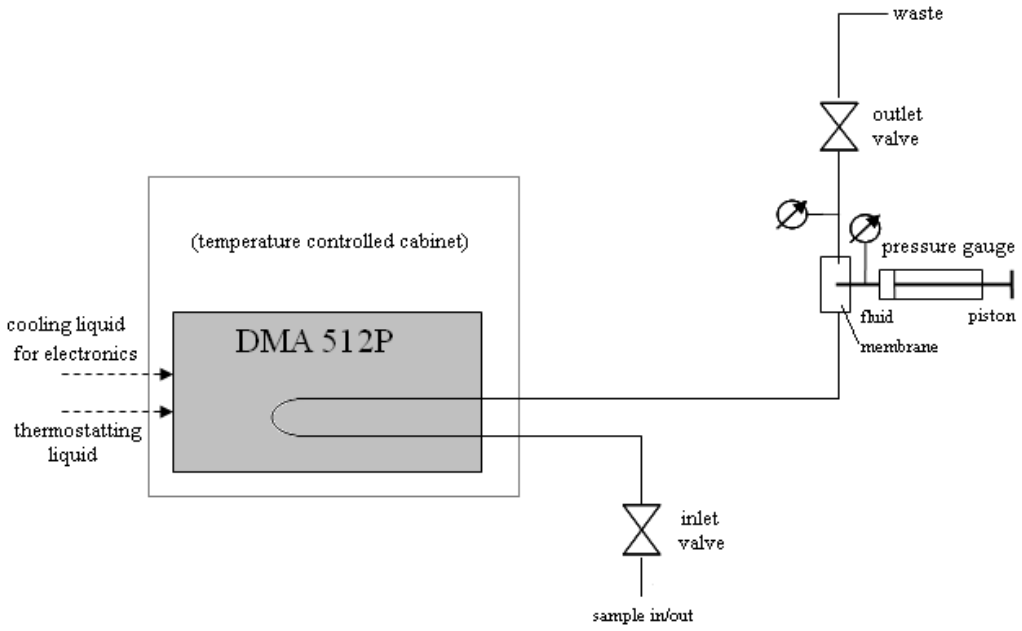


***Figure 2.6*** *Schematic of installation of the DMA 512P cell and set-up to apply high pressures to the samples*

### 2.2.5 High Pressure Reaction Cell

Figure 2.7 shows the cell used for the phase transfer reaction studies. It was constructed in-house from 316 stainless steel and had a maximum working pressure of 300 bar. Burst discs rated to 400 bar were fitted for safety. The internal volume of the cell was approximately 12 $cm^3$. The temperature of the cell was measured using an iron/constantan thermocouple. The temperature of the reactor was regulated to within 0.5 °C of the set point using a CAL 9300-controlled heater. Agitation in the reactor was maintained by use of a magnetically stirred PTFE flea.

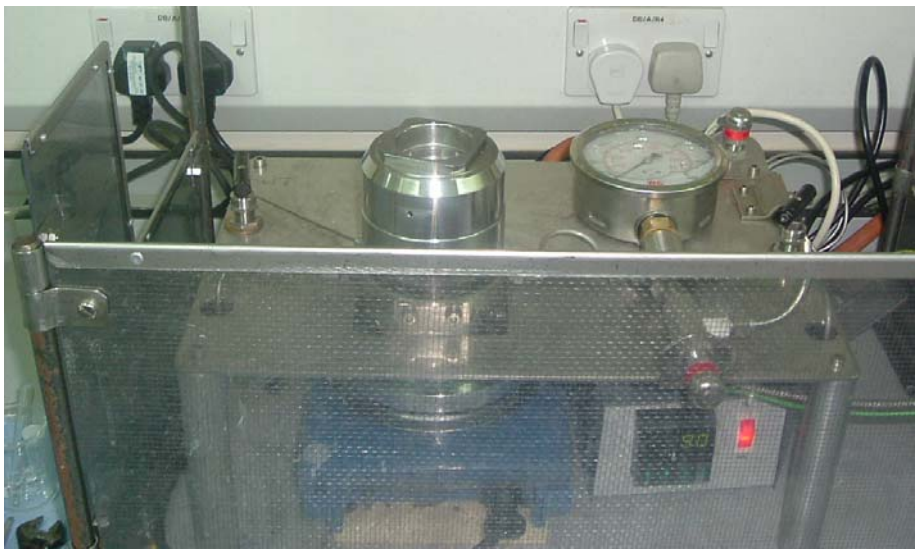

***Figure 2.7*** *The high pressure apparatus used for carrying out biphasic reactions*

### 2.2.6 High Pressure Esterification Cells

***Figure 2.8*** *High pressure vessels used for reaction chemistry, with 50 mL, and 100 mL volume capabilities. Cells are constructed of 316 Stainless Steel and rated to 300 bar*

### 2.2.8 High Pressure View Cell

An optical view cell (Figure 2.9) was employed to examine the change in phase behaviour of a solvent on expansion with a gas. The system was set up in a small cylindrical cell of approximate volume 9 $cm^3$. Visual observations were made possible from the presence of two sapphire windows at either end of the vessel. Temperature and pressure were controlled by connecting the cell to the high pressure apparatus shown in Figure 2.2.


***Figure 2.9*** *High pressure view cell used for visual observations*

### 2.2.9 Gas Chromatography-Mass Spectrometry (GC-MS)

The chromatograms were carried out on a Perkin Elmer Claurus 500 Gas Chromatograph using a Perkin Elmer-Elite Series PE-5 (30 m x 0.25 mm, Film = 0.25 nm, 5% diphenyl, 95% dimethyl polysiloxane) as column chromatography. The oven was set at a fixed temperature, and run-times did not exceed three minutes. The carrier gases were $H_2$ (45 mL/min), and compressed air (450 mL/min).

Gas Chromatography parameters:

Oven temperature: 125 °C

Injector temperature: 230 °C.

Detector temperature: 270 °C.

## 2.3 Experimental Methods

### 2.3.1 Solvatochromism

The optical cell shown in Figure 2.3 was used to measure the solvatochromic shift of the indicator dye at atmospheric and moderate pressures. A small amount of the desired dye was loaded into the cell and subsequently heated and pressurised to the desired conditions. The system was left to equilibrate for one hour then absorbance spectra were taken. It was assumed that the dilute concentration of dye had no effect on the $CO_2$ and liquid phase behaviour. The wavelength of absorbance maximum was calculated from the average of five spectra.

The program UV PROBE was used to obtain the maximum absorbance of the UV-Vis spectra of the solvatochromic dyes in each solvent mixture. The spectrum of the solvatochromic probe in the solvent was measured at a resolution of 0.05 nm per data point. A numerical smooth was performed on the date of the first order derivative to determine the peak maxima. $\lambda_{max}$ values were expressed in wavenumber as kK where, 1kK = 1000 $cm^{-1}$. The estimated uncertainty in the wavelength maximum is less than 1 nm.

### 2.3.2 Dielectrometry and Solubility Studies

The cell shown in Figure 2.4 was used to carry out relative permittivity dielectric measurements on a range of solvents. The solvent was loaded into the reaction vessel ensuring that the plates of the capacitor were fully immersed in the dielectric solution. The relative permittivity, $\boldsymbol{\varepsilon_r}$, was measured in this capacitance cell with capacitance $\boldsymbol{C_0}$ such that the measured capacitance, $C$ was given by,

$$C = \varepsilon_r C_0 \qquad \textbf{(2.1)}$$

Cell capacitances were measured using a logarithmic sweep method from 110 to 1 kHz with a 10 mV ac voltage amplitude using an AUTOLAB frequency response analyser controlled by ZPLOT software. The acquired data were analysed using ZVIEW software. The uncertainty of each capacitance measurement was approximately 50 fF.

The capacitor was tested with several pure solvents of known dielectric constant where the dielectric constant was found to vary by no more than 1 % from literature values. The dielectric constant was calculated from the average cell capacitance obtained from five experimental runs.

### 2.3.3 Densitometry

Prior to any measurements, the densitometer was calibrated to determine the calibration constants. Within a closed loop, the organic liquid was pumped from the high pressure reactor through a high-pressure high-temperature densitometer (Anton Paar DMA512P). Density readings were taken after the solvent/expanded solvent had reached equilibrium, which was noted by obtaining a steady reading on the evaluation unit.

The density of the sample was determined by measuring the period of oscillation of the tuning fork in which it is placed. The tube has an unknown but fixed mass $M_u$ and, and for a set temperature-pressure parameter, and unknown internal volume $V_u$ (T,P). The sample with density ρ(T,P) is passed through the tube, and the process which it undergoes can be modelled as a body of mass M suspended on the end of a spring with elasticity constant C(T,P) (which is representative of that of a tuning fork) and subjected to frictionless oscillation.

The natural frequency of the oscillator, $f$, can be defined by:

$$f = \frac{1}{2\pi}\sqrt{\frac{C}{M}} = \frac{1}{2\pi}\sqrt{\frac{C}{M_u + \rho V_u}} \qquad \textbf{(2.2)}$$

The period of oscillation, $\Lambda$, is given by:

$$\Lambda = 2\pi\sqrt{\frac{M_u + \rho V_u}{C}} \qquad \textbf{(2.3)}$$

Thus, the sample density $\rho$ (g cm$^{-3}$), can be calculated from the measurement of $\Lambda$:

$$\rho(T,P) = A(T,P)\,\Lambda^2 + B(T,P) \qquad \textbf{(2.4)}$$

Where;

$$A(T,P) = \frac{C(T,P)}{4\pi^2 V_u(T,P)} \quad \text{and} \quad B(T,P) = -\frac{M_u}{V_u(T,P)} \qquad \textbf{(2.5)}$$

***Calibration of the Densitometer***

Apparatus constants A and B were determined by measuring the periods of oscillation with filled-in standards of known density at the pressure and temperature of interest.

$$\rho = A * P^2 - B \qquad \textbf{(2.6)}$$

$$A = \frac{\rho_1 - \rho_2}{P_1^2 - P_2^2} \qquad \textbf{(2.7)}$$

$$B = \frac{P_2^2 * \rho_1 - P_1^2 * \rho_2}{P_1^2 - P_2^2} \qquad \textbf{(2.8)}$$

ρ …… unknown density of sample

$\rho_1$……density of standard 1

$\rho_2$……density of standard 2

$P_1$……period of oscillation, standard 1

$P_2$….. period of oscillation, standard 2

P……..period of oscillation, sample

### 2.3.4 Phase Transfer Reaction

A mixture of benzyl chloride (254 mg, 2.0 mmol), potassium bromide (1.19 g, 10.0 mmol), toluene (4.0 mL), water (4.0 mL) was loaded into the reaction cell. The system was first purged a couple of times with $CO_2$ to remove residual air. The reactor was then filled with $CO_2$ to the specified pressure using a model P50-series piston controlled pump (Thar Technologies Inc.; Pittsburg, PA) and the pressure was monitored (±2 bar) using a Swagelok manometer. The mixture was heated to the appropriate temperature, and left to react for the specified amount of time. After cooling to room temperature, the organic phase was filtered off using toluene as

eluent. A sample of the solution collected was analysed by gas chromatography to determine the conversion to desired product.

Variation of the temperature, pressure, agitation, and solvent type were also investigated. The reaction was further optimised on the basis of these results. For experimental reasons[1] the use of a glass vial inside the reactor cell was employed to contain the reaction mixture, and ease its removal on reaction completion.

### 2.3.5 Transesterification

*Biodiesel Reaction*

The hydrolysis of vegetable oils was investigated with a conventional base catalyst. 5 g (0.9 mol) KOH was dissolved in 1 l absolute ethanol and shaken until dissolved. 1 g of this solution was mixed with 5 g of oil (rapeseed or soybean) and shaken in a small stoppered flask. The flask was heated at 40 $^{o}$C and stirred mechanically at 200 RPM for 24 hours. The reaction was allowed to stand for one hour. Separation of glycerol from the KOH-catalysed reaction in ethanol did not occur. The reaction mixture and flask were washed 'gently' with luke warm water until a clear residue was obtained to remove any residual soap formed during the reaction. A sample of the remaining product was then dissolved in DCM, and analysed via GC-MS. Ethyl caprate was used as an internal standard.

### 2.3.6 Miscibility Studies.

The cell in Figure 2.6 was used for determining the phase behaviour of solvent pairs. The miscibility of the solvents used in dielectrometry and solvatochromism studies was studied by observing the changes incurred on expansion with 50 bar $CO_2$. A 1:1 volume ratio of one solvent with a different solvent was prepared and placed into the view cell. The miscibility/immiscibility of this solvent pair was noted, and the mixed solvent was then 'expanded' (pressurised with $CO_2$). Any changes in phase behaviour were noted. In order to improve visualisation, a small amount of coloured dye was added to clarify the formation of any secondary phases. 15 solvents were studied, amounting to data for 105 different solvent pairs.

[1] Depressurisation led to loss of reaction mixture through the exhaust.

# CHAPTER 3

## Solvatochromism in Gas eXpanded Liquids

---



---

## 3.1 Introduction

### 3.1.1 Solvatochromism

Gas expanded liquids are cosolvent mixtures composed of a room temperature organic solvent and a gas such as $CO_2$. They can be considered as a 'compromise' between the use of conventional solvents, which are a major contributor towards pollution, and benign $CO_2$, whose poor solvent qualities and high pressure requirements have led to its limited application. As discussed in Chapter 1, despite the interest in applications, the nature of solvation in expanded liquids is yet to be fully characterised. Published data on solvation consists primarily of solubility determinations of organic solutes in the gas-antisolvent process.[1, 2] The molecular side of solvation such as the composition of the local environment surrounding a solute is still yet to be fully explored. Understanding the solvation of solutes in these mixed liquid-gas solvents is of great importance in solution thermodynamics and solution chemistry.

The complex nature of solute-solvent interactions means that it is not possible to determine solvent polarity by simply measuring an individual solvent property. This has led to the wide-scale use of empirical scales of polarity which are experimentally simple to perform and based on chemical properties. Solvent polarity is best described by molecular-microscopic empirical solvent parameters derived from suitable solvent-dependent reference processes, with individual solvent molecules surrounding the ions or dipoles of the reference solute, leading to a loose or tight solvation shell.

Solvatochromism is observable spectroscopically as the influence of the "medium" on the electronic absorption and emission spectra of molecules.[3] It is the difference in solvation energies between the two electronic states which lead to the observed absorption or emission transition which result in a solvatochromic shift. With increasing polarity, greater stabilisation of the excited state relative to the ground state results in a bathochromic shift, and a decrease in stabilisation results in a hypsochromic shift.

The observed shift depends on the chemical structure and physical properties of both the solvent molecules and chromophore, which in turn determine the strength of the intermolecular solute-solvent interactions in the equilibrium ground state and the excited state. As a general rule, molecules with a large change in their permanent dipole moment exhibit stronger solvatochromism upon excitation. The polarity of a

solvent is defined as a function of its static relative permittivity, $\varepsilon_r$, in the Onsager model of dielectrics.

$$f(\varepsilon_r) = \frac{2(\varepsilon_r - 1)}{(2\varepsilon_r + 1)} \qquad \textbf{(3.1)}$$

As stated by Onsager, a reaction field is the electric field which results from an interaction between an ideal non-polarisable point dipole and a homogeneous polarisable dielectric field in which the dipole is immersed. The solute molecules experience an electric field due to the orientation and/or electronic polarisation of the solvent molecules by the solute dipole.

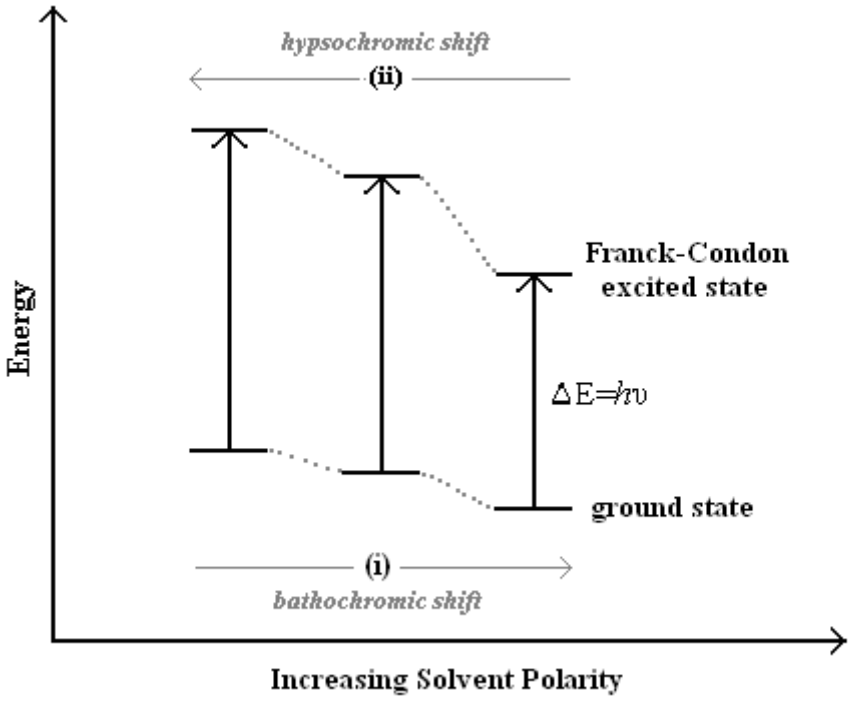


***Figure 3.1*** *Solvent effects on the electronic transition energy*

*(i) Bathochromic shift*
*(ii) Hypsochromic shift*

The magnitude of this shift is dependent upon the extent of change in the dipole moment of the solute, and its value during the transition, and also the degree to which interactions are formed between solute and solvent molecules (Figure 3.1). Solvatochromism is a result of differential solvation of the ground and first excited state by a chromophore. If an increase in polarity by solvation leads to better stabilisation of the ground state molecule than the excited state, negative solvatochromism is observed, and vice versa.

### 3.1.2 Empirical Scales of Solvent Polarity

Solvent strength is characterised by relating the shifts of UV-Vis absorption maxima in solvent-sensitive chromophores to the presence of solute-solvent interactions.[4] It is a very loosely defined concept, and it is also very complex to quantify and segregate all the specific and non-specific physicochemical interactions that are present between a solute and solvent. The interactions can be grouped generally into two categories, namely electrostatic or charge transfer interactions, and specific hydrogen bond interactions. The first empirical parameter was the *Y*-scale of solvent ionising power introduced by Winstein *et al*. in 1948.[5] Solvent polarities were established based on *Y*-values and they prompted other authors to propose scales of solvent polarities based on a given solvent sensitive property. Brooker and co-workers made the first suggestion that solvatochromic dyes could serve as visual indicators of solvent polarity.[6] However, in 1958 it was Kosower who was first to set up a real spectroscopic solvent polarity scale. Kosower took the longest wavelength intermolecular charge transfer transition of 1-ethyl-4-methoxycarbonylpyridinium iodide as a prototypical process. This dye was shown to exhibit a marked negative solvatochromic effect. A hypsochromic shift of the longest wavelength intermolecular charge transfer band of 105 nm results when a solvent change is made from pyridine to methanol. This polarity parameter more commonly became defined as the *Z*-scale.

$$E_T(kcal \cdot mol^{-1}) = h \cdot c \cdot \tilde{\upsilon} \cdot N_A = 2.859 \cdot 10^{-3} \cdot \tilde{\upsilon}(cm^{-1}) \equiv Z \qquad \textbf{(3.2)}$$

where $E_T$ is the molar transition energy, $h$ is Planck's constant, $c$ is the velocity of light, $\tilde{\upsilon}$ is the wavenumber of the photon producing the excitation, and $N_A$ is Avogadro's number. *Z*-values encompass the range from water (94.6) to *i*-octane (60 kcal $mol^{-1}$, and have originally been defined for 21 pure solvents, and 35 binary

solvent systems. Many solvent polarity scales have since been devised, but the two most widely used are the $E_T$ (30) scale,[4] and the π* scale of Kamlet et *al*.[7] The $E_T(30)$ scale is formed on the basis of a solvatochromic probe molecule, pyridinium *N*-phenolate betaine, while the π* scale is based on the absorption spectra of several nitroaniline based indicator dyes.

### 3.1.3 The $E_T$ Scale

Used to define solvent polarity, it is the most widely used single parameter empirical scale. The solvent polarity values are based on a negatively solvatochromic (hypsochromically shifted) betaine dye. Dimroth and Reichardt examined 32 derivatives of 4-(*N*-pyridinio)-phenolate which were classified; $E_T(1)$ to $E_T(32)$ by their capability of indicating polarity via the energy of transition ($E_T$). Probe $E_T(30)$ was the most effective and thus became the standard indicator for solvent polarity (Figure 3.2).

Polar solvents such as water and DMSO stabilise the charged zwitterionic ground state more than the dipolar excited state, and so a more pronounced energy change is noticed for the π→π* transition than that observed in less polar media. The original solvent polarity scale, more commonly referred to as the $E_T(30)$ scale, was defined as the transition energy (kcal $mol^{-1}$) of the longest wavelength absorption band for the dye. Normalised $E_T^N$ values have been introduced because of the introduction of SI units, and values have been referenced against extreme polar (water) for which $E_T^N$ is 1.00 and nonpolar (TMS) where $E_T^N$ is 0.00. The equation for its calculation is given below.

$$E_T^N = \frac{E_T(solvent) - E_T(TMS)}{E_T(water) - E_T(TMS)} = \frac{E_T(solvent) - 30.7}{32.4} \qquad \textbf{(3.3)}$$

Experimentally, $E_T^N$ values are quickly and easily obtained, providing a useful and convenient scale. Reichardt's $E_T(30)$ dye shown in Figure 3.2 is only sparingly soluble in water, and completely insoluble in nonpolar solvents. To overcome such solubility difficulties the dye was modified by the addition of *tert*-butyl groups thus increasing its solubility in hydrocarbons.[8] Aside from its sensitive response to changes

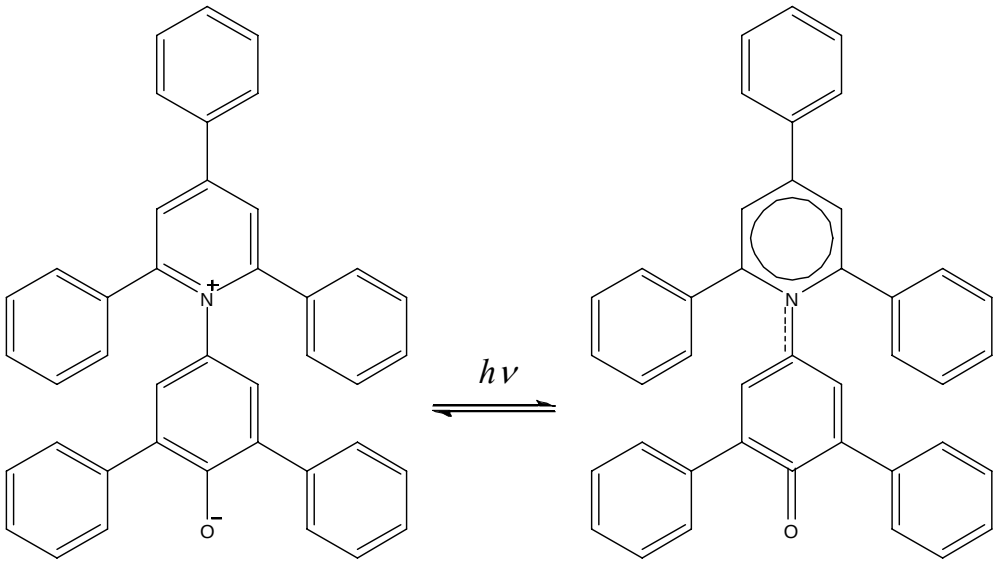


(1a) (1b)

| Solvent | $(C_6H_5)_2O$ | $C_6H_5OCH_3$ | $CH_3COCH_3$ | *i*-$C_5H_{11}OH$ | $C_2H_5OH$ | $CH_3OH$ | $H_2O$ |
|---|---|---|---|---|---|---|---|
| λmax (nm) | 810 | 769 | 677 | 608 | 550 | 515 | 453 |
| Solution Colour | - | yellow | green | blue | violet | red | - |
| | Increasing Solvent Polarity → | | | | | | |

***Figure 3.2*** *4-(2,4,6-triphenylpyridinium)-2,6-diphenylphenoxide Reichardt's $E_T(30)$ probe molecule and its wavelength of maximum absorbance in a range of solvents*

in solvent polarity, the solvatochromic absorption band of the pyridinium-*N*-phenoxide betaine dye also depends on differences in temperature, pressure, and the addition of electrolytes. Limitations in this polarity scale arise as it is based on a single probe molecule and so it cannot experience the diversity of interactions that the whole range of solvents can offer. This problem was undertaken by Kamlet and Taft who devised a multi-parameter polarity scale.

### 3.1.4 Kamlet and Taft Polarisability/dipolarity (π*) Scale

The π* scale of polarities and polarisability relies on three independent parameters (π*, α, β) derived from solvatochromic shift data of different molecules. It was formulated on the basis of solvent effects on p→π* and π→π* electronic transitions of uncharged molecules.[3] The characterisation of organic liquids by various properties can make them suitable for dissolving or providing reaction media for different solutes. Typical physical quantities include polarity, density, relative permittivity, and vapor pressure. Linear solvation energy relationships (LSER) have been proposed to correlate a number of solvent effects on a solute.[9] The Kamlet-Taft expression relating to LSER has been found to be very successful:

$$XYZ = XYZ_0 + a\alpha + b\beta + SPPE \qquad \textbf{(3.4)}$$

The terms $XYZ_0$, $a$, and $b$ are coefficients characteristic of the process being monitored and give an indication as to the sensitivity towards the associated solvent properties. Examples of such properties include reaction rate, equilibrium constant, or a position/intensity of spectral absorption. There are two other solvent strength scales which complement the π* scale which account for specific hydrogen bonding interactions; the $\alpha$-scale[10] (hydrogen bond donor acidity); and the $\beta$-scale (hydrogen bond acceptor basicity).[11] The determination of $\alpha$ and $\beta$ values are primarily obtained by the energies of the longest wavelength absorption peaks of certain carefully selected probe solutes in specified solvents. These measurements are then subtracted from the effect that non-HBD and/or non-HBA solvents would have on the probe which is carried out in independent experiments. The $a$ and $b$ coefficients are the corresponding hydrogen bonding constants associated with the solute and finally, *SPPE* represents the polarisability/dipolarity effect of the solvent. The solvent

strength scales for α and β have been carefully constructed and given numerical values and they exclusively describe the HBD and HBA properties of the solvents without being influenced by other properties such as polarity or polarisability. For some processes any of the solvent independent $XYZ_0$, $a$,$b$ and/or $s$ coefficients may be negligibly small, in such cases the corresponding terms have no influence in the characterisation of the solvent effects for these processes.

Initial construction of the π* scale involved the selection of several primary indicator solutes which had to satisfy specific requirements to a certain practicable extent.[7] The π* scale was then developed on the basis that solvent-induced shifts on the peak position of a UV-Vis absorption maxima of certain indicator solutes in liquid solvents were characteristic of the HBA, HBD, and SPPE values for various solvents. Solvatochromic comparisons of UV-Vis spectral data were assembled to compile the π* scale which incorporated polarity and polarisability in order to give a catalogue of single-valued SPPE parameters. The scale has since been expanded and further refined as other solvatochromic indicators have been added.[12, 13] An arbitrary π* scale of solvent polarities has been established for which optimised average π* values were normalised to give π* of 0.0 for cyclohexane, and π* of 1.0 for DMSO. Table 3.1 shows Kamlet-Taft parameters for a few selected solvents.

When π* factors are used to quantify SPPE effects, the Kamlet-Taft expression for LSER can be revised,

$$XYZ = XYZ_0 + s\pi^* + a\alpha + b\beta \qquad \textbf{(3.5)}$$

with ***s,*** a constant characteristic of the solute which represents the susceptibility of XYZ to changing SPPE. The π* parameter is a quantitative index of polarisability and dipolarity which provides a comprehensive indication for the ability of a solvent to stabilise a charge or a dipole (induced dipole) based on dielectric effects. π* is a measure of the residual polarity or polarisability of the solvent after hydrogen bonding influences have been removed.

***Table 3.1*** *Kamlet-Taft α, β and π* parameters for selected solvents.*

| **Solvent** | **α** | **β** | **π*** |
|---|---|---|---|
| Water | 1.2 | 0.47 | 1.09 |
| Methanol | 1.0 | 0.66 | 0.60 |
| Ethanol | 0.9 | 0.75 | 0.54 |
| Dimethyl sulfoxide | 0.0 | 0.76 | 1.00 |
| Acetonitrile | 0.2 | 0.40 | 0.75 |
| Acetone | 0.1 | 0.43 | 0.71 |
| Dichloromethane | 0.1 | 0.10 | 0.82 |
| Benzene | 0.0 | 0.10 | 0.59 |
| Toluene | 0.0 | 0.11 | 0.54 |
| *n*-Hexane | 0.0 | 0.00 | -0.04 |
| Cyclohexane | 0.0 | 0.00 | 0.00 |

Earlier work by Figueras[14] presented convincing substantiation that shifts in $\lambda_{max}$ of an indicator dye are of limited value for solvent polarity scales where hydrogen bond interactions are possible. In order to overcome this problem, hydrogen bond interactions were excluded from the scale by careful choice of solvents that were neither HBD nor HBA thus named, non-hydrogen bonding (NHB) solvents. If only NHB solvents are used, both the $\alpha$ and $\beta$ term can be ignored. As a result of these simplifications, the revised Kamlet-Taft expression can be reduced to:

$$\upsilon_{max} = \upsilon_0 + s\pi^* \qquad \textbf{(3.6)}$$

Where $\upsilon_{max}$ is the wavenumber of the maximum absorbance in the UV-Vis and $\upsilon_0$ is the reference wavenumber determined from the absorbance maximum for a standard solvent (cyclohexane). The π* polarity scale has been characterised for more than 250 liquid solvents.[15] Compared to the number of $\pi^*$ studies in liquid and supercritical solvents, very limited investigations have been carried out in gas expanded solvents. One such example is the use of the solvatochromic characterisation technique to

examine the properties of CXLs.[16] The solvent strength of various solvents was investigated as a function of gas expansion using carbon dioxide at pressures up to 70 bar. Reports showed that an increase in pressure lead to a strong decrease in polarity as a result of increased dissolution of $CO_2$ in the solvent.

Wyatt *et al*.[17] have also reported solvatochromism in gas expanded liquids. They measured the solvatochromic shift of six probe indicators in binary mixtures of $CO_2$ expanded methanol, and $CO_2$ expanded acetone. UV-Vis spectroscopy data was collated to give $E_T(30)$, α, β, and π* parameters for the entire range of solvent compositions for each binary mixture. They found that π* values for the binary mixtures decreased with increasing amounts of $CO_2$, suggesting a reduction in polarity of the mixtures upon expansion. β values showed a similar trend for expanded methanol, however, in $CO_2$ expanded acetone the probe used was less susceptible to increasing amounts of $CO_2$ and so little change was observed. Both π* and β were shown to decrease towards the direction that led them to approach their respective values for pure carbon dioxide. Measurement of α values showed an opposing trend, where data progressed away from the value for that of pure carbon dioxide. The α values showed the least susceptibility to change when the solvents were expanded, and it was concluded that taking into account scientific error, α values remained the same as the α values for pure methanol or acetone.

Thorough utilisation of a GXL requires a more meticulous understanding of its cybotactic region, the region where the structure of the solvent is influenced by the degree of solute-solute and solute-solvent interactions.[18] Solvatochromic studies in supercritical fluids have shown them to exhibit an enhancement of the local density in the cybotactic region of the solute molecule compared to the bulk density of the solvent near the solvents critical point.[19-21] The establishment of heterogeneities in the cybotactic region necessitates the set up of more specific experiments which probe the local environment. A comprehension of the non-uniformity of the local solvent structure in GXLs can help determine how the chemistry of the solutes is affected.

The aim of this work is to collate data for the polarisability/dipolarity π* parameter and the hydrogen bond donor acidity parameter, α, for a range of $CO_2$ expanded organic solvents. These parameters will help determine the changes in the local environment (cybotactic region) when a solvent is pressurised with $CO_2$ at 50 bar. The data will give key information on local solvent polarity which can be used as a selection tool for applications where polarity is a major consideration when

choosing a solvent. The solvents will be classified into two categories, non hydrogen bonding (NHB) and hydrogen bond donor (HBD) solvents. Parameters such as temperature, pressure and volume of the experimental cell will be kept constant throughout the study.

## 3.2 Results and Discussion

### 3.2.1 Reichardt's Single Parameter Approach

Reichardt's dye is known to dissolve in a range of solvents from nonpolar to polar. The main advantage of using this probe is that the solvatochromic absorption band is at longer wavelengths than most other dyes, and this generates a wide range of solvatochromic behaviour. $E_T(30)$ values are simply defined as molar transition energies (kcal $mol^{-1}$) of the betaine dye dissolved in the solvent under study. A high $E_T(30)$ value corresponds to high solvent polarity. $E_T(30)$ values range from 30.7 for tetramethylsilane up to 63.1 for water Since the majority of its solvatochromic range lies in the visible part of the spectrum, it is possible to visually estimate solvent polarity by simply observing the change in solution colour. As a means of calibrating the use of the UV-Vis spectrometer along with the high pressure cell, Reichardt's dye was used as the probe. It is clear to see from Figure 3.3 how the range of solvents chosen for this study differ in polarity ranging from nonpolar cyclohexane to polar water.

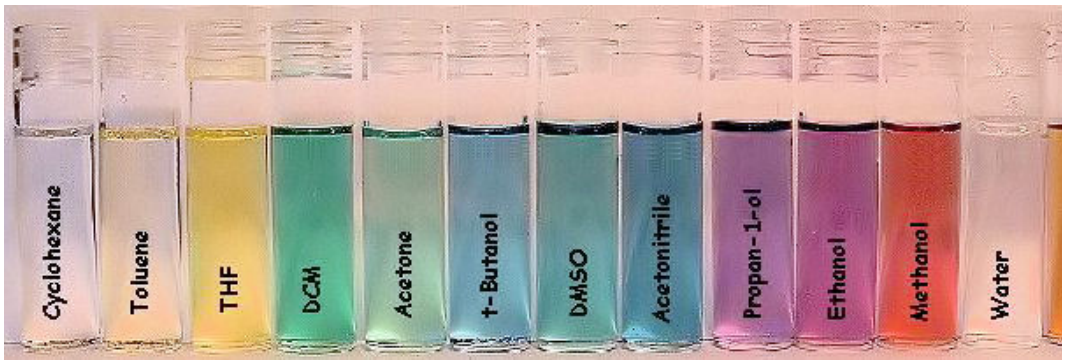


***Figure 3.3*** *Solvatochromic behaviour of Reichardt's Dye $E_T(30)$ in solvents of increasing polarity from left to right*

The data recorded for the solvents under ambient pressure conditions is presented in Table 3.2.

***Table 3.2*** *Data for the solvatochromic absorption of Reichardt's dye in the solvents listed and their $CO_2$ expanded equivalents. The data in the table were recorded in this study apart from the shaded column which represents data reported in the literature*

| **Solvent** | **λ nm** | **$E_T$(30)** | **Lit $E_T$(30)[22, 23]** | **GXL $E_T$(30)** |
|---|---|---|---|---|
| Cyclohexane | 925.4 | 30.89 | 30.89 | 29.72 |
| Toluene | 843.1 | 33.91 | 33.91 | 29.97 |
| THF | 764.3 | 37.41 | 37.41 | 30.31 |
| DCM | 702.0 | 40.73 | 40.71 | 30.51 |
| Acetone | 677.8 | 42.18 | 42.20 | 30.40 |
| t-Butanol | 660.3 | 43.30 | 43.30 | - |
| DMSO | 634.1 | 45.09 | 45.09 | 31.09 |
| Acetonitrile | 626.8 | 45.61 | 45.60 | 30.56 |
| Butanol | 569.4 | 50.21 | 50.20 | - |
| Propan-1-ol | 563.6 | 50.73 | 50.69 | - |
| Ethanol | 551.0 | 51.89 | 51.89 | - |
| Methanol | 516.5 | 55.35 | 55.39 | - |

A good correlation is observed for solvents at ambient pressure with values reported in the literature.[26] However, for the expanded solvents, initial experimentation showed that when protic solvents were subjected to moderate pressures of $CO_2$, the dye became protonated and did not absorb in the UV-Vis region and this resulted in a 'bleaching' effect. Protonation at the phenolic oxygen on addition of trace amounts of acid immediately changed the colour of the dye to a pale yellow.[24] It is also notable to mention that all solvents have a similar $E_T$ value when pressurised with $CO_2$ showing that in expanded conditions the dye loses its wide spectroscopic window. A modified version of the $E_T$(30) dye was employed to circumvent this issue. $E_T$(33) is similar in structure to $E_T$(30) but two of the *t*-phenyl groups have been replaced by chlorines as shown in Figure 3.4. It has already been used for previous solvatochromic studies where protonation has been a problem and also has a wide spectrum range as shown in Figure 3.5.

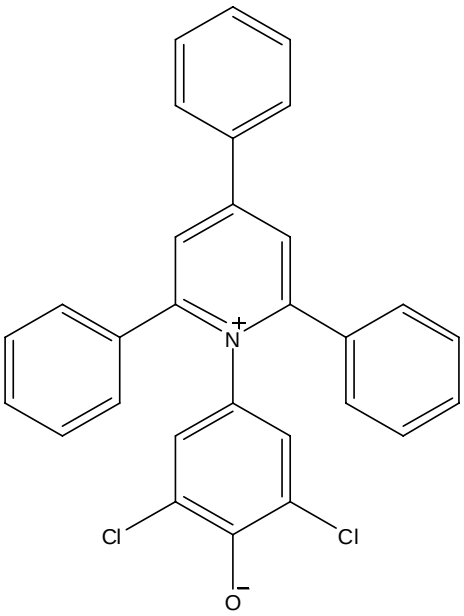


(2)

***Figure 3.4*** 2,6-Dichloro-4-(2,4,6-triphenyl-*N-pyridino*)phenolate*, Reichardt's $E_T(33)$ probe molecule exhibits an unusually high solvatochromic band shift*[4, 24, 25]

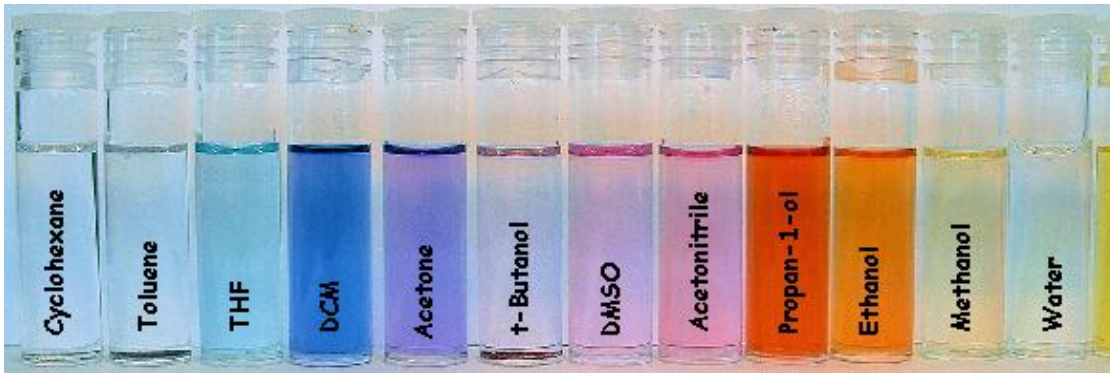


***Figure 3.5*** *Solvatochromic behaviour of Reichardt's $E_T(33)$ dye in a range of liquid solvents with increasing polarity from left to right. The lowest energy intramolecular charge-transfer absorption band is displaced hypsochromically by ca. 357 nm when shifting from a relatively nonpolar diphenyl ether (810 nm) to polar water (~453 nm)*

Transition energies calculated (using equation **3.2**) for the substituted Reichardt's $E_T(33)$ dye in pure, and $CO_2$-expanded solvents, are shown in Table 3.3. As expected, on expansion with $CO_2$ at 50 bar all solvents show a corresponding decrease in polarity. Figure 3.6 correlates the calculated transitions energies for both the $E_T(30)$ and the $E_T(33)$ dye for solvents at ambient pressure conditions. This validates the use of the $E_T(33)$ dye as a suitable replacement probe to avoid problems with protonation by hydrogen bonding solvents as seen with $E_T(30)$. A good linear

correlation is observed. Figure 3.7 shows that the solvatochromic shift is much greater as the polarity of the liquid solvent increases, and so a greater change in polarity is observed for the alcohols and DMSO when they are expanded with $CO_2$. The greatest change is observed for methanol, where $CO_2$-expanded methanol (measured $E_T(33)$ of 42.30) is comparable to the polarity of toluene at ambient conditions ($E_T(33)$ of 42.60). A lesser change in polarity is observed for nonpolar solvents such as cyclohexane and toluene, but it is believed that this is due to the similarity of the nonpolar nature of both the solvent and $CO_2$.

***Table 3.3*** *Data for the solvatochromic absorption of Reichardt's $E_T(33)$ dye in the solvents listed and for their expanded counterparts.*

| **Solvent** | **λ nm** | **$E_T(33)$** | **GXL $E_T(33)$** |
|---|---|---|---|
| Cyclohexane | 722.0 | 39.60 | 39.14 |
| Toluene | 671.2 | 42.60 | 39.43 |
| Tetrahydrofuran | 618.9 | 46.20 | 39.77 |
| Dichloromethane | 583.0 | 49.04 | 39.99 |
| Acetone | 548.8 | 52.10 | 39.86 |
| *t*-Butanol | 502.5 | 56.90 | 41.06 |
| Dimethyl Sulfoxide | 518.9 | 55.10 | 40.55 |
| Acetonitrile | 518.4 | 55.15 | 40.02 |
| Butanol | 498.1 | 57.40 | 43.70 |
| Propan-1-ol | 487.9 | 58.60 | 44.40 |
| Ethanol | 472.2 | 60.55 | 42.20 |
| Methanol | 443.6 | 64.45 | 42.30 |

From a practical viewpoint, $E_T$ values are quickly and easily obtained, providing a very useful and convenient scale. However, limitations arise from this more general polarity scale based on a single probe molecule because a single compound cannot experience the diversity of interactions that the whole range of solvents can offer. Kamlet and Taft's parameters $\alpha$, $\beta$ and $\pi^*$ overcome this problem by employing the use of a series of seven dyes to produce a scale for specific and nonspecific polarity of liquids.[27] Whilst it unquestionably gives a more detailed description of the solvents properties the method by which it is determined is more time consuming and requires extra measurements and further calculations.

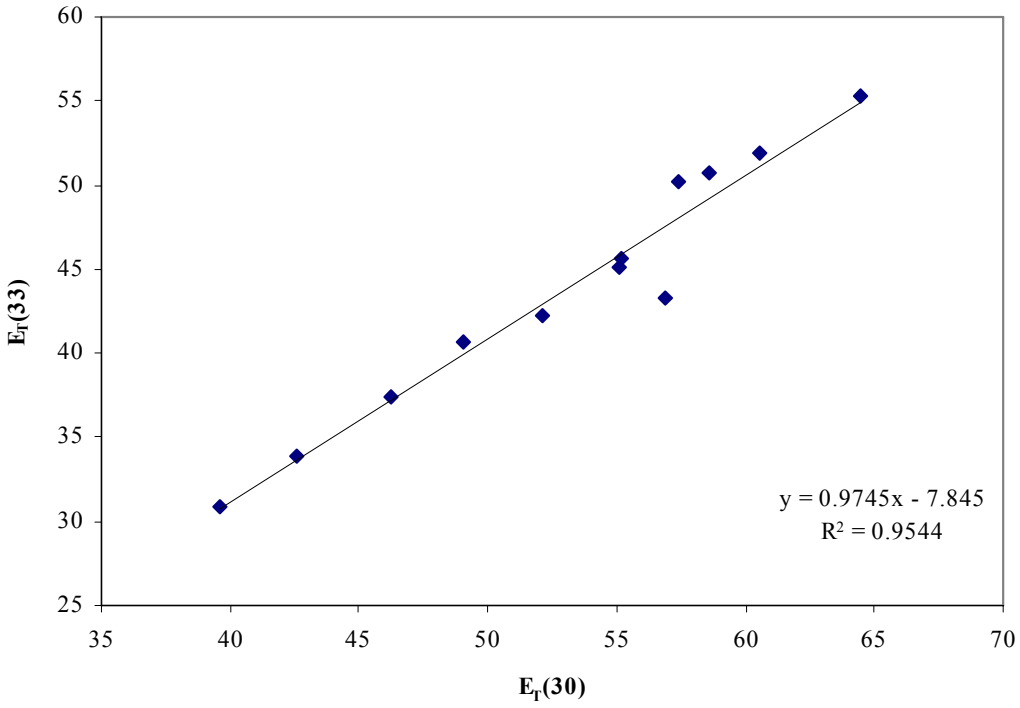


***Figure 3.6*** *Correlation between transition energies calculated for Reichardts $E_T(30)$, and $E_T(33)$ at ambient pressure conditions*

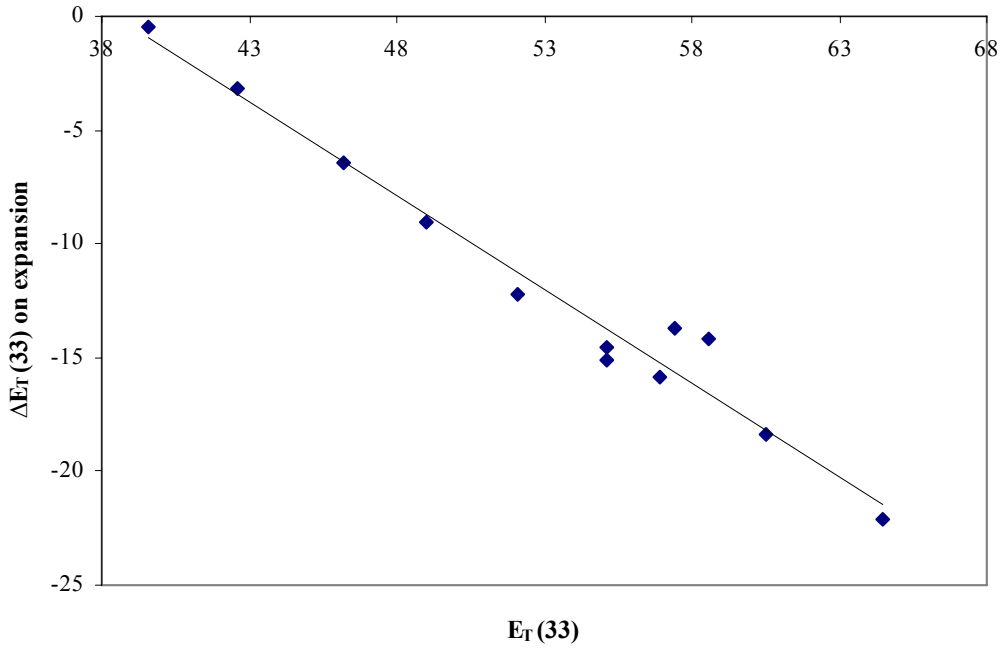


***Figure 3.7*** *Data correlation for Reichardts $E_T(33)$ probe, showing the degree to which solvatochromism was observed on expansion*

### 3.2.2 Kamlet and Taft Multi-Parameter Approach

In addition to the single parameter $E_T$ scale, Kamlet and Taft's π* scale was investigated to probe the changes in hydrogen bonding that occurred during $CO_2$ expansion of the solvents.

Wyatt *et al.*[17] calculated π* values using the shift for two different probes standardised to give a value of 0.0 for cyclohexane and 1.0 for dimethyl sulfoxide. This meant that the calibration for each parameter was carried out based on only two sets of data, that for cyclohexane and DMSO. Similar calibration methods were adopted for the calculation of β and α using different solvents to standardise each parameter. In the current work, all of the solvents in this study will be used to calibrate the solvatochromic parameters of the indicator dye as the use of more solvents makes it possible to 'fit' data more precisely, and thus calculate the coefficients of each parameter being analysed.

The electronic transitions of dyes are strongly dependent upon the degree of solute-solvent hydrogen bonding interactions. The solvents can be classified into three categories;

a) neither hydrogen bond donating nor accepting (non-hydrogen bonding) solvents
b) hydrogen bond donating solvents
c) amphiprotic solvents

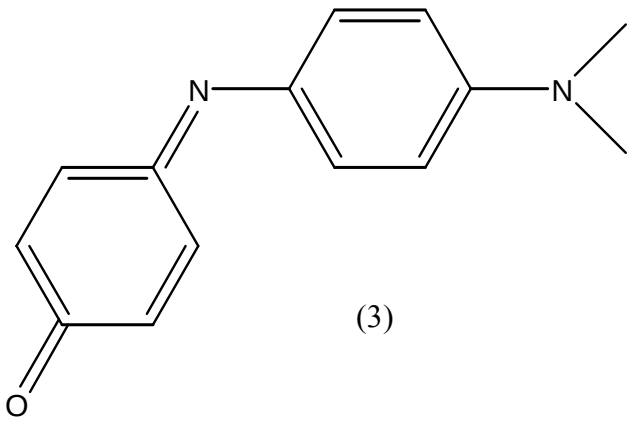


(3)

***Figure 3.8*** *Structure of Phenol blue*

Phenol Blue, *N*-(4-dimethylamino-phenyl)benzoquinonemonoimine) is a suitable model solvatochromic dye. It is unambiguous in its response to solvent polarity in aprotic media; its dialkylamino and carbonyl groups allow only hydrogen bond acceptor behaviour toward amphiprotic and hydrogen bond donor solvents. Its single electronic absorption peak in the visible region is Gaussian in shape and has a high molar absorptivity. Phenol Blue is a positively solvatochromic dye.[14]

Theoretical studies have previously been studied[28-30] looking into its solvent-independent electronic properties examining the sensitivity of the absorption maximum to the solvent environment. A greater solvent sensitivity is possible for Phenol Blue because the π bonding of the chromophore is more delocalised within the larger dye species than the four primary nitroaniline indicators. The visible spectrum of Phenol Blue has a single intense absorption band at ~550 nm which corresponds to a π-π* transition. It is capable of acting as HBD substrate in hydrogen bond acceptor solvents, but not in hydrogen bond donor solvents. The red shift of the absorption maxima ($\lambda_{max}$) from a nonpolar to a polar aprotic solvent exceeds 55 nm and is comparable in magnitude to Nile Blue A, Oxazone (Nile Red) and other uncharged dyes in non-hydroxylic solvents. The sensitivity of the absorption maxima to the solvent environment has been examined from the view point of theoretical mechanisms.[31]


***Figure 3.9*** *Change in absorbance of phenol blue shown for solvents ranging from nonpolar cyclohexane, to polar water*

The solvatochromic behaviour of Phenol Blue can be predicted from the bulk properties of a solvent using a second order quantum mechanics perturbation theory. The resulting McRae equation (equation 3.7) relates intrinsic solvent strength via the dye's solvatochromic behaviour to bulk relative permittivity, $\varepsilon_r$, and bulk refractive index, *n*, to derive a two-variable expression.[14, 32] The McRae equation can be applied to those indicator solutions in binary aprotic solvents showing regular behaviour, and

has since been re-stated by Figueras in terms of the transition energy $(E_T)_M$ as shown[33]:

$$(E_T)_M = A\left[\frac{n^2-1}{2n^2+1}\right] + B\left[\frac{\varepsilon_r - 1}{\varepsilon_r + 2} - \frac{n^2-1}{n^2+2}\right] + C \qquad \textbf{(3.7)}$$

Where A, B and C are constants specific of phenol blue[14] for $(E_T)_M$ in kcal mol$^{-1}$ (-33.0, -4.4, and 57.92 respectively). This equation, does not account for specific interactions such as hydrogen bonding. The validity of experimental data has been compared with that of Kolling and Goodnight who used this equation to model the behaviour of 13 solvents in phenol blue.[33] Data for this work is presented in Table 3.4.

***Table 3.4*** *Literature data and spectral parameters for NHB and HBD solvents at 25°C.*

| **Solvent** | **Relative Permittivity $(\varepsilon_r)$[34]** | **Refractive index $(n)$[35]** | **Phenol blue λ (nm)** | **Observed[(a)] $E_T$** | **Calculated[(b)] $(E_T)_{Mb}$** | **$(E_T)_M$ - $E_T$** |
|---|---|---|---|---|---|---|
| DCM | 8.93 | 1.424 | 591.1 | 48.37 | 49.14 | 0.77 |
| Cyclohexane | 2.02 | 1.426 | 550.3 | 51.95 | 51.20 | -0.76 |
| Toluene | 2.38 | 1.496 | 573.6 | 49.84 | 50.35 | 0.51 |
| DCE | 10.37 | 1.444 | 590.7 | 48.40 | 48.82 | 0.42 |
| Acetone | 20.56 | 1.358 | 582.1 | 49.12 | 49.12 | 0.01 |
| Acetonitrile | 35.94 | 1.344 | 585.3 | 48.85 | 49.03 | 0.18 |
| DMSO | 46.45 | 1.479 | 604.0 | 47.33 | 47.75 | 0.41 |
| THF | 7.58 | 1.407 | 576.6 | 49.58 | 49.46 | -0.12 |
| Ether | 4.20 | 1.352 | 561.3 | 50.94 | 50.73 | -0.21 |
| *N,N*-DMF | 36.71 | 1.430 | 593.7 | 48.16 | 48.22 | 0.06 |
| Methanol | 32.66 | 1.328 | 609.3 | 46.92 | 49.22 | 2.30 |
| Ethanol | 24.55 | 1.361 | 603.1 | 47.41 | 49.01 | 1.60 |
| Propan-1-ol | 20.45 | 1.385 | 601.7 | 47.52 | 48.87 | 1.35 |
| Propan-2-ol | 19.92 | 1.377 | 597.9 | 47.82 | 48.96 | 1.14 |
| Butanol | 17.51 | 1.399 | 601.3 | 47.55 | 48.83 | 1.28 |
| *t*-Butanol | 12.47 | 1.387 | 590.9 | 48.38 | 49.17 | 0.79 |

*[(a)] Transition energies measured from $\lambda_{max}$ of phenol blue. Literature data confirmed experimentally.[14, 33, 36-38]*

*[(b)] Transition energies (kcal/mol) computed from experimental values, $\lambda_{max}$ of phenol blue in each of the pure HBD solvents using equation **3.7**.*

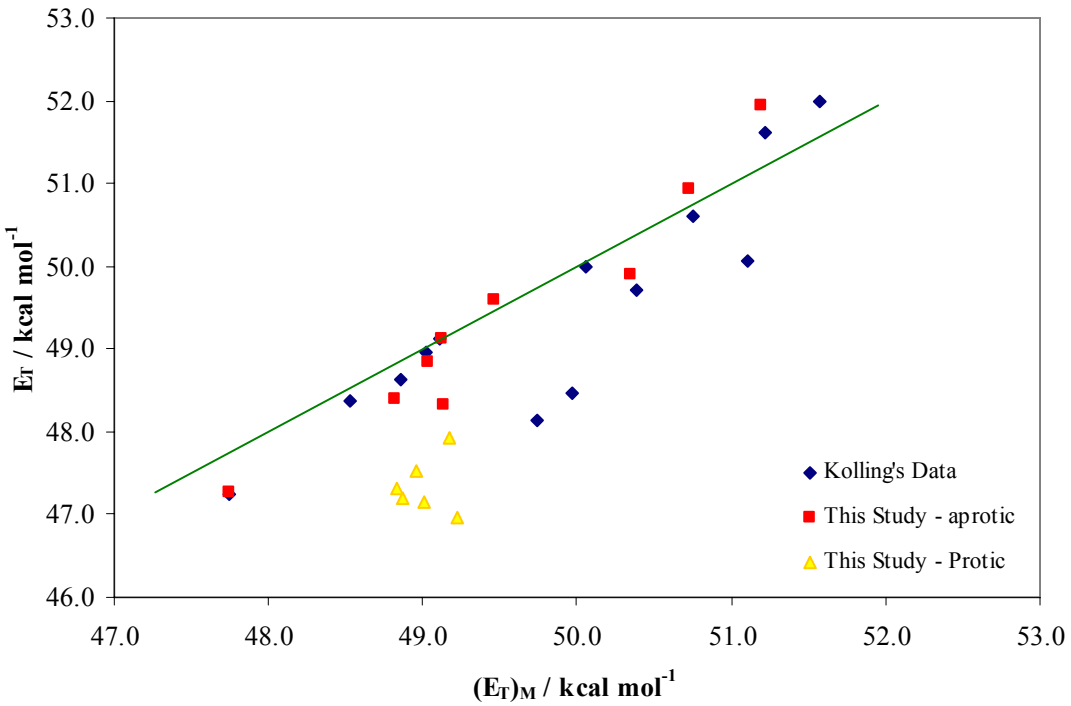


***Figure 3.10*** *Plot of the calculated $(E_T)_M$ derived from the McRae equation against experimental $E_T$*

The solvents used by Kolling *et al*. differ from some of the solvents used in this study, however this should not pose a problem as it is the trend between the experimental and the calculated transition energies which are being compared, not the actual numbers. Figure 3.10 shows that a more linear trend is observed from the data plotted for the solvents used in this study (red dots with dotted line), compared to those of Kolling (blue diamond). When data for the transition energies are plotted for hydroxylic solvents (yellow triangles), the data points appear to be noticeably displaced from the general trend observed for aprotic solvents. The calculation of transition energies does not take into account hydrogen bonding influences and it is thought that this is why only the alcohols are displaced from the general trendline as they are the only solvents with significant hydrogen bonding character.

It can be seen that for solvents with intermediate polarity, experimental $E_T$ values are significantly lower than the value predicted by the McRae equation. This indicates that the dye is stabilised to a greater degree than can be accounted for by assuming the mixtures are homogeneous (which is assumed by using the McRae analysis). Kim and Johnston[39] have shown that this added stabilisation is the result of

enrichment in the local environment about the dye molecules in the more polar component of the mixture and so, the solution may only contain 50 % of a solvent, but the environment sensed by the dye is to a much greater amount.

Kolling and colleagues further developed a method which incorporated the use of the transition energy of phenol blue, and showed that it is a suitable indicator which can be used for the spectrophotometric measurement of solvent polarity. They demonstrated that Phenol Blue is superior to the nitroanilines in distinguishing between weaker hydrogen bond donors, thus showing the capability of this method to calculate π* and α. This method was also shown to be successful in the determination of π* and α for HBD and amphiprotic solvents such as alcohols. Studies concerning the solvatochromism of Phenol Blue (and its derivatives) are relatively few, though work carried out by Figueras[14, 37] and McRae[36] have elucidated the mechanisms for the behaviour of Phenol Blue in both aprotic and protic media.

A calibration incorporating the use of two different dyes was required to calculate both π* and α. Abbott and Eardley have previously reported the pressure dependency of π* for supercritical solvents using Nile Red as an indicator solute.[40] The experimental data obtained from the McRae test was used along with a second series of data based on the dye Nile Red (Figure 3.11) which has a close structural relationship to Phenol Blue. The spectral range of Nile Red is shown visually in Figure 3.12.

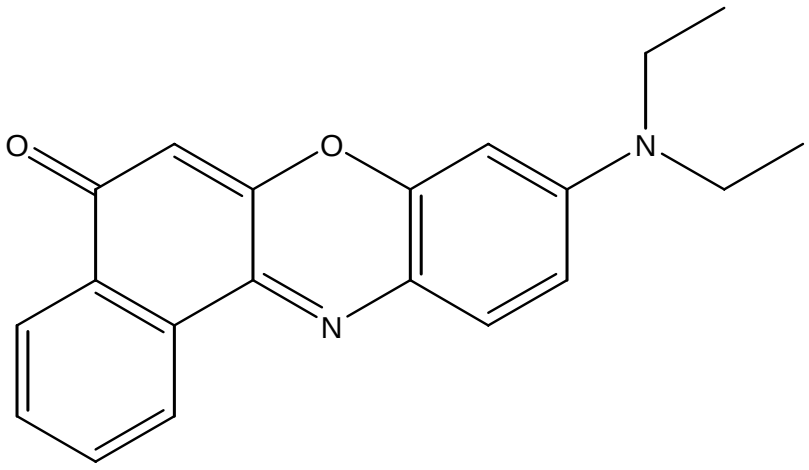


(4)

***Figure 3.11*** *Structure of Nile Red*

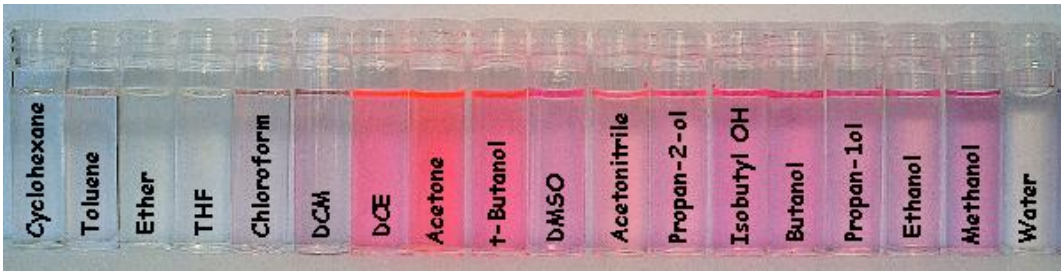


***Figure 3.12*** *Nile Red in a range of solvents with increasing polarity from left to right*

To obtain the π* values for the expanded solvents, the susceptibility constant '*s*' for the two solvatochromic dyes was determined by measuring their absorption spectra in 16 liquid solvents of differing polarity. Using solvents with a known π* value the coefficient *s* for a specific solute was determined as the slope of a graph of the maximum absorption energy $\upsilon_{max}$ versus the polarity, π* as shown in Figures 3.13 and 3.14. A negative *s* value is indicative of a solute that has an electronically excited state that is more stabilised than its ground state when π* is increased. The data obtained were fitted to the equations 3.8 and 3.9 below and an iterative least-squares method was used to find the best fit against literature π* values resulting in the specific regression functions shown below in Table 3.5

*Nile Red:* $$\nu_{max} = 19.993 - 1.725\pi^* \quad \textbf{(3.8)}$$

*Phenol Blue:* $$\nu_{max} = 18.238 - 1.604\pi^* \quad \textbf{(3.9)}$$

***Table 3.5*** *Susceptibility constants for the solvatochromic probes used in this work*

| Dye | s value | $\nu_o$ (kK) | $R^2$ value |
|---|---|---|---|
| Phenol Blue | 1.604 | 18.238 | 0.997 |
| Nile Red | 1.725 | 19.993 | 0.976 |

Table 3.5 shows that a very good correlation was obtained in all cases ($R^2 > 0.97$). These constants were used to re-calculate the π* of the liquid solvents, and the difference between calculated π* and literature π* was determined.

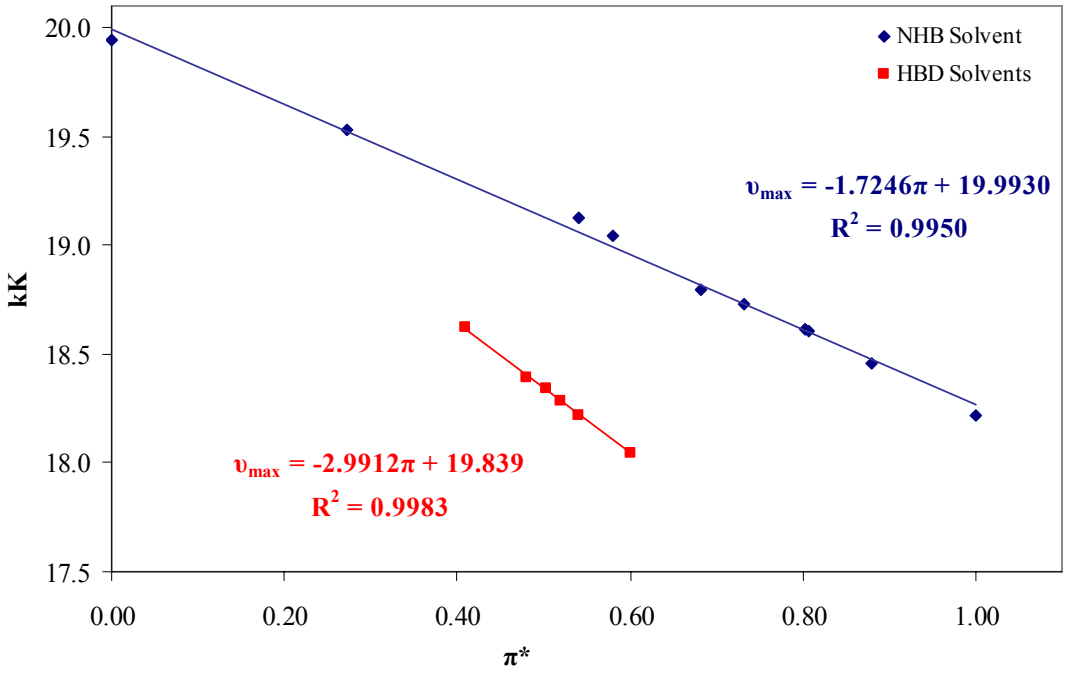


***Figure 3.13*** *Plot of π* versus maximum wavelength absorption readings, $\upsilon_{max,}$ for Nile Red in NHB solvents (blue), and HBD solvents (red) at ambient pressure*

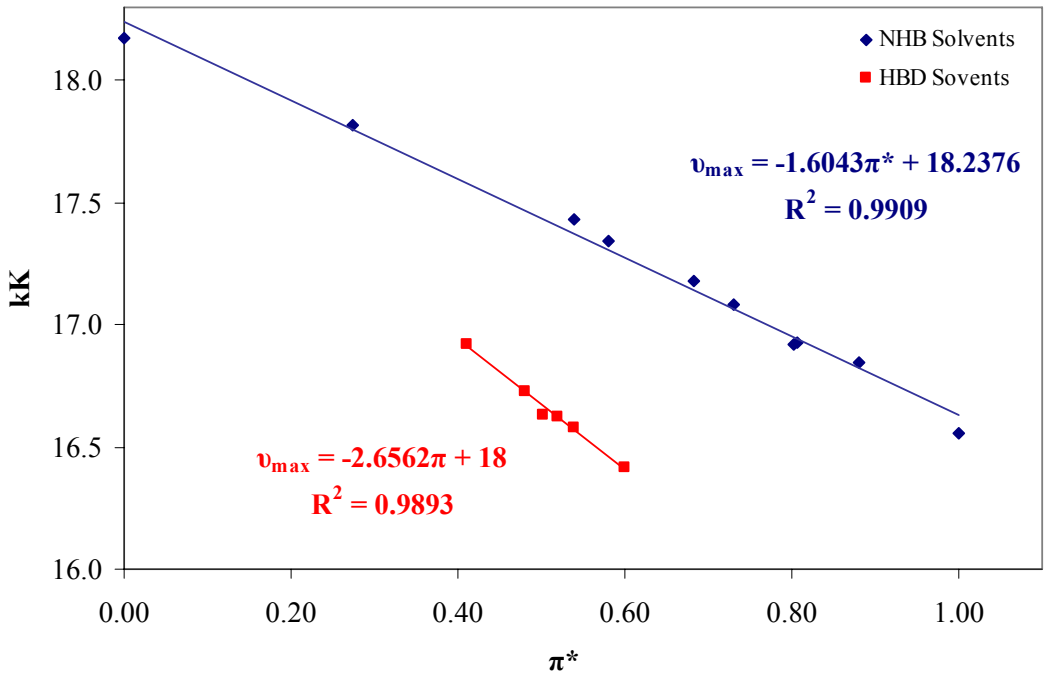


***Figure 3.14*** *Plot of π* versus maximum wavelength absorption readings $\upsilon_{max}$ for Phenol Blue in NHB solvents (blue), and HBD solvents (red) at ambient pressure*

***Table 3.6*** *Solvatochromic data for Phenol Blue and Nile Red in a range of solvents at ambient pressure consitions*

| **Solvent** | ***Nile Red*** | | ***Phenol Blue*** | | **Literature[1] π*** | **Calculated π*** |
|---|---|---|---|---|---|---|
| | **$\nu_{max}$ (nm)** | **$\nu_{max}$ (kK)** | **$\nu_{max}$ (nm)** | **$\nu_{max}$ (kK)** | | |
| Dichloromethane | 537.2 | 18.62 | 591.1 | 16.92 | 0.802 | 0.812 |
| Cyclohexane | 501.4 | 19.94 | 550.3 | 18.17 | 0.000 | 0.034 |
| Toluene | 522.9 | 19.12 | 573.6 | 17.43 | 0.540 | 0.503 |
| Dichloroethane | 537.4 | 18.61 | 590.7 | 16.93 | 0.807 | 0.810 |
| Acetone | 532.0 | 18.80 | 582.1 | 17.18 | 0.683 | 0.677 |
| Acetonitrile | 534.0 | 18.73 | 585.3 | 17.09 | 0.731 | 0.727 |
| DMSO | 548.8 | 18.22 | 604.0 | 16.56 | 1.000 | 1.039 |
| Tetrahydrofuran | 525.0 | 19.05 | 576.6 | 17.34 | 0.580 | 0.553 |
| Ether | 512.1 | 19.53 | 561.3 | 17.82 | 0.273 | 0.266 |
| N,N-Dimethyl formamide | 541.7 | 18.46 | 592.7 | 16.87 | 0.880 | 0.880 |
| *Methanol* | *554.1* | *18.05* | *609.3* | *16.41* | *0.600* | *1.200* |
| *Ethanol* | *548.8* | *18.22* | *603.1* | *16.58* | *0.540* | *1.062* |
| *Propan-1-ol* | *546.9* | *18.28* | *601.7* | *16.62* | *0.520* | *1.030* |
| *Propan-2-ol* | *543.8* | *18.39* | *597.9* | *16.73* | *0.480* | *0.964* |
| *Butanol* | *545.2* | *18.34* | *601.3* | *16.63* | *0.503* | *1.009* |
| *t-Butanol* | *537.1* | *18.62* | *590.9* | *16.92* | *0.410* | *0.829* |

[1] Literature data for π* from Kamlet and Taft[15, 41, 42].

Table 3.6 shows that for NHB solvents, calculated π* values were within very good agreement with published values. Using the same method, the HBD solvents showed a large deviation from expected values similarly to that observed by the McRae analysis for Phenol Blue. The work on NHB solvents was continued by looking into the change in polarity when the solvents were exhibited to a moderate pressure of $CO_2$, only π* data was collected for this work due to the absence of hydrogen bonding, and the results are shown in Table 3.6.

It has been suggested that similarly to nitroaniline indicators Phenol Blue is not strong enough an acceptor to resolve extremely weak HBD behaviour such as that exhibited by dichloromethane and acetonitrile,[32] therefore α was not determined for weakly HBD solvents and from this point on they were treated as non hydrogen bonding solvents. The solvatochromic data for the solvent systems formed upon $CO_2$ expansion are shown in Table 3.7. Equations 3.8 and 3.9 were used to calculate the new values for π*. The change in π* was recorded as the difference between π* of the solvent at ambient pressure and the calculated π* of its expanded equivalent.

In this study, all solvents resulted in an overall decrease in polarity when expanded. The degree to which polarity was changed showed no trend against the initial polarity of the pure solvent, however work reported here shows that a significant change in polarity is observed when a solvent is expanded, and it is thought that the change in π* is dependent on both liquid solvent polarity and the solubility of $CO_2$ in the solvent. By comparing the π* data for solvents before and after expansion it is possible to see that gas expanding the solvents allows significant changes in solvent properties to be obtained. The data reported here is in contrast to those reported by Wyatt *et al*.[17] where the solvatochromic parameters of gas expanded liquids appear to remain fairly constant and are similar to that of the pure liquid as $CO_2$ is added until high compositions of $CO_2$ are reached. Their study, however, was limited to the analysis of only two solvent systems, methanol and acetone.

***Table 3.7*** *Solvatochromic data for Phenol Blue and Nile Red in a range of solvents at 50 bar pressure of $CO_2$*

| **Expanded Solvent Data** | ***Nile Red*** | | ***Phenol Blue*** | | **π* (1 atm)** | **π* (50 atm)** | **Change π*** |
|---|---|---|---|---|---|---|---|
| | **$\nu_{max}$ (nm)** | **$\nu_{max}$ (kK)** | **$\nu_{max}$ (nm)** | **$\nu_{max}$ (kK)** | | | |
| Dichloroethane | 537.2 | 18.62 | 591.1 | 16.92 | 0.812 | 0.487 | -0.325 |
| Cyclohexane | 501.4 | 19.94 | 550.3 | 18.17 | 0.034 | -0.067 | -0.101 |
| Toluene | 522.9 | 19.12 | 573.6 | 17.43 | 0.503 | 0.177 | -0.325 |
| Dichloroethane | 537.4 | 18.61 | 590.7 | 16.93 | 0.810 | 0.566 | -0.244 |
| Acetone | 532.0 | 18.80 | 582.1 | 17.18 | 0.677 | 0.432 | -0.245 |
| Acetonitrile | 534.0 | 18.73 | 585.3 | 17.09 | 0.727 | 0.530 | -0.197 |
| Dimethyl Sulfoxide | 548.8 | 18.22 | 604.0 | 16.56 | 1.039 | 0.938 | -0.101 |
| Tetrahydrofuran | 525.0 | 19.05 | 576.6 | 17.34 | 0.553 | 0.367 | -0.186 |
| Ether | 512.1 | 19.53 | 561.3 | 17.82 | 0.266 | 0.043 | -0.223 |
| N,N-dimethyl formamide | 541.7 | 18.46 | 592.7 | 16.87 | 0.880 | 0.841 | -0.039 |

Phenol Blue is known to be subject to specific interactions with alcohols.[33] Figures 3.13 and 3.14 presented earlier show that data points for HBD solvents in both Phenol Blue and Nile Red were displaced from the regression line. These solvents are expected to be displaced from the line by statistically significant amounts, and are presumed to reflect specific solute-solvent interactions. A linear regression of these HBD solvents alone, gave the following equations relating solvatochromic behaviour.

*Nile Red:* $$\nu_{max} = 19.839 - 2.991\pi^* \quad \textbf{(3.10)}$$

*Phenol Blue:* $$\nu_{max} = 18.000 - 2.656\pi^* \quad \textbf{(3.11)}$$

The π* values for alcohols at ambient pressure are reported in Table 3.8. Literature data are also included for comparison.

***Table 3.8*** *Solvatochromic data for Phenol Blue and Nile Red in different alcohols at ambient pressure.*

| Solvent | *Nile Red* | | *Phenol Blue* | | Literature[1] π* | Calculated π* |
|---|---|---|---|---|---|---|
| | $\nu_{max}$ (nm) | $\nu_{max}$ (kK) | $\nu_{max}$ (nm) | $\nu_{max}$ (kK) | | |
| Methanol | 554.1 | 18.05 | 609.3 | 16.41 | 0.600 | 0.598 |
| Ethanol | 548.8 | 18.22 | 603.1 | 16.58 | 0.540 | 0.537 |
| Propan-1-ol | 546.9 | 18.28 | 601.7 | 16.62 | 0.520 | 0.520 |
| Propan-2-ol | 543.8 | 18.39 | 597.9 | 16.73 | 0.480 | 0.482 |
| Butanol | 545.2 | 18.34 | 601.3 | 16.63 | 0.503 | 0.508 |
| *t*-Butanol | 537.1 | 18.62 | 590.9 | 16.92 | 0.410 | 0.407 |

[1] Literature data for π* from Kamlet and Taft[15, 41, 42].

Literature π* data and π* values obtained in this work showed a very good correlation. Due to the presence of hydrogen bonding in these solvents, equation 3.12 was used to calculate π* and α simultaneously.

$$\upsilon_{\max} = \upsilon_0 + s\pi^* + a\alpha \qquad \textbf{(3.12)}$$

The solvatochromic comparison method must satisfy certain conditions before solute-solvent hydrogen bonding interactions can be determined successfully. Firstly, a plot of corresponding $\upsilon_{max}$ values for two probes of differing hydrogen bonding ability should show a linear relationship with a statistically acceptable correlation coefficient when determined against a range of solvents of varying polarity where hydrogen bonding is excluded. This has been determined, and shown in Figure 3.13 and 3.14. Secondly, data points for those solvents that are hydrogen bond donors should be should be displaced from the regression line (in the same direction) by statistically significant amounts. This clause has also been satisfied as displayed by the displaced red line shown for protic solvents in the same figures. Finally, the direction of the displacement should be within a consistent manner of the chemical nature reflecting a reasonable order of solvent HBD strengths.

The hydrogen bond itself is an intermolecular or intramolecular interaction, which has a strength of around 20 kJ $mol^{-1}$. Its strength is comparable to a van der Waals force but a hydrogen bond has directionality which can result in discrete recognisable units made-up of two or more single molecules. Hydrogen bonds were first commented on by Latimer and Rodebush in 1920.[43] They were used to explain among other effects, the high boiling points of compounds containing the groups -OH, $-NH_2$ or >NH in relation to isomeric molecules with no hydrogen directly attached to the oxygen or nitrogen. From this initial work it was found that a hydrogen bond is an attractive interaction between two closed shell species, which is represented by the broken line in figure 3.15. Hydrogen bonding can only occur if the red spheres in Figure 3.15 are highly electronegative and small for example F, O or N, and one of which must also possess a lone pair of electrons.

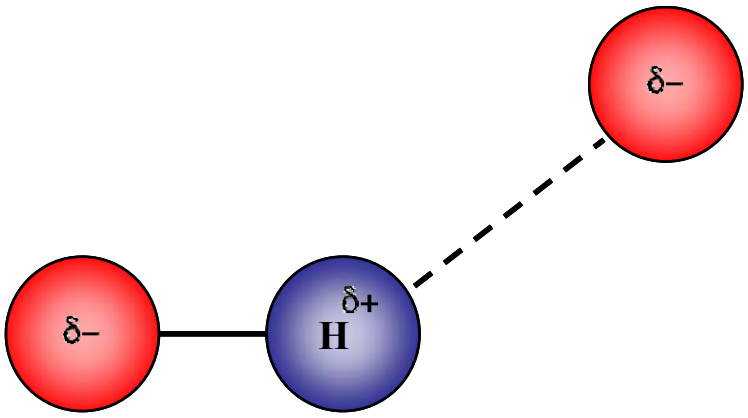


***Figure 3.15*** *Representation of a hydrogen bond*

As α has been defined as the measure of the ability of a solvent to donate a hydrogen atom towards the formation of a hydrogen bond, it is only protic and protogenic solvents that have non-zero α values. For the solvents used in this study there are 9 out of 16 solvents which have zero α values. Employing the use of only this subset of solvents would have been skewed by the non-inclusion of zero values, and would therefore result in a very different set of calculated coefficients. For this analysis, coefficients were calculated by analysis of the entire set of α values inclusive of those solvents with no HBD capability. Microcal Origin 6.0 was used to carry out a multiple regression analysis on literature π* and literature α data for solvents at

ambient pressure, and resulted in the coefficients shown in equations 3.13 and 3.14. The π* and α data are presented in Table 3.9.

*Nile Red:* $$\nu_{max} = 19.9657 - 1.0241\pi^* - 1.6078\alpha \quad \textbf{(3.13)}$$

*Phenol Blue:* $$\nu_{max} = 18.2086 - 0.9990\pi^* - 1.4883\alpha \quad \textbf{(3.14)}$$

Similarly to the NHB solvents, an overall decrease in polarisability/dipolarity was observed for each solvent on expansion with $CO_2$. Generally, shorter chain alcohols showed a more pronounced change in terms of both π* and α data. This relates well with solubility studies in alcohols where it has been shown that $CO_2$ solubility decreases in alcohols as the alkyl chain length is increased.

The observed polarity change could be due to two factors. Firstly, it could be seen as a direct result of the application of pressure to the system, and secondly, it could be due to an indirect result of a difference in density and/or composition of the liquid phase. The peak in Phenol Blue's spectrum used in this study arises from a π-π* transition in which the excited state has a dipole moment of about 2.5 debye greater than the ground state.[25] This excited state is more stabilised by polar solvents (relative to the ground state) and this results in a red shift in the dye's spectrum. This is reflected by experimental data where in pure acetone $\lambda_{max}$ occurs at 582.1 nm, and cyclohexane at 550.3 nm. When the system is pressurised, the liquid phase becomes rich in carbon dioxide and because of the nonpolar nature of $CO_2$ this significantly decreases the polarity of the resulting mixture. If a direct pressure effect was dominant, the polarity of the mixture would increase with an increase in pressure.[44]

Relatively large changes in α are also observed, with alcohols such as methanol and ethanol showing a decrease in hydrogen bond character by approximately one-third of the original values determined. Table 3.9 reports data from this work on the hydrogen bonding character of expanded alcohols. This does not correlate with the trend observed by Wyatt *et al*.[17] as they only noticed a change in α when $CO_2$ mole fractions were increased to such pressures where the expanded fluid consisted of greater than 90 % $CO_2$.

***Table 3.9*** *The change in polarity and hydrogen bonding when various alcohols were exhibited to moderate pressures of $CO_2$.*

| Expanded Alcohols Data | π* (1 bar) | π* (50 bar) | Δπ* | α (1 bar) | α (50 bar) | Δα |
|---|---|---|---|---|---|---|
| Methanol | 0.598 | 0.372 | -0.226 | 0.925 | 0.638 | -0.286 |
| Ethanol | 0.537 | 0.291 | -0.246 | 0.848 | 0.535 | -0.313 |
| Propan-1-ol | 0.520 | 0.336 | -0.183 | 0.825 | 0.593 | -0.232 |
| Propan-2-ol | 0.482 | 0.346 | -0.136 | 0.778 | 0.606 | -0.173 |
| Butanol | 0.508 | 0.439 | -0.069 | 0.810 | 0.723 | -0.087 |
| t-Butanol | 0.407 | 0.373 | -0.033 | 0.682 | 0.640 | -0.042 |

It is thought that the difference in solvatochromic characterisation between Wyatt's work and this study arise from the use of different methods of calibration. Wyatt's calibration involved the use of just two solvents, whereas this work employed sixteen solvents to build the calibration model. Small changes in calculated coefficients using the multiple regression method can result in significant changes in polarisability and hydrogen bonding character. Figure 3.16 plots the change in α seen in the protic solvents, against the change in π*. The graph obtained shows a very good linear relationship between the two parameters determined, where the calculated change in α for solvents on expansion with $CO_2$ at 50 bar is almost exactly equivalent to the change in π* for the same solvent systems. This reduction in α, means that as the solvents undergo expansion, the hydrogen bonding in the alcohols breaks down. The effect of hydrogen bond disruption is more-so in methanol and ethanol *i.e.* solvents which have a large hydrogen bond donor ability to start of with, and to a lesser extent in the weaker hydrogen bonding alcohols such as propanol and butanol.

Figure 3.17 shows the polarisability/dipolarity, π*, of a range of organic solvents and the degree to which π* changes when they are expanded with 50 bar of $CO_2$ at ambient temperature. The local polarity values were obtained with an uncertainty of ± 2 % and values obtained at ambient pressure were in good correlation with published data.[15] The raw data for this work can be found in Tables 1 to 4 in the Appendix. Results show that local polarity of all solvents decreased when expanded with $CO_2$. A lesser change in polarisability was observed for more polar

solvents, and less so for nonpolar solvents. DCM and toluene showed the largest change in polarisability when expanded with π* for DCM decreasing from 0.812 to 0.487, and π* for toluene decreases from 0.503 to 0.177, a reduction by more than half its original value for the pure liquid solvent.

All solvents when expanded resulted in a change in π* which approached that for pure $CO_2$. As carbon dioxide has a relatively low π* (for liquid $CO_2$, π* = -0.882), it would be expected that the expanded liquid would result in a local polarity to be somewhere in the region between that of the pure solvent and of $CO_2$.

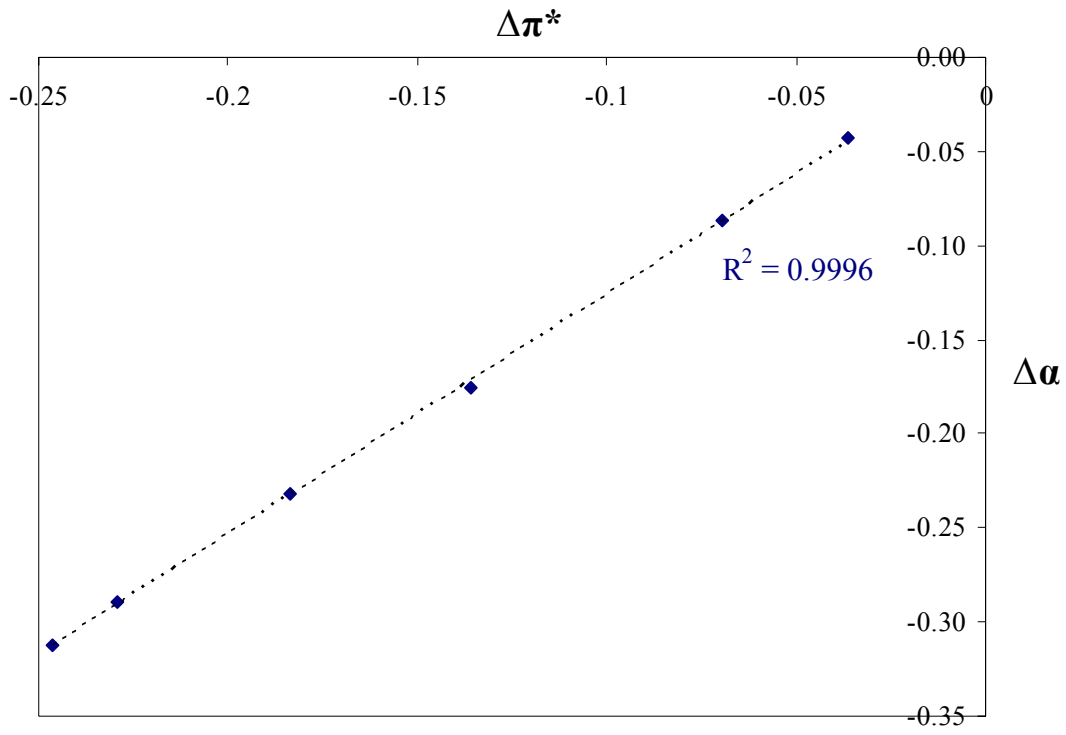


***Figure 3.16*** *Shows the linear correlation between the change in π* and α when the alcohol solvents (hydrogen bond donors) are expanded with $CO_2$ at 50 bar. The extent to which α changes on expansion is equivalent to the degree of change noticed for the π* parameter. This shows that alcohols exhibit significant changes in polarity when expanded with $CO_2$ gas, with both a reduction in the polarity/polarisability as well as a reduction in the hydrogen bonding capability of the solvent*

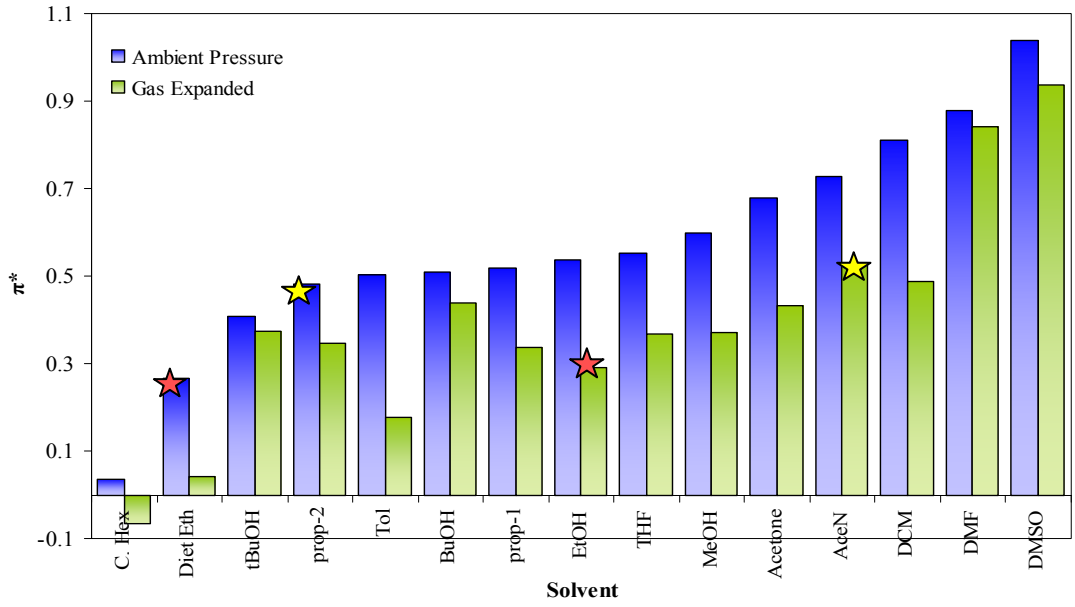


***Figure 3.17*** *The π* polarity/polarisability for a range of solvents (blue) and expanded solvents (green) when pressurised with $CO_2$ at 50 bar pressure, and 25 $^oC$. Solvents are plotted in order of increasing π*, from nonpolar cyclohexane to polar DMSO*

Where π*;

★ Expanded Ethanol ~ Diethyl Ether at ambient pressure

★ Expanded Acetonitrile ~ 2-Propanol at ambient pressure

### 3.3 Summary

Spectroscopic measurements of a range of binary mixtures of organic solvent with carbon dioxide have been recorded to calculate solvatochromic parameters for gas expanded liquids. This work has investigated two different solvatochromic methods using a single polarity scale (based on transition energies of a betaine dye) and a multi-parameter scale which looks at the dipolarity/polarisability and hydrogen bond donating acidity in terms of Kamlet-Taft solvatochromism parameters. Sixteen solvents ranging from nonpolar cyclohexane to polar DMSO were investigated for analysis by both polarity scales. The $E_T$ scale was chosen initially because of the wide spectrum range of Reichardt's $E_T(30)$ dye, but it was found that on expansion the broad spectral range was lost, and protonated solvents observed a 'bleaching' effect and so measurements for expanded alcohols were not possible due to weak or no absorption in the UV-Vis range. $\pi^*$ and $\alpha$ were determined using Kamlet & Taft's method at ambient temperature (25 ºC) and at 50 bar pressure of $CO_2$. Experimental results for the probes used, in both protic and aprotic solvents at ambient pressure were in good agreement with the literature. Data obtained for gas expanded solvents showed a significant change in polarity upon addition of $CO_2$, modifying the properties of traditional organic solvents making these mixtures more economically attractive solvents especially as the $CO_2$ is not left as a residue after depressurisation.

This work has shown that Kamlet-Taft parameters can provide a solvent strength scale that facilitates comparisons between $CO_2$ expanded traditional solvents and their un-expanded equivalents and that it is possible to devise a whole new solvent scale based on expanded liquids where this work has shown that a mixture such as $CO_2$ expanded acetone has comparable solvent polarity to that of *t*-butanol at ambient pressure and $CO_2$ expanded ethanol has an equivalent polarity to that of ether under ambient conditions. Although solvatochromic data are not completely appropriate for the determinations of solvent power or absolute solubilities, they have shown promise of providing an insight into the local solvent surroundings in both single solvents (liquid solvents) and binary mixtures (expanded solvents). To probe the cybotactic region in greater detail requires more information about $CO_2$ solubility and solvent density; this will be discussed further in the next chapter.

### 3.4 References


1. J. Badilla, C. J. Peters and J. D. Arons, *Journal of Supercritical Fluids*, 2000, **17**, 13-23.
2. S. D. Yeo and E. Kiran, *Journal of Supercritical Fluids*, 2005, **34**, 287-308.
3. P. Suppan and N. Ghoneim, *Solvatochromism*, Royal Society of Chemistry: Cambridge, 1997.
4. C. Reichardt, *Chemical Reviews*, 1994, **94**, 2319-2358.
5. E. Grunwaldt and S. Winstein, *Journal of the American Chemical Society*, 1948, **70**, 841-846.
6. L. G. S. Brooker, A. C. Craig, D. W. Heseltine, P. W. Jenkins and L. L. Lincoln, *Journal of the American Chemical Society*, 1965, **87**, 2443-2450.
7. M. E. Jones, R. W. Taft and M. J. Kamlet, *Journal of the American Chemical Society*, 1977, **99**, 8452-8453.
8. D. J. Adams, P. J. Dyson and S. J. Tavener, *Chemistry in Alternative Reaction Media*, John Wiley & Sons Ltd, West Sussex, 2004.
9. J. L. M. Abboud, R. W. Taft and M. J. Kamlet, *Journal of the Chemical Society-Perkin Transactions 2*, 1985, 815-819.
10. R. W. Taft and M. J. Kamlet, *Journal of the American Chemical Society*, 1976, **98**, 2886-2894.
11. M. J. Kamlet and R. W. Taft, *Journal of the American Chemical Society*, 1976, **98**, 377-383.
12. V. Bekarek, *Journal of the Chemical Society-Perkin Transactions 2*, 1983, 1293-1296.
13. O. W. Kolling, *Analytical Chemistry*, 1984, **56**, 2988-2990.
14. J. Figueras, *Journal of the American Chemical Society*, 1971, **93**, 3255-&.
15. M. J. Kamlet, J. L. M. Abboud, M. H. Abraham and R. W. Taft, *Journal of Organic Chemistry*, 1983, **48**, 2877-2887.
16. S. P. Kelley and R. M. Lemert, *American Institute of Chemical Engineers Journal*, 1996, **42**, 2047-2056.
17. V. T. Wyatt, D. Bush, J. Lu, J. P. Hallett, C. L. Liotta and C. A. Eckert, *Journal of Supercritical Fluids*, 2005, **36**, 16-22.
18. V. Bekarek, *Journal of Physical Chemistry*, 1981, **85**, 722-723.
19. C. R. Yonker and R. D. Smith, *Journal of Physical Chemistry*, 1988, **92**, 235-238.

20. M. Maiwald and G. M. Schneider, *Berichte Der Bunsen-Gesellschaft-Physical Chemistry Chemical Physics*, 1998, **102**, 960-964.
21. J. E. Adams, *Abstracts of Papers of the American Chemical Society*, 1994, **208**, 131-PHYS.
22. C. Reichardt, A. Blum, K. Harms and G. Schafer, *Liebigs Annalen-Recueil*, 1997, 707-720.
23. C. Reichardt and G. Schafer, *Liebigs Annalen*, 1995, 1579-1582.
24. C. Reichardt, *Pure and Applied Chemistry*, 2004, **76**, 1903-1919.
25. C. Reichardt, S. Asharinfard, A. Blum, M. Eschner, A. M. Mehranpour, P. Milart, T. Niem, G. Schafer and M. Wilk, *Pure and Applied Chemistry*, 1993, **65**, 2593-2601.
26. C. Reichardt, M. Eschner and G. Schafer, *Liebigs Annalen Der Chemie*, 1990, 57-61.
27. M. J. Kamlet, T. N. Hall, J. Boykin and R. W. Taft, *Journal of Organic Chemistry*, 1979, **44**, 2599-2604.
28. M. Barra, L. M. Croll, A. Tan and W. L. Tao, *Dyes and Pigments*, 2002, **53**, 137-142.
29. J. E. Brady and P. W. Carr, *Journal of Physical Chemistry*, 1985, **89**, 5759-5766.
30. D. Beysens and P. Calmettes, *Journal of Chemical Physics*, 1977, **66**, 766-771.
31. J. O. Morley and A. L. Fitton, *Journal of Physical Chemistry A*, 1999, **103**, 11442-11450.
32. O. W. Kolling, *Analytical Chemistry*, 1981, **53**, 54-56.
33. O. W. Kolling and J. Goodnight, *Analytical Chemistry*, 1973, **45**, 160-164.
34. J. A. Riddick, W. B. Bunger and T. K. Sakano, *Organic Solvents: Solvent Properties and Methods of Purification*, 4th edn., J. Wiley and Sons, New York, 1986.
35. D. R. Lide, ed., *CRC Handbook of Chemistry and Physics*, 84th edn., Boca Raton, 2003.
36. E. G. McRae, *Journal of Physical Chemistry*, 1957, **61**, 562.
37. J. Figueras, P. W. Scullard and A. R. Mack, *Journal of Organic Chemistry*, 1971, **36**, 3497-&.
38. O. W. Kolling and J. Goodnight, *Analytical Chemistry*, 1974, **46**, 482-485.

39. K. P. Johnston, S. Kim and J. Combes, *ACS Symposium Series*, 1989, **406**, 52-70.
40. A. P. Abbott and C. A. Eardley, *Journal of Physical Chemistry B*, 1999, **103**, 2504-2509.
41. M. J. Kamlet, J. L. Abboud and R. W. Taft, *Journal of the American Chemical Society*, 1977, **99**, 6027-6038.
42. M. J. Kamlet, P. W. Carr, R. W. Taft and M. H. Abraham, *Journal of the American Chemical Society*, 1981, **103**, 6062-6066.
43. M. R. W. Latimer W, H. , *Journal of the American Chemical Society.*, 1920, **42**, 1419.
44. S. W. Kim and K. P. Johnston, *American Institute of Chemical Engineers Journal*, 1987, **33**, 1603-1611.

# CHAPTER 4

## Physical Properties of Gas eXpanded Liquids

---



---

## 4.1 Introduction

### 4.1.1 Solubility in High Pressure Systems

Solubility is amongst one of the most important physicochemical properties of solutes dissolved in high pressure systems. Solubility data are typically presented in the form of solubility isotherms, where it is readily apparent that solubility increases rapidly at lower pressures around the critical pressure, whereas at higher pressures the increase in solubility is less pronounced. The shape of the solubility isotherm reflects changes in the density with pressure. Very little work has been carried out to investigate solubility in systems of moderate (gas expanded) pressures away from the critical point.

The ability of a sc fluid to dissolve solids was first reported more than 100 years ago by Hannay and Hogarth.[1] They studied the solubility of inorganic salts in sc ethanol. Since then, the interest in the quantitative determination of solubility has increased continuously. Several substances have been employed in the form of SCFs to carry out different processes, sc $CO_2$ is most frequently used. Over the last few decades, the solubilities of solids and liquids in sc fluids have been measured extensively.[2-8]

The most common methods employed to date for measuring solubilities are gravimetric, chromatographic and spectroscopic techniques, of which the gravimetric method developed by Eckert,[9] Paulaitis,[10] Reid[11] and their co-workers in the late 1970s is most widely used. Of these methods, previous experience in the Abbott group has suggested that online spectroscopic techniques give the most meaningful data but they can only be used if the solute has one or more absorption bands in the UV-Vis-IR wavelength ranges, which can be used to determine its concentration. Implementation of these techniques is sometimes problematic and can meet certain experimental difficulties. Gravimetric methods resulted in aerosol formation, and the sensitivity of the method was poor. Furthermore, relatively small changes in pressure frequently vary the solubility by several orders of magnitude, which complicates the measurements.

A suitable experimental technique for the measurement of solubility in expanded systems needs to be fast, simple and precise. Previous researchers have used dielectrometry as the approach to measure the solubility of compounds in pressurised systems.[12, 13] This technique has the advantage that it can be used when solubilities are

high (> $10^{-3}$ mol $dm^{-3}$) or if the solution is turbid. This method is also capable of relating solid solubility to the local and bulk properties of the solvent.

Solubility is measured as a function of the expanded liquid, the solute, the temperature, and the pressure. In order to reduce the parameters, several procedures have been adopted to describe and correlate the solubility (or enhancement factor) of solutes in both expanded liquids and sc fluids and their changes with temperature and density. Equations of State (EOS) are frequently used to describe the change of solubilities with thermodynamic parameters because of their diversity.

### 4.1.2 Relative Permittivity

As seen in Chapter 3, on a microscopic level, solvatochromic shift data present information on local solvation in the cybotactic region of a solute molecule, and can therefore be directly compared with properties such as the free energy of a solute in a given solvent. However, knowledge of its macroscopic electronic properties is required before a solvent can be employed in a chemical context. The relative permittivity is a fundamental property of the bulk solvent, essential to the quantification of solute-solvent and solute-solute interactions.

The relative permittivity, $\varepsilon_r$ (also known as dielectric constant, $\varepsilon$) plays a particularly important role in the characterisation of solvents. It stands out over other criteria due to the simplicity of electrostatic models of solvation, and hence, it has become a useful measure for solvent polarity. For a dielectric material in a ground state, electrons are bound to their parent atoms and are fixed to their equilibrium positions.

Relative permittivities are determined by analysing the impedance of a solvent between two parallel plates of a capacitor. If solvent molecules do not have permanent dipoles of their own, then dipoles will be induced by the external field which will separate the charge within the molecules. Thus, molecules with charged or induced dipoles are forced by the charged plates into an ordered arrangement, leading to the *polarisation* as shown in Figure 4.1. The greater the extent of polarisation, the larger the drop in electric field strength. The relative permittivity is, therefore, representative of the ability of a solvent to separate charge and to orientate its dipoles.

As this behaviour is comparable to the orientation of the solvent around an electrolyte, the relative permittivity is a good indicator of the ability of a solvent to dissolve ionic compounds. Solvents with large relative permittivity's usually act as dissociating solvents and are called polar solvents as opposed to apolar or nonpolar solvents which exhibit low relative permittivities. Dielectric properties often run in accordance with the solvent power of the solute, in the case of ionic solutes, solvents with a high dielectric facilitate dissolution by separating the ions.

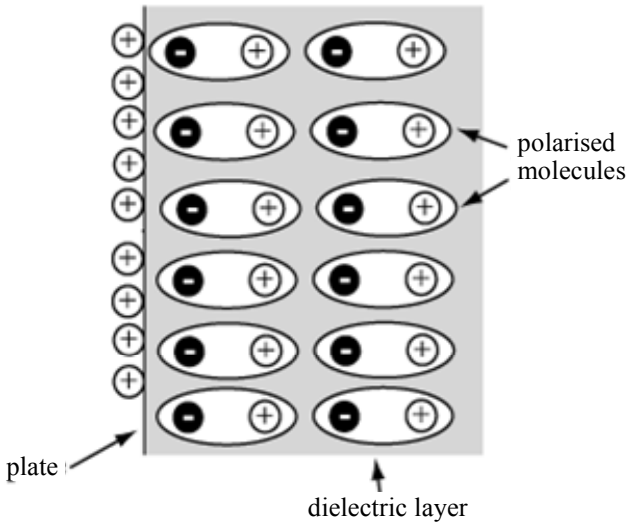


***Figure 4.1*** *Reduction of the effective charge on a capacitor plate by lining-up polarised dielectric molecules*

Experimentally, the relative permittivity is measured relative to the effect of the same applied field when placed in a vacuum, the equation for which is shown below.

$$\mathcal{E} = \mathcal{E}_r.\mathcal{E}_0 \qquad \textbf{(4.5)}$$

Where; $\varepsilon_0$ is the permittivity of free space, measured in farads per metre, and $\varepsilon_r$ is the relative permittivity of the insulator used. The relative permittivity is then the ratio of the natural permittivity of the material ($\varepsilon_r$) to the permittivity of free-space ($\varepsilon_o$). It is seen to be a direct measure of the polarisability of a material and will govern both the phase variation and attenuation of an imposed field in the material.

### 4.1.3 Measurement of Relative Permittivity

Capacitance (C, measured in Farads) is a measure of the amount of charge (Q, measured in coulombs) stored on each plate of a capacitor for a given potential difference or voltage (V, measured in volts) which appears between the plates where:

$$C = \frac{Q}{V} \tag{4.6}$$

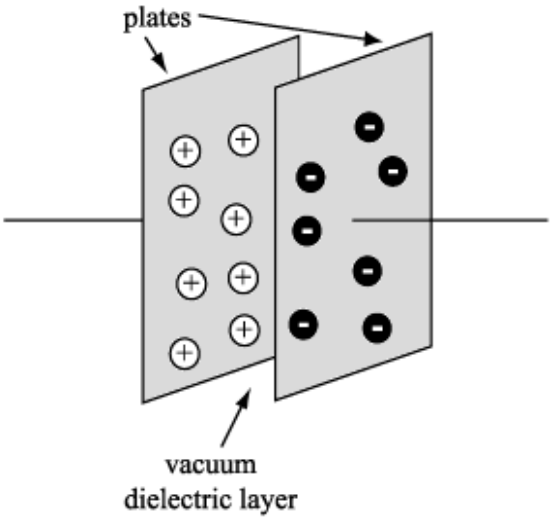


***Figure 4.2*** *A parallel plate capacitor*

Capacitance exists between any two conductors insulated from one another. The above equation used to calculate capacitance is only valid if the conductors have equal but opposite charge, $Q$, and the voltage, $V$, is the potential difference between the two conductors. The capacitance is directly proportional to the surface areas of the plates, and is inversely proportional to the separation between the plates as shown in Figure 4.2. It is also very dependent on the dielectric of the material. Dielectric materials are rated based upon their ability to support electrostatic forces. The higher the relative permittivity the greater the ability of the dielectric to support electrostatic forces. Therefore, as the relative permittivity increases, capacitance increases.

The relative permittivity, $\boldsymbol{\varepsilon_r}$, is measured via capacitance, $\boldsymbol{C}$ such that the measured capacitance is given by:

$$C = \varepsilon C_0 \qquad \textbf{(4.7)}$$

where $C_0$ is the capacitance of a vacuum. If the geometry of the conductors and the dielectric properties of the insulator between the conductors are known, capacitance can be calculated. In the case of a parallel-plate capacitor:

$$C = \varepsilon_0 \varepsilon_r \frac{A}{d} \qquad \textbf{(4.8)}$$

where: C is the capacitance in farads

A is the area of each plane electrode, measured in square metres

d is the separation between the electrodes, measured in metres

### 4.1.4 The Dielectrometry Technique

Previous research carried out in the area of solubility techniques utilised the dielectrometry technique. It was used to measure the solubility of polar solutes in sc fluids.[14, 15] Polar solutes cause a change in the relative permittivity of the medium and the extent of this relative permittivity change with respect to the pure solute (at the same temperature and pressure) can be related to the solute concentration and hence its solubility. It is a simple method to use, inexpensive and allows for direct *in situ* measurements of solute solubility in pressurised fluids.

So far, very few cases have applied this technique for solubility measurements in high pressure reaction media. Leeke *et al.* have used a cloud-point technique to verify data obtained using the dielectrometry method for solubility determinations of phenylboric acid, iodobenzene, and biphenyl in carbon dioxide at 353 and 383 K and between pressures of 100 to 300 bar.[16] Kordikowski *et al.*[17] reported volume expansion and vapour liquid equilibria of binary mixtures of polar solvents and near critical solvents. They obtained bubble point curves, density, volume and composition data for a variety of near-critical solvents. They expanded six different solvents with $CO_2$ and ethane. Their studies found that plotting volume expansion versus mole fraction for each solvent system resulted in the same result.

Chang and Randolph have also studied solvent expansion and solute solubility prediction in GXLs.[18] They determined the expansion behaviour of two binary systems in the miscible liquid-phase region, while relating this to partial molar

volume change for each component in the liquid phase. They then went on to look at solute solubility in expanded systems relating to the GAS process. Lazzoroni[19] and colleagues reported vapour-liquid equilibria, molar volume, and volume expansion for several binary mixtures of organic solvent with $CO_2$ as a function of temperature and pressure. The solubility of $CO_2$ in these solvents was explained by consideration of the interaction of $CO_2$ in solution. Benzene was compared with THF, but THF exhibited a greater $CO_2$ solubility. It was assumed that $CO_2$ acted as a Lewis acid and could interact with the basic ether functionality of THF and less so with the aromatic ring of benzene. Despite the zero net dipole moment of $CO_2$, its high solubility in polar solvents is an attribution of its quadrupolar character.

Other literature published in the area includes monitoring the solubility of $CO_2$ as a function of pressure for various solvents,[17] and an insight into the ability to alter the physicochemical properties (polarity, dielectric and gas solubility) of a liquid solvent on expansion.[20]

Reighard and colleagues studied the phase behaviour of methanol and $CO_2$ mixtures at temperatures between 25 °C to 100 °C, and pressures of 3 to 20 MPa.[21] The range of methanol mole fractions where high pressures are required to form and maintain a single phase was found to be between 0.5 and 0.7.

Further research on expanded methanol systems included those reported by Smith *et al.* They investigated the dielectric properties of methanol and $CO_2$ mixtures at 40 to 50 °C and at a pressure of 11 MPa.[22] An increase in relative permittivity was found as the mole fraction of methanol was increased. It was summarised that $CO_2$ had an initial effect on the methanol hydrogen bond networks which inhibited dipole movement through strong dipole-quadrupole interactions that were later weakened for higher molar concentrations of $CO_2$.

## 4.2 Results and Discussion

### 4.2.1 Calibration of Dielectrometry Technique

Firstly, before any new relative permittivity measurements were obtained, it was necessary to test the validity of the dielectrometry technique to determine accurate and reliable data. The relative permittivity of water was measured at ambient pressure and at variety of temperatures and the data were compared to values reported in the literature. One of the anomalous properties of water is the unusually high relative permittivity ($\varepsilon_r$ = 78.4 at 25 °C). Figure 4.3 shows the change in relative permittivity of water as a function of temperature. The reported relative permittivity reading is the average of five replicate readings where results were found to vary by no more than ± 0.03.

The general trend shows that as the temperature is increased the relative permittivity decreases. At temperatures greater than 86 ºC, water has dielectric properties comparable to that of formic acid at room temperature ($\varepsilon$ = 58.5). Normally, in an applied electric field, polar molecules tend to align themselves with the field. Although water is a polar molecule, its hydrogen-bonded network tends to oppose this alignment. Because of its exceptional cohesive properties, water has a high relative permittivity. On cooling, the dielectric of liquid water climbs to 87.9 at 0 °C.[23] The relative permittivity similarly reduces if the hydrogen bonding is broken by other means such as strong electric fields.

The change in dielectric with temperature gives rise to considerable and anomalous changes in its solubilisation and partition properties, and so the physical properties of water are very dependent on the operating temperature. A good agreement between the data reported here, and that found in the literature confirms the validity of this technique as a suitable model to measure capacitance and determine the relative permittivity for other solvents. The values for water reported here are slightly lower than those previously reported,[23] however, the difference lies within experimental uncertainty in $\varepsilon$.

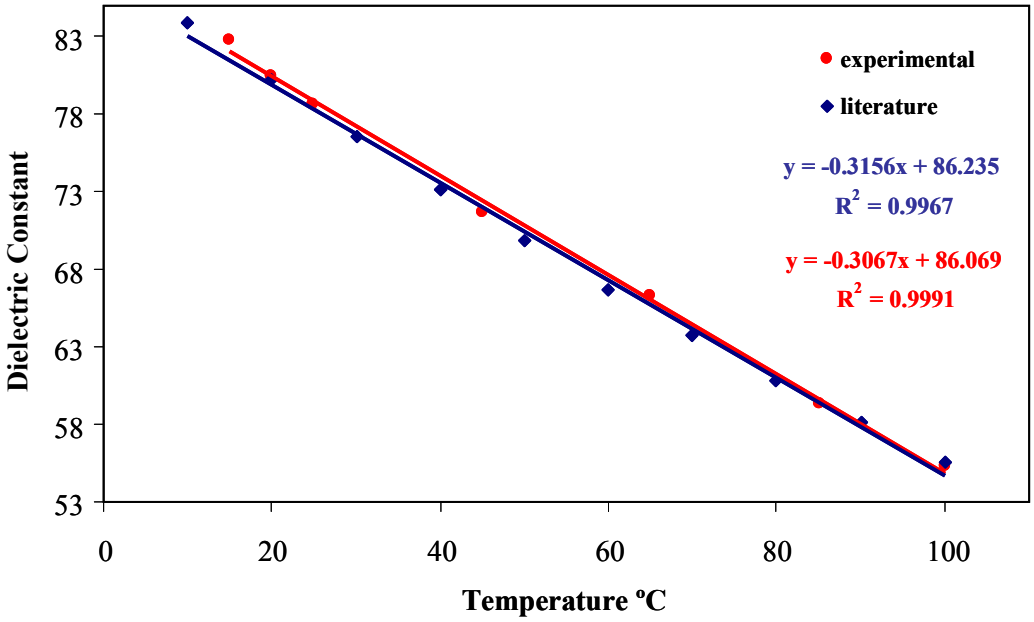


***Figure 4.3*** *Comparison of experimental and literature data[23] for the change in relative permittivity of water as a function of temperature.*

### 4.2.2 Screening of Gas Expanded Solvents

$CO_2$ has a small polarisability and no dipole moment, so additives increase the polarisability of the solvent (refractive index) and the dielectric. Polar cosolvent molecules also interact with functional groups on solutes. The dissolution of $CO_2$ into liquid organic solvents allows a rapid change in polarity from polar to nonpolar media simply by the application of moderate pressure of $CO_2$. Cosolvents may increase solubilities up to an order of magnitude, although enhancement is dependent on cosolvent concentrations. A range of organic solvents from nonpolar cyclohexane to polar DMSO were analysed using the dielectrometry technique. The cell capacitance was measured for each solvent and plotted against relative permittivity values reported in the literature. These calibration graphs was then used to calculate the relative permittivity of the $CO_2$ expanded solvents. The change in capacitance between the liquid solvent and its expanded equivalent was recorded and converted to the dielectric scale.

Figure 4.1 shows the relative permittivity, $\varepsilon_r$, of a range of organic solvents and the degree to which ε changes when they are expanded under 50 bar of $CO_2$ at ambient temperature. The relative permittivity values were obtained using the method outlined in Section 2.3.2 with an uncertainty of ± 2 %. The raw data are listed in Tables 5 and 6 in the Appendix. Values obtained at ambient pressure were in good correlation with published data.[24] Results show that the relative permittivity of all solvents decreased when expanded with $CO_2$. A greater change in relative permittivity was observed for more polar solvents, and less of a change for nonpolar solvents. DMSO showed the largest change in relative permittivity when expanded with its relative permittivity decreasing from 49 to 21, a reduction by more than half its original value for the pure liquid. All solvents when expanded resulted in a change in relative permittivity which approached that for pure $CO_2$. As carbon dioxide has a relatively low relative permittivity (for liquid $CO_2$, $\varepsilon_r = 1.6$),[25] it would be expected that dissolution of $CO_2$ into the solvent would change the relative permittivity of the mixture to be somewhere in the region between that of the solvent and of $CO_2$.

The bulk polarity of all solvents changed quite significantly, as seen in the three examples in Figure 4.4. The $\varepsilon_r$ of $CO_2$ expanded acetone is equivalent to that of unexpanded THF; the $\varepsilon_r$ of $CO_2$ expanded DMSO with liquid propan-2-ol and the ε of $CO_2$ expanded DCM with pure *t*-butanol. The relative permittivity of the binary mixture is dependent on the mole fraction of $CO_2$ present in the expanded phase.

The dissolution of $CO_2$ into liquid organic solvents to generate expanded liquids results in significant changes in the polarity of a solvent medium. Technologically, this permits an almost instant shift in polarity from polar to nonpolar media simply by adding moderate pressures of $CO_2$. Traditionally, solvents are selected to have dielectric properties that help to maximise solubility of the reagents and/or catalyst and also improve the rate of the desired reaction. The results reported above, show that a wide-range of dielectric properties can be achieved by forming GXLs where Figure 4.4 demonstrates that a solvent such as DMSO can be instantly tuned to have dielectric properties similar to that of propan-1-ol.

These mixed systems can be tuned even further by simply varying the relative amount of each component in the mixture allowing a wide spectrum of dielectric properties. These solvents could potentially be used to replace undesirable pure

solvents but in most cases, the mixture compositions provide beneficial properties compared to the pure solvent because of enhanced mass transport.

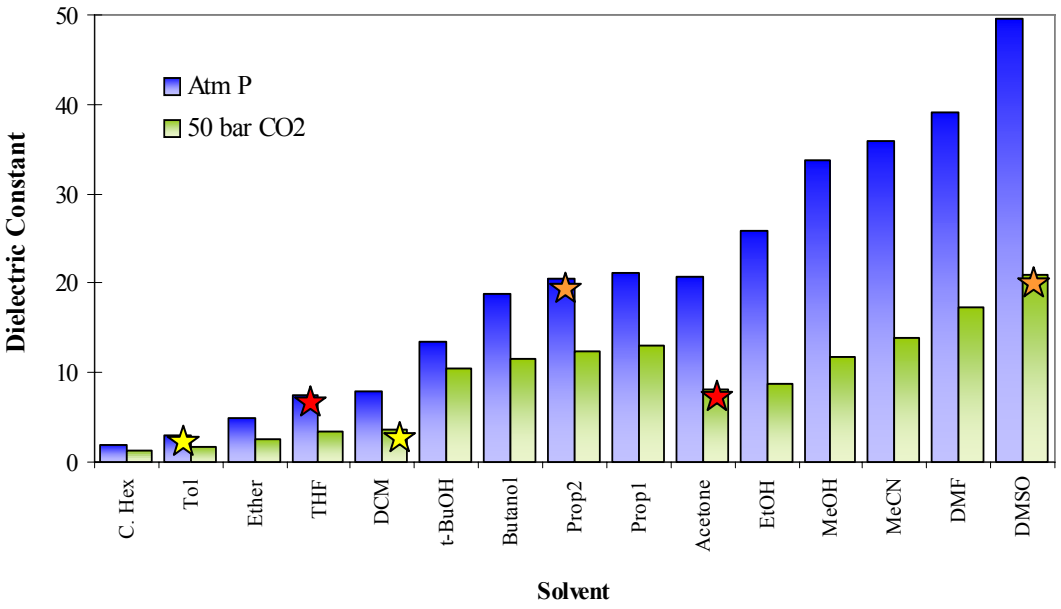


***Figure 4.4*** *The relative permittivity for a range of solvents (blue) and expanded solvents (green) when pressurised with $CO_2$ at 50 bar pressure, and 25 $^oC$. Solvents are plotted in order of increasing dielectric polarity, from nonpolar cyclohexane to polar DMSO*

Where;

★ Expanded Acetone ~ THF at ambient pressure

★ Expanded DMSO ~ 2-Propanol at ambient pressure

★ Expanded DCM ~ Toluene at ambient pressure

While there is potential that solvents such as acetone or ethanol could replace more toxic solvents such as DCM, it is the chemical reactivity that generally controls solvent selection. The potential replacement of other solvents may come from the reduced volume of solvent, although this is naturally at the expense of process complexity.

The limited solubilities of most compounds in $scCO_2$ have led to their modification by the use of cosolvents such as methanol and acetone. Fedetov and Hourri showed that supercritical systems with added cosolvents also have the benefits of improved mass transfer and enhanced solvent power.[26] However, in comparison to cosolvent modified sc $CO_2$, GXLs are able to cover a wider range of solvent properties. The distinction lies in the different 'roles' of $CO_2$ in each pressurised system. In SCFs the solvent power is dependent on the solubility of liquid cosolvent in $CO_2$, whereas with GXLs, the limitation arises from the solubility of $CO_2$ in the liquid solvent. Thus $CO_2$ acts as a 'solvent' in SCFs, but more like a 'solute' in GXLs.

### 4.2.3 Solvation Effects and Correlation with Local Polarity

Solvents are primarily a 'bulk medium'; the dielectric properties of the solvent are of primary importance and can be determined through continuum solvation models to calculate the Gibbs free energies of solvation $\Delta G_{sol}$ of charges, dipoles, and quadrupoles in polarisable media. The free energy of solvation is determined by equation 4.9.

$$\Delta G_{sol} = \Delta G_{elec} + \Delta G_{vdw} + \Delta G_{cav} (+ \Delta G_{hb}) \qquad \textbf{(4.9)}$$

Where; $\Delta G_{elec}$ is the electrostatic energy of interaction

$\Delta G_{vdw}$ is the Van der Waals interaction between solute and solvent

$\Delta G_{cav}$ is the free energy of formation for a cavity in the dielectric medium

and, $\Delta G_{hb}$ is an explicit hydrogen bonding term

The local electric field in a liquid assembly of permanent dipoles was defined by Onsager in 1936.[27] It was approximated that a point dipole occupying a spherical cavity polarises the surrounding dielectric continuum giving rise to an electric field which in turn will act on the charge distribution inside the cavity. It has been shown

previously[28] that the reaction field, ***R***, created by an electrostatic field of polar molecules surrounding a solute can be determined using

$$R = \frac{2(\varepsilon_r - 1)\mu_G}{(2\varepsilon_r + 1)a^3} \qquad \textbf{(4.10)}$$

Where; $\mu_G$ is the dipole moment of the solute in the ground state, and *a* is the radius of the cavity occupied by the solute. If the reaction field is accountable for the stabilisation of the excited state of the indicator solute, then it is possible to correlate the Kirkwood function, $(\varepsilon_r\text{-}1)/(2\varepsilon_r+1)$ with π*. Figure 4.5 shows that there is a good correlation between these two parameters for the alcohols, however this is less valid for NHB solvents. This is analogous to the trends seen with the analysis of the solvatochromism data in Chapter 3 where the alcohols were always noticeably displaced away from the general trend of the aprotic solvents.

A strong correlation between the π* scale of solvent polarity and the Dimroth-Reichard $E_T$ scale of polarity exists.[29] However, plotting $E_T$ values against the Kirkwood function shows a better, though non-linear, correlation between the two functions. Figure 4.6 shows that the entire range of solvents correlate well with the dielectric function. The difference in Figure 4.5 and 4.6 arises from the fact that $E_T$ values are based on a single-parameter solvent scale and thus do not probe hydrogen bonding as a separate factor. The displacement of hydrogen bonding solvents seen in Figure 4.5 where π* is plotted is therefore not observed in Figure 4.6.

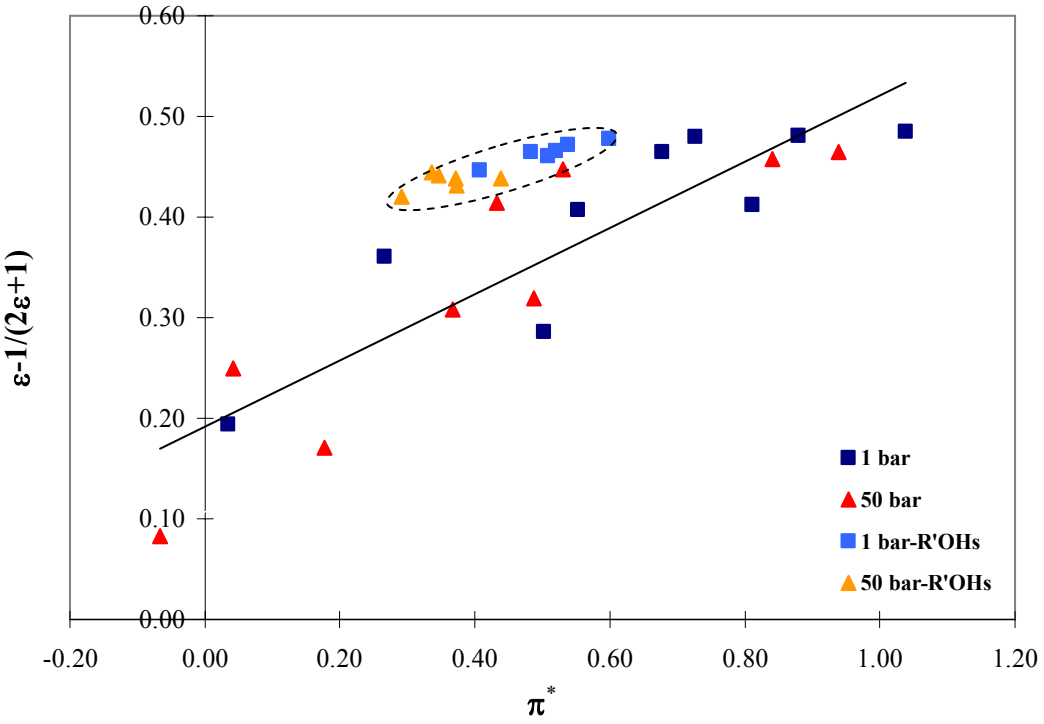


***Figure 4.5*** *Correlation between polarisability, π* and the Kirkwood function (ε-1)/(2ε+1)*

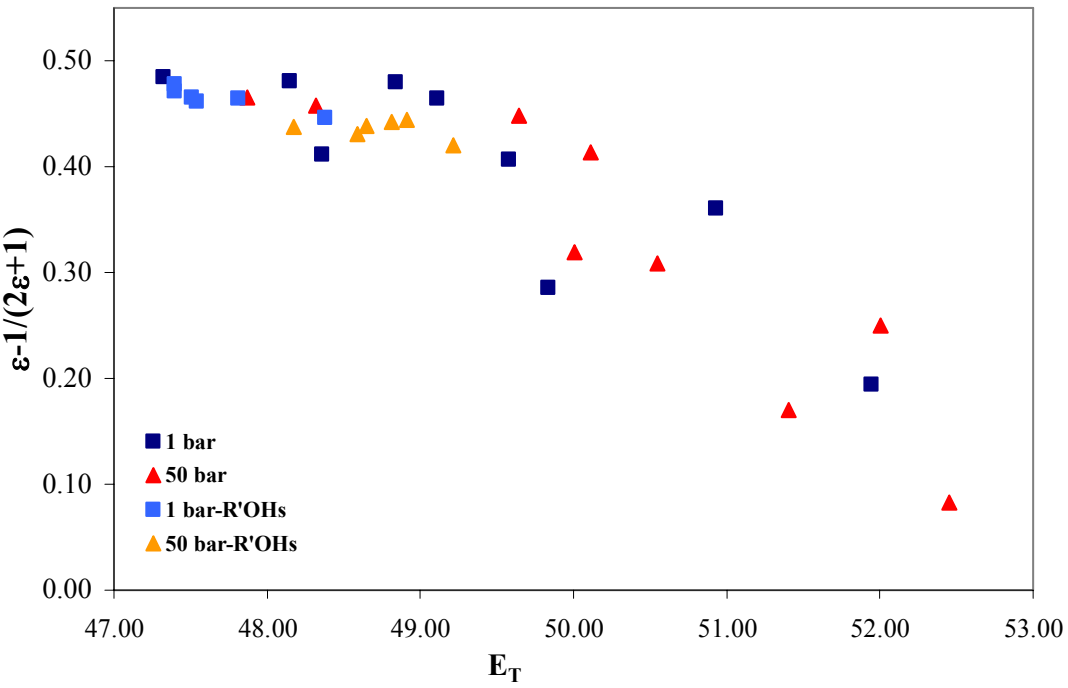


***Figure 4.6*** *Correlation between Reichardt's $E_T$ polarity scale and the Kirkwood function (ε-1)/(2ε+1)*

Figure 4.7 shows the correlation between the $E_T$ parameter and the experimental relative permittivity for all 15 solvents studied. The $E_T$ parameter is a single parameter polarity scale which allows hydrogen bonding properties to be incorporated allowing for a direct comparison of local (solvatochromic) and bulk (dielectric) properties. The trend shown in Figure 4.7 suggests that the relative change in $\pi^*$ upon expansion is to a much lesser extent than the change in relative permittivity. This implies that the degree to which $CO_2$ modifies the polarity of a solvent locally is much greater than that measured in the bulk of the solvent. In studies where polar cosolvents were added to $scCO_2$ it was found that a higher concentration of polar constituent was present around the indicator solute. It is logical to assume that the same phenomenon (preferential solvation) occurs in a GXL. The extent of $CO_2$ inclusion in the cybotactic region will depend upon the polarity of the expanded solvent more than the solubility of $CO_2$.

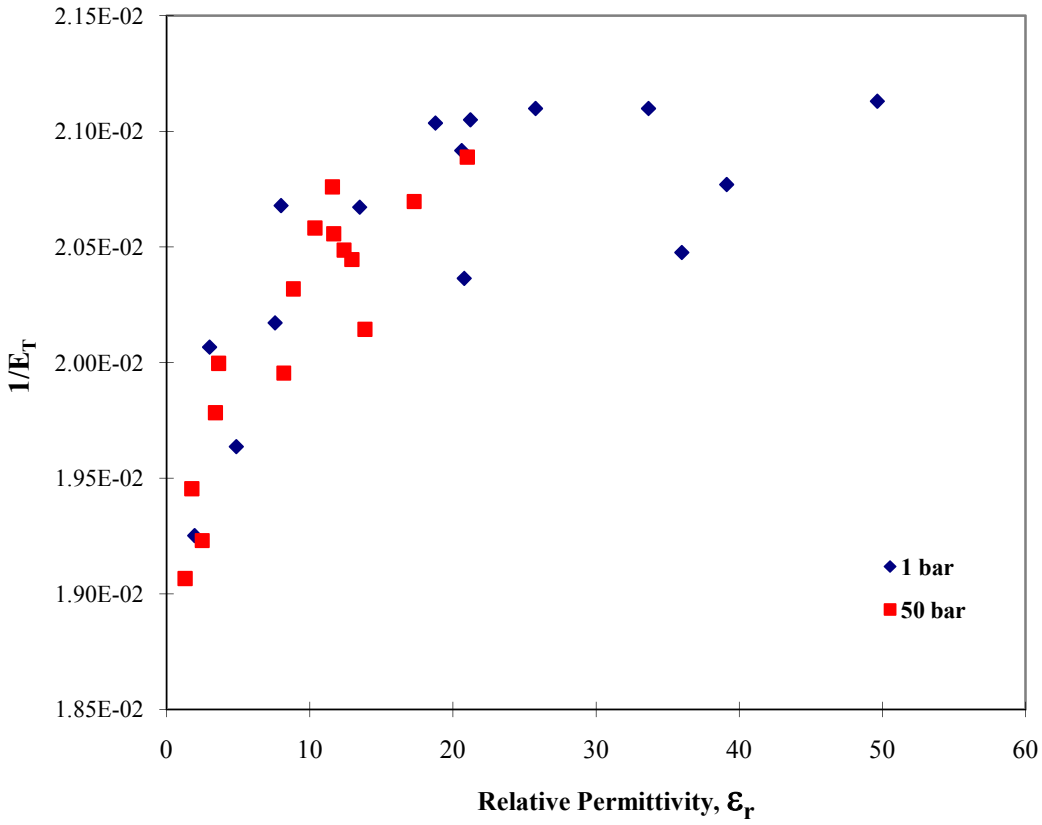


***Figure 4.7*** *Plot of $1/E_T$ versus ε for all solvents under ambient and $CO_2$ expanded pressures*

### 4.2.4 Solubility of $CO_2$ in liquids

The solubilities of various gases in liquids have been actively studied both experimentally and theoretically. $CO_2$ solubility in organic solvents has been reported by various authors.[30-32] Currently, there is no general method for which gas solubility can be predicted.[33] Previous methods provide a general procedure for predicting values of solubility as some necessary intermolecular parameters are unknown for most cases and models are usually empirically based utilising correlation and factor analysis. Several authors have encompassed a semi-empirical approach based on regular solution theory which despite certain limitations has become well accepted.[32, 34-41] Methods employing a more rigorous approach such as those by Pierotti and Goldman[42-45] have not provided sufficiently accurate predictions of solubility data even when intermolecular potential parameters are available.

In terms of solubility determination, carbon dioxide appears as a notable exception for the calculation of gas solubilities. Compressed $CO_2$ solubilises into an organic solvent the liquid expands volumetrically, which results in the formation of a GXL. Not all solvents expand to the same extent when subjected to the same pressure of $CO_2$, and the differences result from the varied solubility of $CO_2$ in the liquid solvents. Large discrepancies have been reported between experimental and calculated solubilities of $CO_2$.[45] Katayama *et al.*[46] found that strongly to moderately polar solvents showed a greater degree of $CO_2$ dissolution than that predicted by most theories. The unique behaviour of $CO_2$ in polar solvents is thought to be attributed to the fact that, although the molecule does not possess a permanent dipole moment, it does however have a large quadrupole moment.

So far, the dielectrometry technique has only been applied in a few cases for solubility measurements in sc $CO_2$. Fedotov *et al.* initially measured the solubility of a number of polar compounds in sc $CO_2$ such as acetonitrile, acetone, and manganese cyclopentadienyltricarbonyl as a function of pressure.[12, 13] Hourri and co-workers have also used this method to measure the solubility of naphthalene in sc $CO_2$ as a function of temperature and pressure, and have compared their results to published data.[14] Their results showed a good agreement to better than 4 % of those published previously.

More recently, Durling *et al.* have reported the first solubility measurements of a number of *p*-benzoic acids and *p*-phenols in difluoromethane.[15] Their work

confirmed that the previously proposed dielectrometry method for measuring solubilities was also successful in determining solubilities in sc HFC 32. The limitations often coupled with the use of other commonly employed solubility measurement techniques were not observed. The method was described as a quick, simple and precise *in situ* technique that could be applied in different pressurised solvents to measure the solubility of both polar and nonpolar liquid and solid solutes. The solubility of $CO_2$ in expanded solvents was calculated using data obtained from the dielectrometry method earlier in this chapter.

$$\varepsilon_{mix} = \varepsilon_{CO_2} X_{CO_2} + \varepsilon_{solv} X_{solv} \qquad \textbf{(4.11)}$$

Where; $\varepsilon_{mix}$ is the relative permittivity of the expanded solvent, $\varepsilon_{CO_2}$ is the dielectric for pure $CO_2$ at 50 bar, $X_{CO_2}$ is the mole fraction of $CO_2$ in the expanded mixture, $\varepsilon_{solv}$ is the dielectric of the pure liquid solvent, and $X_{solv}$ is the mole fraction of liquid solvent in the expanded mixture.

Figure 4.8 shows the calculated solubility of $CO_2$ in different expanded solvents. Addition of $CO_2$ at 50 bar pressure shows a varying degree of solubility in the range of solvents studied. This is the first time that this technique (dielectrometry) has been used to determine gas solubilities in liquids. Most of the solvents pressurised show a high extent of $CO_2$ dissolution. $CO_2$ was determined to be most soluble in cyclohexane which, when expanded fully was composed of almost 75 % $CO_2$, the poorest solubility was mostly in the alcohols, namely *t*-butanol (~25 %), and *n*-butanol (~40 %). Conversely, the higher alcohols such as methanol and ethanol showed a relatively large change in relative permittivity when expanded, hence $CO_2$ solubility is relatively high and the percentage of pure alcohol in both expanded solvents is less than one third of the mole fraction. This provides a very different picture for GXLs where for most systems the polar solvent is the minor component. GXLs are in fact more comparable to sc fluids than a condensed liquid.

Comparing mole fraction data with the analysis of local polarity from Chapter 3, it is possible to deduce that gas expansion has a relatively small effect on the $\pi^*$ of solvents. In DMSO for example, the dielectrometry method calculates that at 50 bar expanded DMSO contains approximately 60 % $CO_2$. Literature values for DMSO at

ambient pressure are reported as having a π* of 1.0, whereas the measured π* for expanded DMSO was determined in Chapter 3 to be 0.938 at 50 bar. Considering that $CO_2$ has a π* of -0.882 at 50 bar, and that the expanded solvent consists mostly of $CO_2$, a much greater reduction in local polarity would be expected when the solvent is $CO_2$ expanded. The same discrepancies are observed for all the aprotic solvents studied.

Figure 4.9 shows that there is no correlation between the change in relative permittivity and the change in π* on expansion. This is because the two parameters measure different aspects of the solution properties. Solvent structure is influenced by intermolecular forces. Relative permittivity results have shown that the bulk solvent properties are changed to a greater extent to that observed locally through π* measurements. This can be explained schematically in Figure 4.10. Preferential solvation is a local enrichment of the solvation shell in the more polar component. Figure 4.10 shows the aggregation of solvent molecules in the cybotactic region to give the impression that a solute ($CO_2$) is in a solvent-rich environment, whereas in reality there are just as many (if not more) $CO_2$ molecules around.

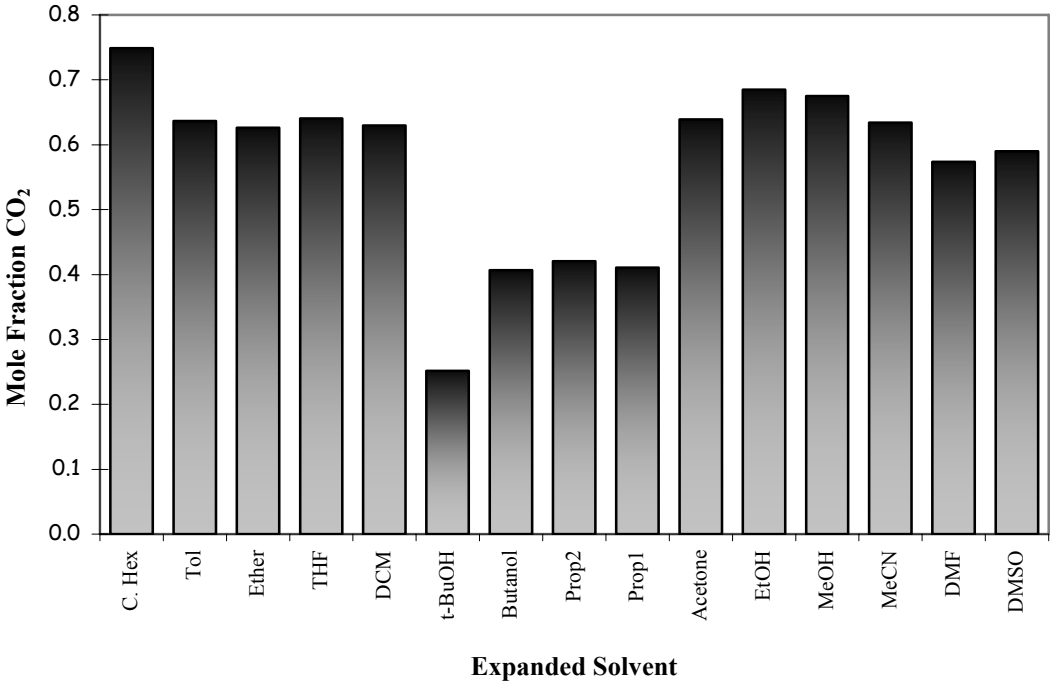

***Figure 4.8*** *Solubility of $CO_2$ at 50 bar in a series of expanded solvents. Solvents are plotted in order of increasing dielectric polarity*

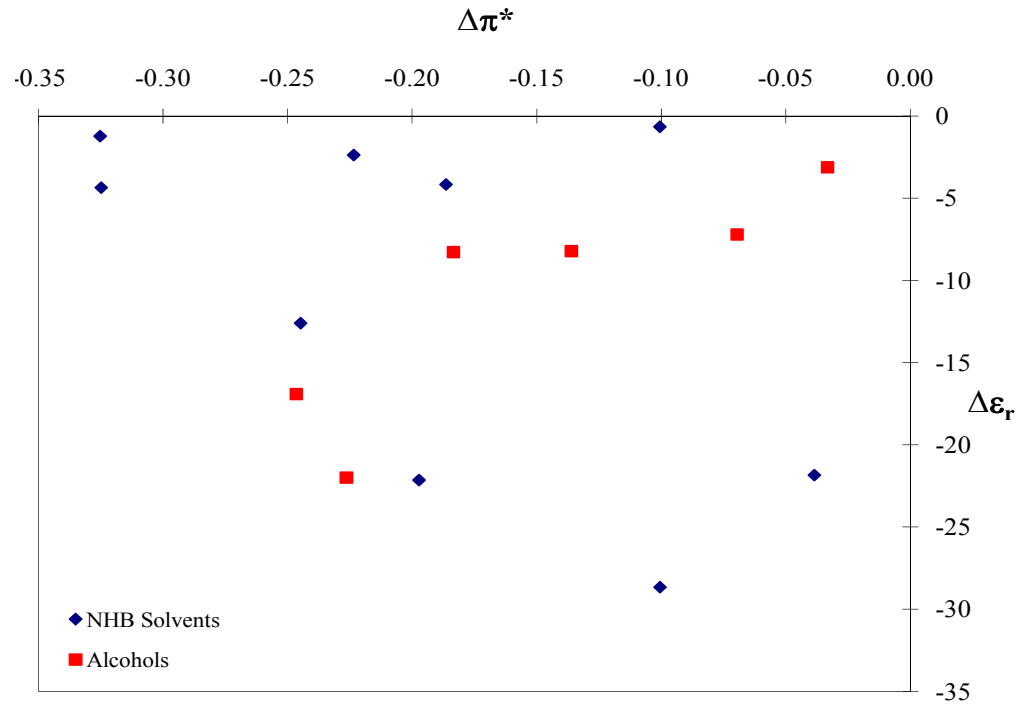


***Figure 4.9*** *Change in local polarity versus change in bulk polarity. The difference in local polarity, and bulk polarity between the expanded solvents and their un-expanded equivalents*

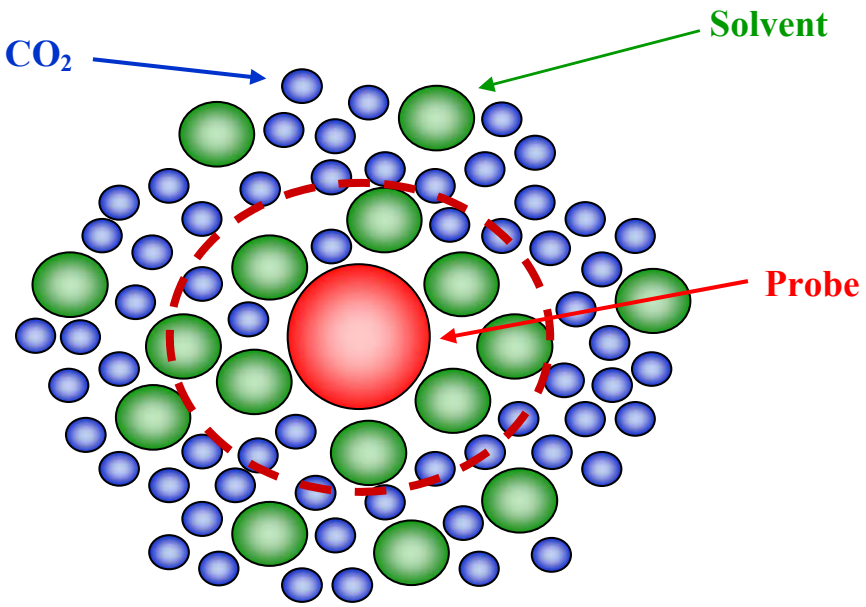

***Figure 4.10*** *Preferential solvation around the cybotactic region*

This explains why relative permittivity data for the solvents on expansion show a greater degree of change as they represent an average of the whole liquid, whereas the solvatochromic method only probes the solvation sheath around the solute molecule, and so when preferential solvation is observed, the liquid solvent properties are maintained even at pressure, and $CO_2$ merely acts as a diluent.

Generally, the role of the solute 'probe' is to perturb the system in which it is being placed, however, it is also possible that if this disturbance is of a significant extent, the solute molecule ceases to act as the 'probe' but instead establishes its own local environment which can be quite different from the bulk of the mixture. This has been encountered for both pure and modified $scCO_2$. Figure 4.11 correlates the relative permittivity of the expanded solvent with its mole fraction of $CO_2$. It is interesting to note that there is a linear correlation between the aprotic solvents, although protic solvents (namely higher alcohols) are outliers in this trend. This is comparable to the data presented in Figure 4.5, and the work discussed on solvatochromic behaviour of alcohols in Chapter 3.

Figure 4.12 demonstrates the correlation between the relative changes in relative permittivity for an expanded solvent as a function of the relative permittivity of the un-expanded liquid. There appears to be a bigger step change for nonpolar solvents, than for polar solvents. This could be expected since in general 'like dissolves like'. Non polar solvents have low relative permittivity's more close to that of pure $CO_2$, allowing for greater dissolution of the gas. This can result in a larger relative change in properties due to increased mole fractions of $CO_2$ gas in the expanded solvents. Polar solvents are less likely to solubilise $CO_2$ to the same extent and thus, the relative change in polarity remains fairly constant for solvents with a relative permittivity between 15 and 50.

The above discussion assumes that the packing of solvent around the solute is relatively constant and that the inclusion of $CO_2$ does little to disturb this. Clearly the solvents all have different packing densities and this is ultimately affected by the inclusion of $CO_2$. To gain a greater insight into the system it is necessary to probe the system densities.

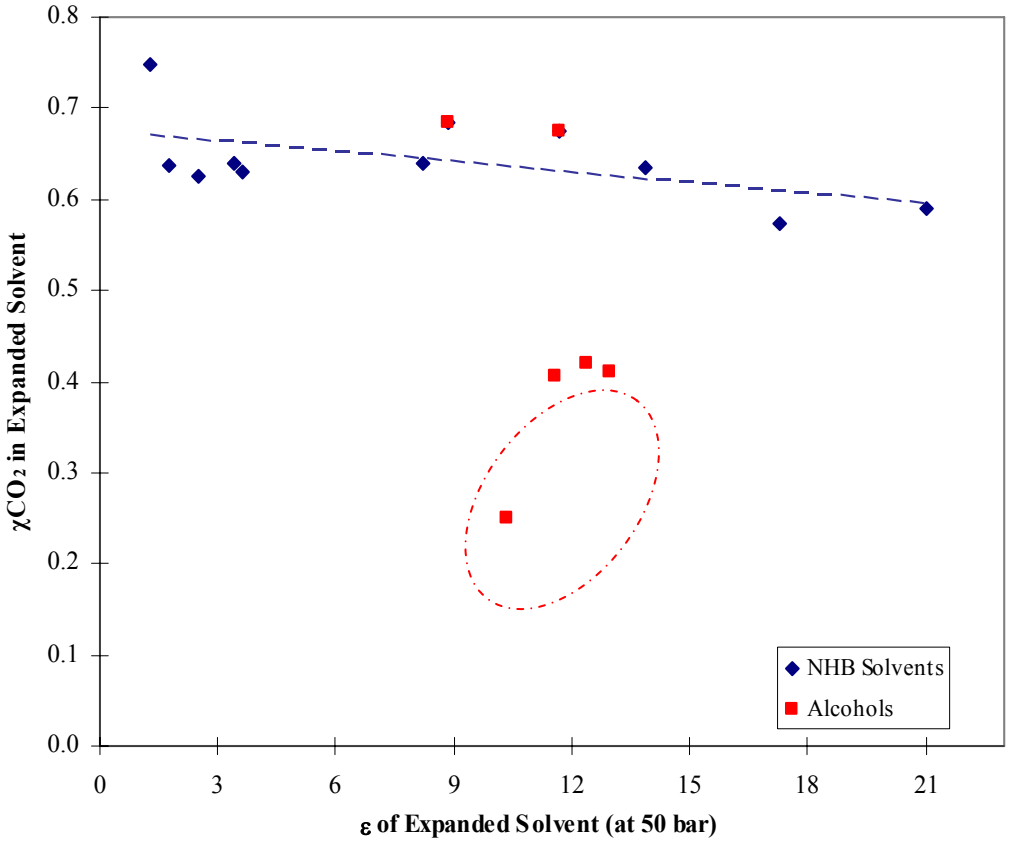


***Figure 4.11*** *Mole fraction of $CO_2$ in the expanded solvent as a function of relative permittivity at 50 bar pressure. The blue dotted line shows the general trend for NHB solvents*

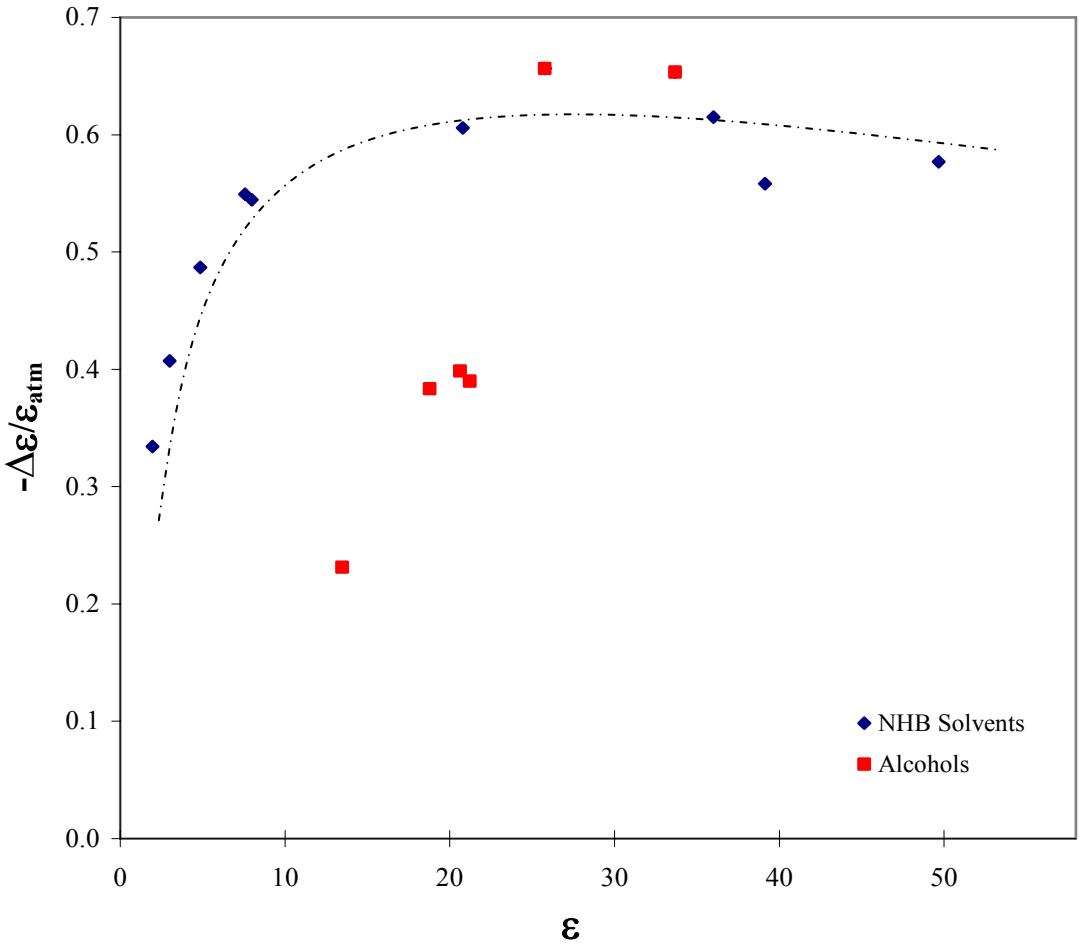


***Figure 4.12*** *Relative changes in relative permittivity on expansion as a function of the relative permittivity at ambient pressure. The blue dotted line follows the general trend of the NHB solvents*

### 4.2.5 Density of $CO_2$ Expanded Solvents

To determine a more accurate picture of a GXL it is important to quantify the change occurring in the molar volume upon expansion. Figure 4.13 shows the density of a range of organic solvents and the degree to which density changes when they are expanded under 50 bar of $CO_2$ at ambient temperature as described in Section 2.3.3. The solvents are plotted in order of increasing density at ambient pressure. The density values were obtained with an uncertainty of ± 2 % and values obtained at ambient pressure were in good correlation with published data.[47] Figure 4.13 shows that the density of the majority of solvents increased when expanded with $CO_2$. The increase in the density might be due to the initial "solvent" behaviour of carbon dioxide. Carbon dioxide "dissolving" in the mixture would then increase the initial density of the solvent up to maximum saturation, *i.e.* more solvent molecules are packed in a given volume.

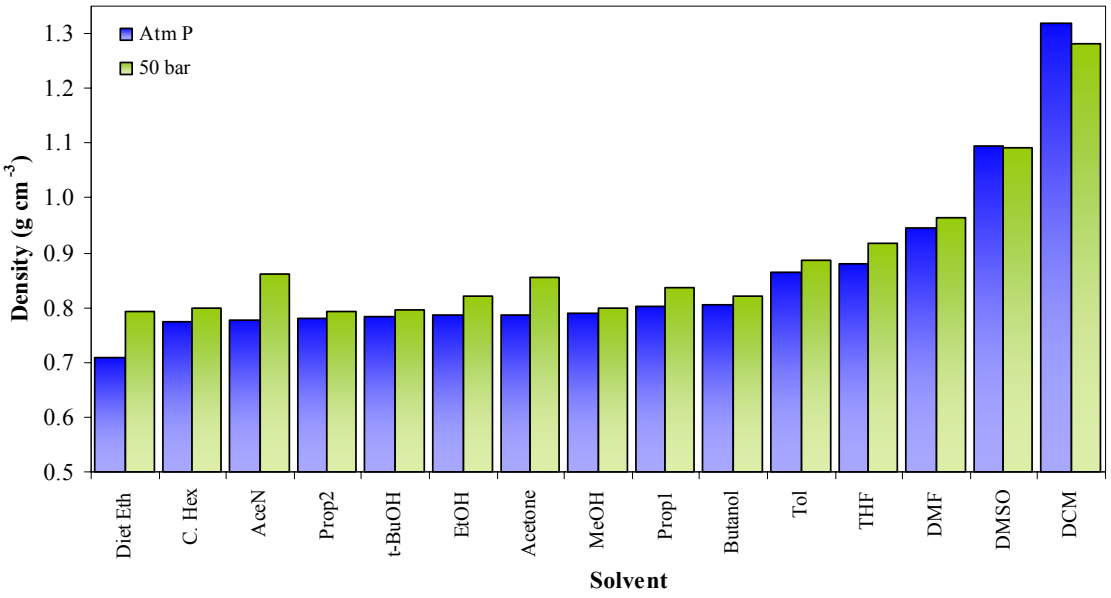


***Figure 4.13*** *Density data values for solvents at ambient pressure (blue), and $CO_2$ expanded equivalents (green) at 50 bar pressure and room temperature (25 $^oC$)and constant volume of solvent*

A more pronounced change in density was noticeable for acetone, ether, and acetonitrile, however there was no observable trend as to which solvents changed the most. The more dense solvents, dichloromethane and dimethyl sulfoxide, showed a reduction in density. It is proposed that all expanded solvents increase in density initially as the mole fraction of carbon dioxide increases up to a maximum, after which point further increases in $CO_2$ solubility result in an opposing effect where density begins to decrease. This density behaviour could be attributed to one or two different phenomena; liquid compression as a result of the application of pressure, and the solubilisation of $CO_2$. Kordikowski *et al.*[17] have reported vapour-liquid equilibria for polar solvents with carbon dioxide. They calculated the volume expansion of the liquid phases by obtaining density measurements for the liquids under various pressure ranges. The density plots of expansion with carbon dioxide showed the occurrence of a maximum for each solvent system, although predominantly linear behaviour was observed between a wide range of pressures (0.2 to 0.7 MPa). Figure 4.14 shows the results for $CO_2$ expansions of six different solvents at ambient temperature.

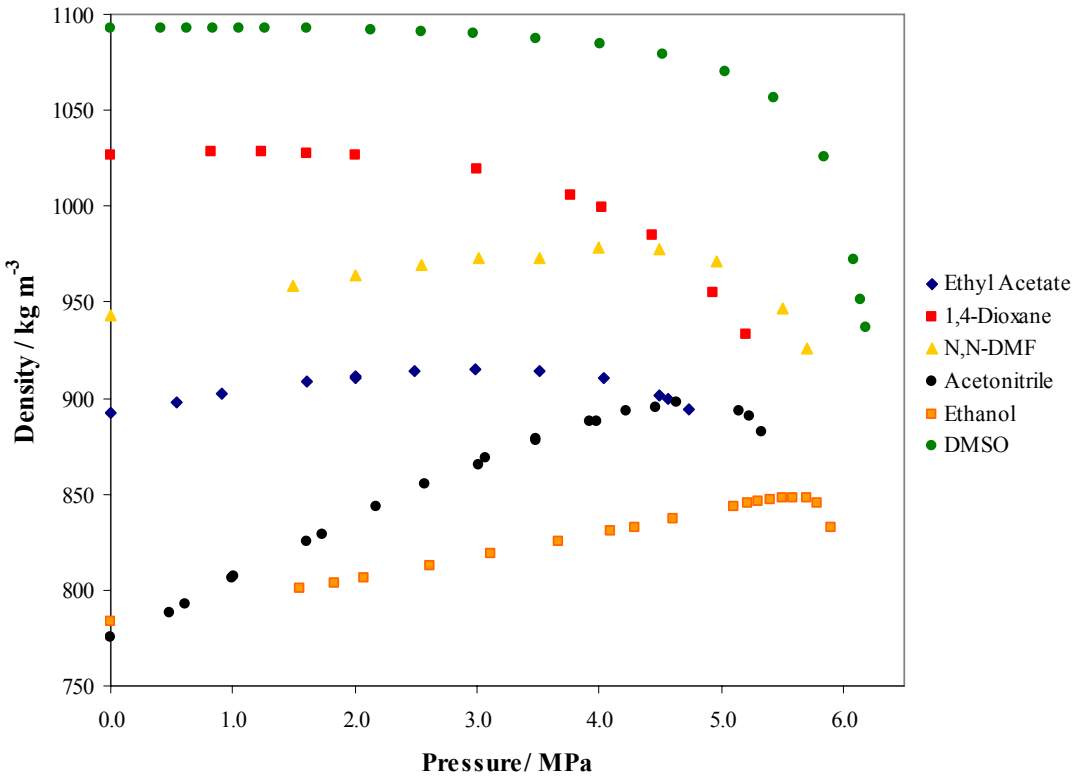


***Figure 4.14*** *Liquid densities for $CO_2$ pressurised in six different solvents at 298.15 K, as a function of pressure*

If solubility was the only factor, then the changes in density would correlate to the solubility of $CO_2$. This is not the case, and hence both factors must play a role. Pressure effects are most likely to be dominant when $CO_2$ solubility in the organic solvent is poor; this results in an increase in the saturated liquid density when the system is subjected to pressure. However, it can also be argued that when dissolution of $CO_2$ into the liquid phase is favoured, the density of the expanded liquid shifts towards the value of the pure $CO_2$ density at 50 bar and room temperature (0.141 g $cm^{-3}$). This value is generally lower than those of organic solvents.

Although the density values of the expanded solvents are similar to those of traditional liquids, the presence of the gaseous component results in solvation and transport properties that are intermediate between that of a dense gas and a pure liquid, thereby enhancing their mass transport ability. To understand the packing in these systems it is helpful to consider the molar density, this is shown in Figure 4.15. The molar density gives information on the spatial occupation of solvent molecules and this data can then be used to calculate the free volume (the space between solvent molecules that is unoccupied and available for solute solvation).

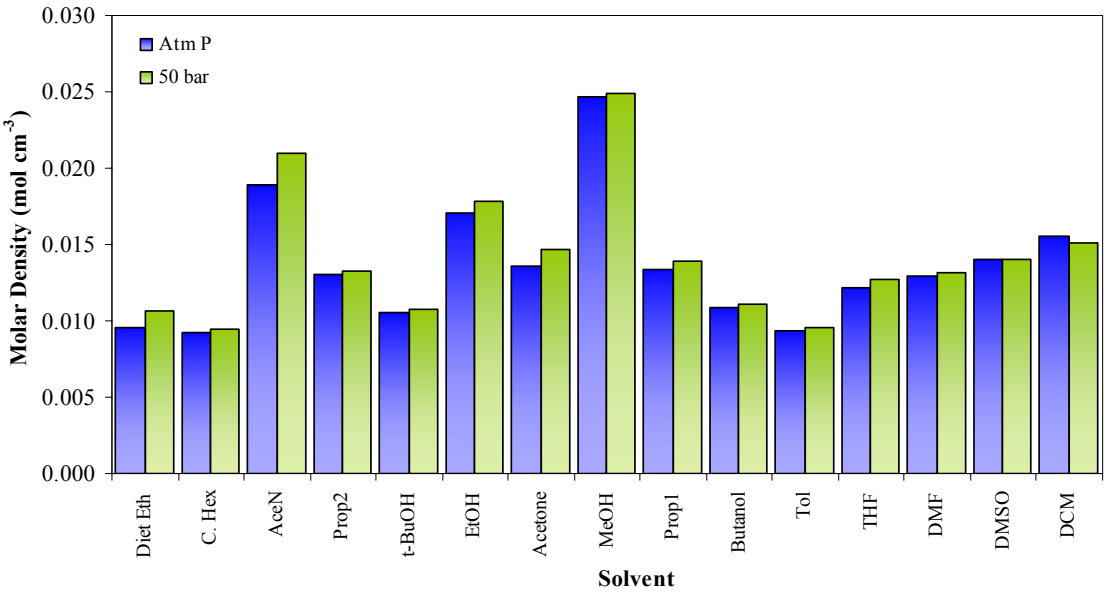


***Figure 4.15*** *Molar density data values for solvents at ambient pressure (blue), and $CO_2$ expanded equivalents (green) at 50 bar pressure and room temperature (25 $^oC$) and constant volume of solvent*

### 4.2.6 Determination of Molar Free Volume

Analysis of the data in this form is slightly misleading, as $CO_2$ is a small but dense molecule and density measurements do not give a significant amount of insight into liquid structure. A more useful proposal is to consider the molar volume of the liquid and determine what changes are happening to the free volume of the liquid upon expansion. The molar free volume, $V_{free}$, of a liquid can be determined from the following equation:

$$V_{free} = (M_w/\rho) - (N_A * V) \qquad \textbf{(4.12)}$$

Where $M_w$ is the molecular mass of the solvent, $\rho$ is the density of the solvent at ambient pressure, $N_A$ is Avogadro's constant, and $V$ is the molecular volume.

Using the data presented in Figure 4.8, $V_{free}$, for the gas expanded liquid can also be calculated by carrying out the same procedure for each of the components as shown in equation 4.12.

Figure 4.17 shows that in contrast to Figure 4.14, where density changes were minimal, gas expansion has a significant effect upon the percentage of free volume between solvent molecules. In general, solvents that exhibit the largest solubilities for $CO_2$ cause the greatest increases in molar free volume and, in terms of the free volume, all of these systems expand with the exception of DCM as shown in Figure 4.7 where the free volume for DCM decreases on expansion.

Figure 4.18 shows that there is a direct correlation between the change in free volume and the mole fraction of $CO_2$ dissolved in the liquid for the protic solvents. The correlation is less marked for the non-hydrogen bonding solvents. The linear correlation for the protic solvents is to be expected; when more $CO_2$ is dissolved the hydrogen bonding structure is disrupted and the free volume increases.

The thermodynamics of $CO_2$ mixing depends upon the relative solvent-solute interactions. To dissolve $CO_2$ in the solvent it is necessary to overcome the intermolecular forces between the solute species (which should be negligible), and the energy released when the $CO_2$ interacts with the solvent and the solvent-solvent interactions required to form a cavity for the solute. In a GXL it is the last of these that will dominate, and this can be quantified using the Hildebrand solubility parameter, δ which is shown in equation 4.13.

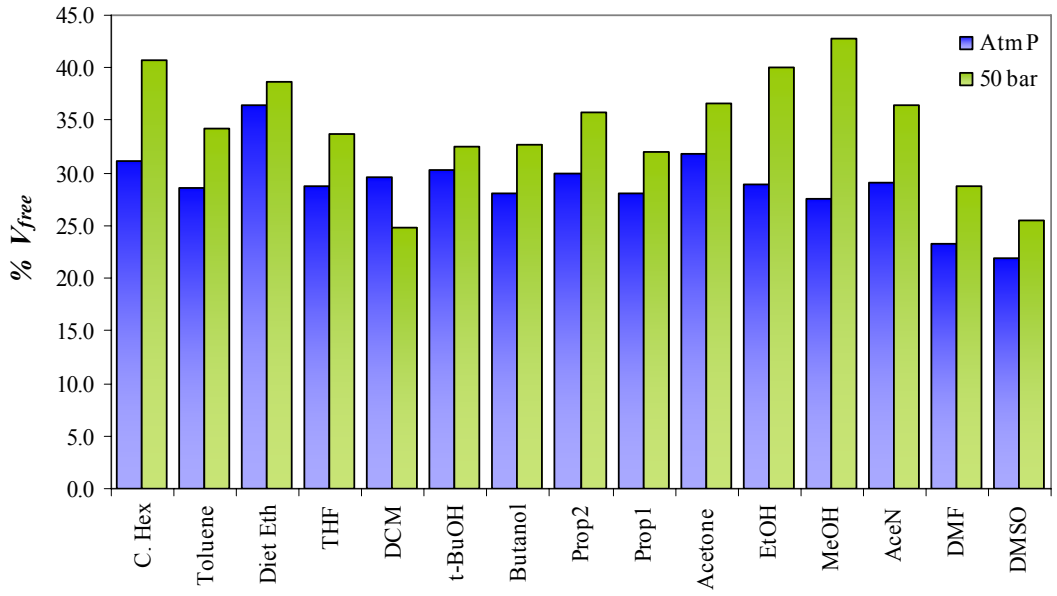


***Figure 4.16*** *Molar free volume in a range of liquids at ambient pressure (blue), and when expanded with 50 bar of $CO_2$ (green)*

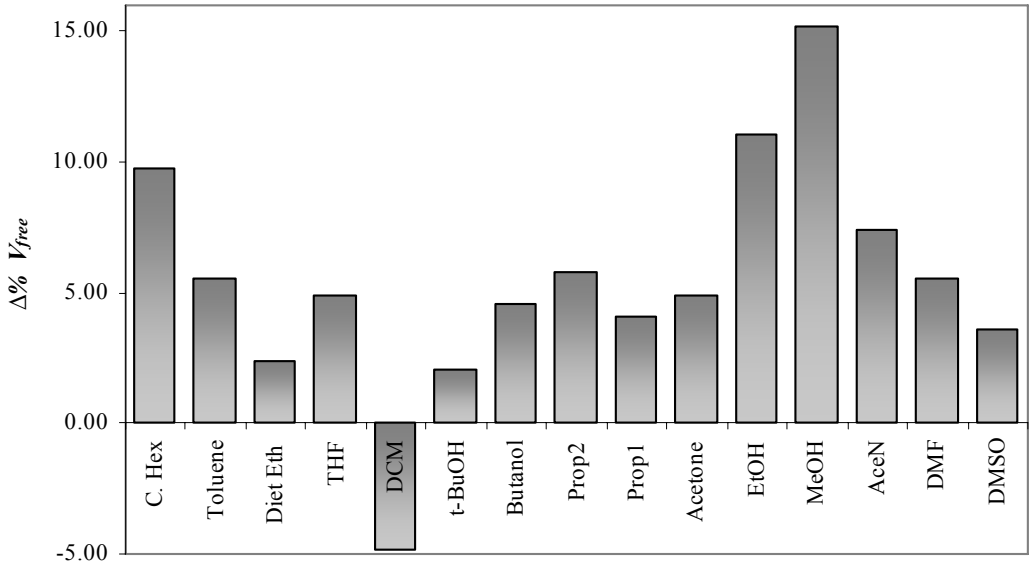


***Figure 4.17*** *Change in molar free volume when liquid solvents are expanded at 50 bar pressure with $CO_2$*

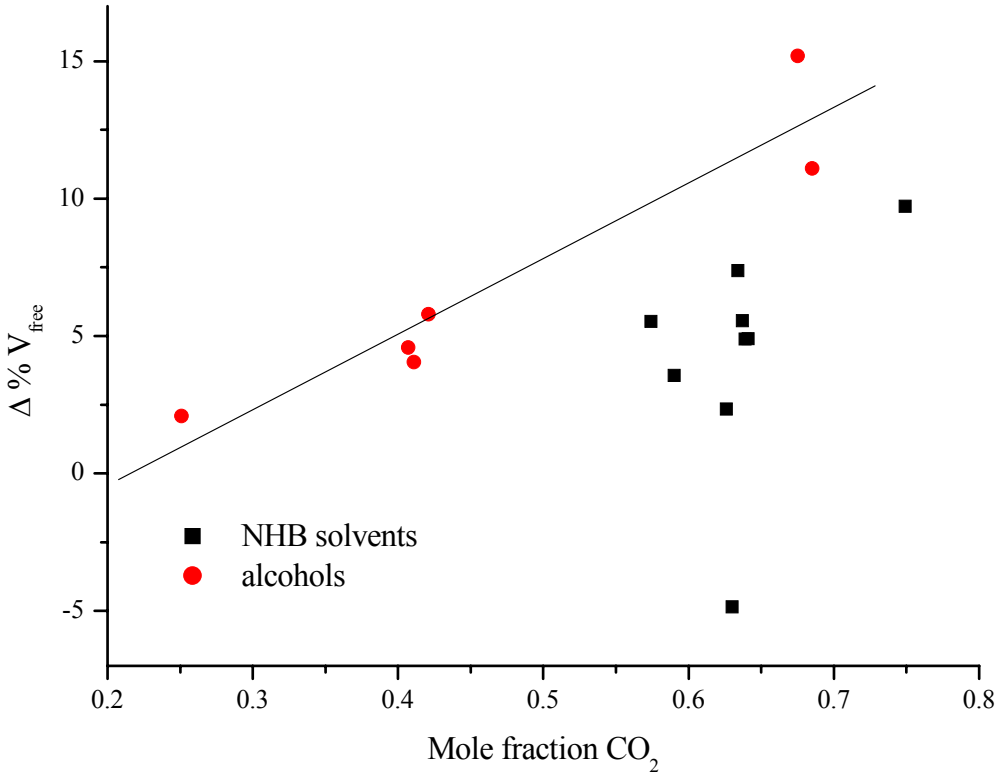


***Figure 4.18*** *Mole fraction of $CO_2$ as a function of the change in molar free volume when the liquid solvents undergo expansion with 50 bar of $CO_2$*

$$\delta = \sqrt{\frac{\Delta H - RT}{V_m}} \qquad \textbf{(4.13)}$$

Where; $\Delta H$ is the change in enthalpy, $R$ is the gas constant (8.314 J $K^{-1}$ $mol^{-1}$), $T$ is the temperature (in Kelvin), and $V_m$ is the molar volume of the solvent. Figure 4.19 shows a good correlation between the change in molar volume upon expansions and δ.

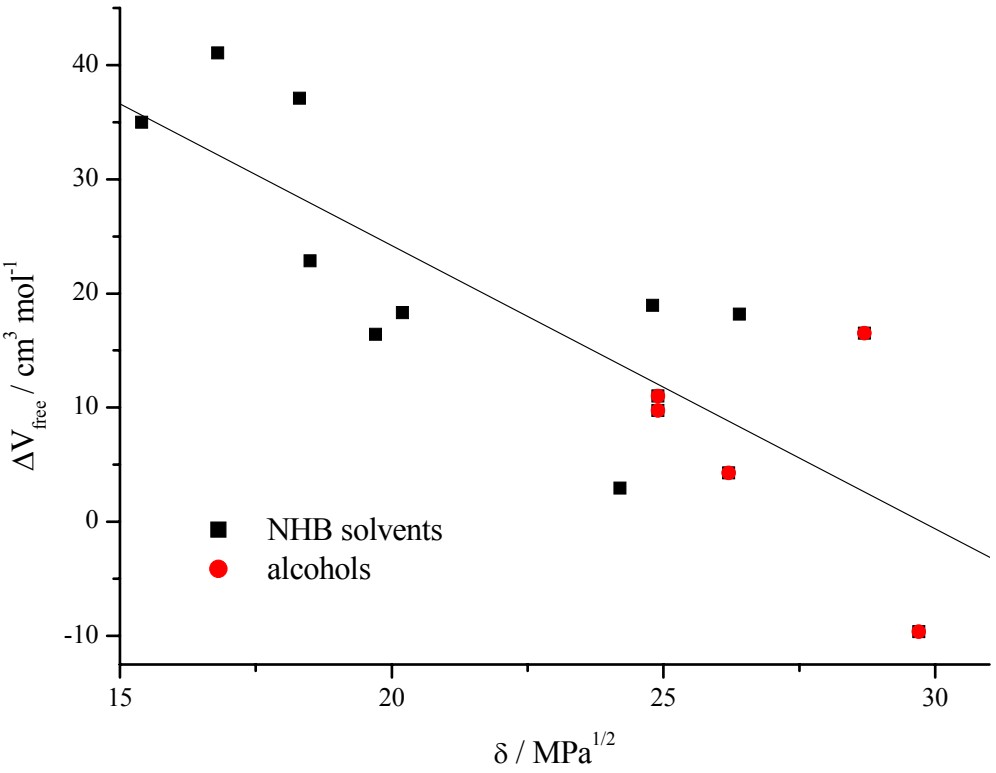


***Figure 4.19*** *Relationship between Hildebrand solubility parameter for the pure liquid*[24] *and the change in molar free volume when a liquid organic solvent is pressurised with 50 bar* $CO_2$

Figure 4.19 shows that there is a linear correlation between the change in molar free volume upon expansions and the Hildebrand solubility parameter showing that the expansion of molecular solvents is controlled by the thermodynamics of cavity formation. This work has shown that the solubility of $CO_2$ in molecular solvents is relatively similar for most of the solvents studied but higher alcohols demonstrate considerably lower solubility, due primarily, to the solvent-solvent interactions. The

density of most solvents only changes by a small amount, but in molar terms the free volumes of the expanded liquids can increase by over 10 %.

### 4.3 Conclusions

This work assesses the validity of a quick, simple, and precise *in situ* technique for determining the relative permittivity of GXLs. Density and relative permittivity data at 25 ºC and 50 bar pressure for a range of $CO_2$-expanded solvents are reported for the first time. The dissolution of $CO_2$ into liquid organic solvents to generate expanded liquids has shown significant changes in the dielectric polarity of a solvent medium. The bulk polarity of all solvents changed quite significantly. In some cases this has allowed an instant shift in polarity from polar to nonpolar media, simply by adding moderate pressures of $CO_2$. Similarities in relative permittivity's were shown between expanded acetone with pure THF, and expanded DMSO with pure propan-2-ol. The exact point at which the relative permittivity of the binary mixture fell was determined to be dependent upon the mole fraction of $CO_2$ present in the expanded phase. Following on from this data, it has also been possible to determine the solubility (mole fraction) of $CO_2$ for each expanded solvent. Most of the solvents pressurised show a high extent of $CO_2$ dissolution. $CO_2$ was determined to be most soluble in cyclohexane which, when fully expanded was composed of almost 75 % $CO_2$, the poorest solubility was mostly in the alcohols, namely *t*-butanol (~25 %), and *n*-butanol (~40 %).

No correlation between the change in relative permittivity and the change in $\pi^*$ was seen on expansion. So far, polarity results have shown that the bulk solvent properties are changed to a greater extent than that observed locally. Preferential solvation around the cybotactic region of the solute is believed to be the reason for $CO_2$ acting as more of a diluent on a local level. This can be confirmed with solvatochromic data determined in chapter three where local polarity was investigated.

The character and content of a solvent are what determine the solvation behaviour of expanded liquids over a given compound.[48] $CO_2$ expanded media have shown to generate a range of tuneable physical properties for which they can be used to generate a continuum of alternative solvent media with variable solvent power, as a function of pressure (extent of expansion), or their composition, thus offering a multitude of opportunities for industrial applications.

## 4.4 References


1. J. B. Hannay and J. Hogarth, *Proceedings of the Royal Society of London*, 1879, **29**, 324.
2. G. Anitescu and L. L. Tavlarides, *Journal of Supercritical Fluids*, 1997, **10**, 175-189.
3. G. Anitescu and L. L. Tavlarides, *Journal of Supercritical Fluids*, 1997, **11**, 37-51.
4. G. Anitescu and L. L. Tavlarides, *Journal of Supercritical Fluids*, 1999, **14**, 197-211.
5. S. V. Rodrigues, D. Nepomuceno, L. V. Martins and W. Baumann, *Fresenius Journal of Analytical Chemistry*, 1998, **360**, 58-61.
6. V. F. Cabral, W. L. F. Santos, E. C. Muniz, A. F. Rubira and L. Cardozo, *Journal of Supercritical Fluids*, 2007, **40**, 163-169.
7. Y. Marcus, *Journal of Supercritical Fluids*, 2006, **38**, 7-12.
8. R. N. Maksudov, A. E. Novikov, A. N. Sabirzyanov and F. M. Gumerov, *High Temperature*, 2005, **43**, 854-858.
9. K. P. Johnston and C. A. Eckert, *American Institute of Chemical Engineers Journal*, 1981, **27**, 773-779.
10. R. A. Vanleer and M. E. Paulaitis, *Journal of Chemical and Engineering Data*, 1980, **25**, 257-259.
11. R. T. Kurnik, S. J. Holla and R. C. Reid, *Journal of Chemical and Engineering Data*, 1981, **26**, 47-51.
12. A. N. Fedotov, A. P. Simonov, V. K. Popov and V. N. Bagratashvili, *Journal of Physical Chemistry B*, 1997, **101**, 2929-2932.
13. A. N. Fedotov, A. P. Simonov, V. K. Popov and V. N. Bagratashvili, *Zhurnal Fizicheskoi Khimii*, 1996, **70**, 166-168.
14. A. Hourri, J. M. St-Arnaud and T. K. Bose, *Review of Scientific Instruments*, 1998, **69**, 2732-2737.
15. A. P. Abbott, S. Corr, N. E. Durling and E. G. Hope, *Journal of Chemical and Engineering Data*, 2002, **47**, 900-905.
16. G. Leeke, R. Santos, B. Al-Duri, J. Seville, C. Smith and A. B. Holmes, *Journal of Chemical and Engineering Data* 2005, **50**, 1370-1374

17. A. Kordikowski, A. P. Schenk, R. M. VanNielen and C. J. Peters, *Journal of Supercritical Fluids*, 1995, **8**, 205-216.
18. C. J. Chang and A. D. Randolph, *American Institute of Chemical Engineers Journal*, 1990, **36**, 939-942.
19. M. J. Lazzaroni, D. Bush, R. Jones, J. P. Hallett, C. L. Liotta and C. A. Eckert, *Fluid Phase Equilibria*, 2004, **224**, 143-154.
20. J. Badilla, C. J. Peters and J. D. Arons, *Journal of Supercritical Fluids*, 2000, **17**, 13-23.
21. T. S. Reighard, S. T. Lee and S. V. Olesik, *Fluid Phase Equilibria*, 1996, **123**, 215-230.
22. R. L. Smith, C. Saito, S. Suzuki, S. B. Lee, H. Inomata and K. Arai, *Fluid Phase Equilibria*, 2002, **194**, 869-877.
23. D. R. Lide, ed., *CRC Handbook of Chemistry and Physics*, 84th edn., Boca Raton, 2003.
24. J. A. Riddick, W. B. Bunger and T. K. Sakano, *Organic Solvents: Solvent Properties and Methods of Purification*, 4th edn., J. Wiley and Sons, New York, 1986.
25. F. G. Keyes and J. G. Kirkwood, *Physical Reviews*, 1930, **36**, 754.
26. D. L. Tomasko, B. L. Knutson, F. Pouillot, C. L. Liotta and C. A. Eckert, *Journal of Physical Chemistry*, 1993, **97**, 11823-11834.
27. L. Onsager, *Journal of the American Chemical Society*, 1936, **58**, 1486.
28. C. R. Yonker and R. D. Smith, *Journal of Physical Chemistry*, 1989, **93**, 1261-1264.
29. C. Reichardt, *Chimia*, 1991, **45**, 322-324.
30. W. Kunerth, *Physical Reviews*, 1922, **19**, 512.
31. E. Wilhelm and R. Battino, *Chemical Reviews*, 1973, **73**, 1-9.
32. J. M. Prausnitz and F. H. Shair, *American Institute of Chemical Engineers Journal*, 1961, **7**, 682.
33. F. Gibanel, M. C. Lopez, F. M. Royo, J. Pardo and J. S. Urieta, *Fluid Phase Equilibria*, 1993, **87**, 285-294.
34. J. C. Gjaldbaek and J. H. Hildebrand, *Journal of the American Chemical Society*, 1949, **71**, 3147.
35. J. H. Hildebrand and L. W. Reeves, *Journal of the American Chemical Society*, 1957, **79**, 1313.

36. J. H. Hildebrand and G. Archer, *Journal of Physical Chemistry*, 1963, **67**, 1830.
37. H. Hiraoka and J. H. Hildebrand, *Journal of Physical Chemistry*, 1964, **68**, 213.
38. J. H. Hildebrand and R. G. Linford, *Journal of Physical Chemistry*, 1969, **73**, 4410.
39. J. C. Gjaldbaek and H. Nieman, *Acta Chemica Scandinavica*, 1958, **14**, 611.
40. A. Lannung and J. C. Goldbaek, *Acta Chemica Scandinavica*, 1960, **14**, 1121.
41. J. M. Prausnitz, *Journal of Physical Chemistry*, 1962, **66**, 640.
42. R. Pierotti, *Journal of Physical Chemistry*, 1964, **67**, 1840.
43. S. Goldman, *Journal of Chemical Physics*, 1977, **67**, 727-732.
44. S. Goldman, *Journal of Solution Chemistry*, 1977, **6**, 461-474.
45. S. T. Perisanu, *Journal of Solution Chemistry*, 2001, **30**, 183-192.
46. T. Katayama, M. Tomosaburo and T. Nitta, *Kagaku Kogaku*, 1967, **31**, 559.
47. R. H. Perry and D. W. Green, *Chemical Engineers' Handbook (7th Edition)*, McGraw-Hill, 1997.
48. F. E. Wubbolts, PhD, University of Delft, Netherlands, 2000.

# CHAPTER 5

# Applications of Gas eXpanded Liquids

---



---

## 5.1. Applications in High Pressure

Supercritical $CO_2$, although an inert diluent, has shown the ability to increase reaction rates and selectivity for catalytic homogeneous and heterogeneous reactions.[1-3] Carbon dioxide is the only non-flammable and non-toxic solvent that is miscible with fluorocarbons, hydrocarbons, and the majority of polar low molecular weight organics including ketones, ethers, alkanes and nitriles, however, it shows poor miscibility with water.

The addition of $CO_2$ to fluorous organic biphasic systems has resulted in improved reaction rates in homogenous conditions.[1, 4] SCF solvents have an unusual combination of physical properties, making them attractive solvents for many reactions. The high compressibility of $CO_2$ in the near-critical region means that small changes in temperature and pressure result in large density changes and considerable solubility variations. Therefore $CO_2$ is easily separated from reaction products by a simple method of depressurisation. This chapter investigates various applications where supercritical technologies currently exist with the hope of finding a suitable $CO_2$-expanded replacement.

There are numerous advantages associated with the use of GXLs in chemical synthesis. With a unique combination of properties achievable, they have great potential to benefit many types of different reactions. One of the most prominent advantages of GXLs for chemical synthesis is their adjustable solvating power. There is a considerable amount of knowledge concerning extraction and solubility in SCFs that is available in the literature. Such processes show promise for separation and purification steps in industrially relevant processes. The extractive properties of SCFs have been investigated to separate products from by-products, and for the recovery of homogeneous catalysts. The physical properties of GXLs determined in chapter three and four have shown great promise for their use as substitutes for SCFs. Chapter 5 looks at the phase behaviour, selectivity and solubility data for GXLs as suitable solvents for synthetic uses. Four application areas are considered including, biphasic reactions, solute solubility determinations, and phase behaviour studies.

GXLs and SCFs share many of the same enhanced properties which may be advantageous for increasing reaction rates. Diffusion controlled reactions can be enhanced in both solvent types because of their improved mass transport ability. Local solute-solute clustering noted in chapter three for GXLs can also result in the presence of a local concentration of reactants, thus increasing reaction rates further.

Biphasic reactions are of particular interest due to the mass transfer limitations observed between the liquid-organic and the liquid-aqueous phases. It is hoped that replacing the liquid solvents with at least one gas expanded phase should improve miscibility between the two phases and lead to more efficient product yields.

Another area which will be investigated is selectivity in reactions. The same factors known to affect rates can also affect selectivity by altering the rates of competing reactions. Changes in physical properties of solvents induced on pressurisation of reaction mixtures may result in considerable tuning effects on the selectivity of reaction products based on polarity influences. GXLs have already been established as suitable solvents for precipitation studies as discussed in chapter one. The solubility of compounds in solvents is a key area of research for the consideration of potential process applications. The availability of solubility data can give an indication of the performance of a GXL as a solvent for particular solutes.

The third application area investigated in this chapter is the solubility of solutes in different pressurised solvents (liquid $CO_2$, GXLs, and SCFs). The solubility of a component is mainly influenced by its chemical functionality, the nature of the solvent, and the operating conditions employed. Although the solubility of a single solute in a solvent is not necessarily the same as that determined in a multi-component system, binary solubility data are nevertheless still useful for estimating selectivities for particular solutes. Finally, the fourth application discussed will look into phase behaviour of mixed solvents and the changes in their miscibility/immiscibility with each other when expanded with $CO_2$. Miscibility of liquid solvents is controlled by the enthalpy of mixing, and in order for solvents to mix, the enthalpy of mixing is predominantly negative as generally the enthalpy of mixing is small. Changes in polarisability, polarity, density, and free volume seen for GXLs when pressurised requires a new set of miscibility data to be collated for expanded solvent pairs.

## 5.2 Phase Transfer Catalysis

### 5.2.1 Introduction

The phase transfer method is a mild and catalytic method for achieving functional group exchange (Figure 5.1). Generally, there are two immiscible phases, and a phase transfer catalyst (PTC) is added to the reaction mixture. This is usually a quaternary ammonium or phosphonium halide containing a lipophilic cation. PTC is a widely used technique for conducting reactions between two or more reagents in two

or more phases when the reaction is inhibited, as the reactants cannot simply react together. For this reason, a phase transfer agent is added to transfer one of the reagents to a site where it can conveniently and rapidly react with the other reagent.

One example that illustrates how the phase transfer method operates is the reaction of 1-chlorooctane with aqueous sodium cyanide.[5] Under normal conditions where no catalyst is used, heating this biphasic mixture under reflux with vigorous agitation for up to two days gives no evident reaction with the exception of a possible hydrolysis of the sodium cyanide to form ammonia and sodium formate. On the other hand, with the addition of just 1 wt% of an appropriate quaternary ammonium catalyst - $(C_6H_{13})N^+Cl^-$, 100 % yields are obtained for both conversion and selectivity in just two to three hours.

The sequence of reactions that cause cyanide to be transferred into the organic phase is represented by equilibrium stages, and is shown schematically by the Stark's extraction mechanism in Figure 5.1. It is noteworthy to mention that the transfer rate of interest is the net rate of delivery of cyanide to the organic phase and not merely the rate of the physical process of taking it across from the aqueous to the organic phase. It is important to achieve high rates for both steps of the phase transfer process, and to correlate kinetics of both steps closely through the effect of the catalyst. It is therefore possible to maintain overall reactivity when the rates of both steps are equal.

The vast majority of work in PTC has been concerned with the transfer of anions from aqueous to organic phases for reaction.[6] However, the primary concept of PTC is that any species in principle can be transferred to its non-normal phase and be activated for appropriate reactions.[7] The most frequently encountered problem associated with the use of phase transfer processes is the need to separate the product and catalyst.[8] It is also highly desirable particularly in industrial applications that the catalyst be reusable or recyclable. By use of insoluble catalysts, this problem may be avoided by incorporating facile separation methods such as filtration, centrifugation or phase separation. So far, the most commonly used methods of separation for soluble catalysts are extraction and distillation methods.

**"The Starks Extraction Mechanism"**

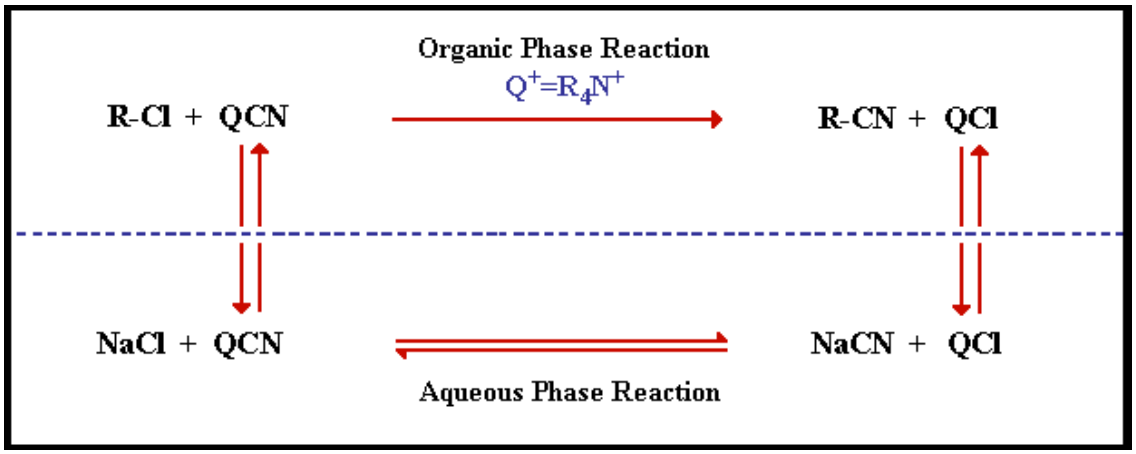


***Figure 5.1*** *Schematic representation of phase transfer catalysed cyanide displacement on 1-chlorooctane*

There are two key stages involved in the phase transfer process:

**Step 1. The "transfer" step**

This involves the transfer of the quaternary ammonium catalyst from the organic to the aqueous phase. For example, exchange of the chloride for the cyanide ion takes place in the aqueous phase, followed by the transfer of the catalytic cyanide from the aqueous to the organic phase.

**Step 2. The "displacement" step**

This is the sequence of reactions that take place in the organic phase which result in the formation of product. For the example given above, this is the displacement reaction between the quaternary ammonium cyanide and 1-chlorooctane in order to produce 1-cyanooctane.

### 5.2.2 Factors affecting PTC

Phase transfer catalysis reactions can be influenced by a number of variables, the most important of which are outlined briefly below. More detailed information on these factors can be found as described by Starks[9] who also discusses other reaction variables that have not been mentioned in this report.

- **Choice of Solvent**

  Phase transfer reactions usually require the participation of a solvent because the organic reagent can be an unreactive solid under reaction conditions. The ability of different combinations of solvent pairs to enable biphasic operation can be estimated on the one hand according to the principle of "like dissolves like" in respect to the solvent for the catalyst. This advantageous characteristic can contribute to improved product purity and yields, and also prevent the use of environmentally hazardous solvent.[10] The fundamentals of miscibility are generally governed by the solvent polarity scale,[11] and are discussed further later on in this Chapter.

- **Agitation**

  Vigorous stirring is employed to aid the transfer of anions from the aqueous to the organic phase. In the absence of agitation, phase transfer reactions are almost always too slow to proceed to a reasonable extent. Stirring increases the interfacial area between the two phases, thus accelerating the rate of transfer of the reactive species.[12]

- **Temperature**

  Increasing the temperature can accelerate the rate of most organic PTC reactions. In most cases, it is likely to be one of the first experimental variables to be optimised. Temperature effects are usually dependent on the type of catalyst being employed, for example, Quaternary ammonium salts usually decompose at high temperatures (120 to 150 $^{\circ}$C).

In the aqueous biphase system, the aqueous phase, containing the water-soluble catalyst, is immiscible with the organic phase, which contains both reactants and reaction products. Product isolation therefore simply involves decantation of the organic phase, leaving the aqueous catalyst-containing solution separated and ready

for further catalytic cycles. This technique combines the advantages of homogeneous catalysis with the ease of separation inherent in heterogeneous systems, thereby "heterogenising" a homogeneous system.[13,14]

Some advantages and properties of using water as a liquid support on aqueous biphase catalysis are listed below:

- Easy to separate from nonpolar solvents or products.
- Inflammable.
- Odourless and colourless, making contamination easily recognisable.
- Density of 1 g/cm$^3$ provides a sufficient difference from most organic substances.
- Very high dielectric constant.
- High thermal conductivity, high specific heat capacity and high evaporation enthalpy.
- Low refraction index.
- High solubility of many gases, especially $CO_2$ (on a volume expansion basis)
- Formation of hydrates and solvates.

Despite the number of advantages outlined above, the aqueous biphase system also has its disadvantages associated with the aqueous process itself. For example, the rate of reaction depends on the solubility of the substrate in the aqueous phase. Therefore, when the substrates are water-immiscible, the reaction can only occur at the limited interface between the two phases and this can significantly reduce the rate of reaction. The technique of aqueous biphase catalysis has had such an impact on the chemistry of biphase reactions that different solutions have been proposed. Fluorous systems[15] have advantages in the "homogeneous" reaction and the "heterogeneous" separation because of a greater degree of control over phase behaviour.

Most PTC reactions reported to date in the literature are based around the aqueous/organic biphasic system. Water is a unique solvent because of its high polarity and its strong capability of forming a network of hydrogen bonds. It is a suitable candidate for biphasic reactions due to its immiscibility with many organic solvents for which catalysts are made preferentially soluble in the organic phase. One of the most challenging aspects of this type of chemistry is the selection of an appropriate phase transfer catalyst as many different features must be considered, including, disposal, recovery, toxicity, cost and availability. The work reported here

was based on an aqueous/organic biphase system for the nucleophilic displacement reaction of a benzyl halide as shown in Figure 5.2.

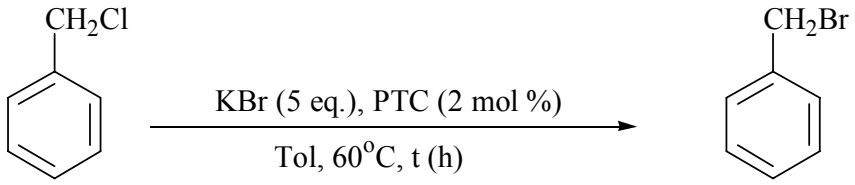


***Figure 5.2*** *Catalysed nucleophilic displacement of benzyl chloride under biphasic conditions.*

The reaction was carried out at moderate pressures of $CO_2$ (50 bar) as described in Section 2.3.4 in the absence of a phase transfer catalyst. Earlier studies have shown that as pressure is increased the mole fraction solubility of $CO_2$ in water increases. The pH of the system is strongly dependent on the extent of solubility of $CO_2$ in water.[16] It was envisaged that the hydrogen bonding network in water could be disrupted by the increased solubility of $CO_2$ when pressurised, thus increasing the miscibility of the aqueous and organic phase.

### 5.2.3 Results and Discussion

Previous studies have shown that expansion with a gas like $CO_2$ can significantly reduce the amount of organic solvent required for the reaction by up to 80 %.[17] Replacement of most of the organic liquid phase results in a significant change in solvent solubility, and it was hoped that by subjecting the system to moderate pressures of $CO_2$, miscibility between the two phases would be enhanced. Carbon dioxide is weakly soluble in water (on a mole fraction basis), and readily forms carbonic acid.

Step 1: Carbonic acid formation

$$CO_2\ (aq) + H_2O \leftrightarrow H_2CO_3\ (aq) \qquad \textbf{(5.1)}$$

Step 2: Carbonic acid equilibrium

$$H_2CO_3\ (aq) \leftrightarrow H^+(aq) + HCO_3^-\ (aq) \qquad \textbf{(5.2)}$$

$$HCO_3^-(aq) \leftrightarrow H^+(aq) + CO_3^{2-}(aq) \quad \textbf{(5.3)}$$

Preliminary results from applying moderate pressures of $CO_2$ to the system showed no significant improvement to product yields. Visual examination of the reaction under high pressure conditions showed that pressurisation led to an increase in the observed volume of the organic phase, and no apparent change in the aqueous phase. As the system was left to equilibrate, a thin layer was formed on-top of the organic phase as depicted in Figure 5.3. The formation of this third layer was due to the presence of liquid $CO_2$, on depressurisation the third layer diffused out.

### 5.2.4 Phase Transfer Reactions in Different Solvent Systems

The biphasic substitution of benzyl chloride was studied in various organic solvent systems and in their gas expanded counterparts. Vigorous stirring speeds were not investigated as for the majority of phase transfer reactions increased agitation does not enhance the desired reaction but has shown to promote the undesired non-catalysed interfacial hydrolysis. As a result, vigorous agitation would simply result in wasted raw materials. The reaction was carried out under identical conditions, uncatalysed, at 60 °C, and with mechanical agitation at 200 rpm for two hours with an unsaturated aqueous phase (containing 5 mmol of salt). The final product and by-product yields were compared for the reaction

**$CO_2$-Expanded Biphasic Reaction**

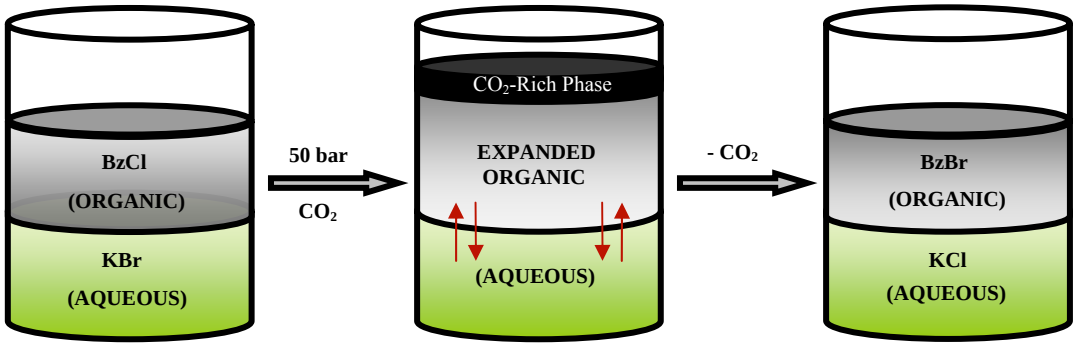


**Figure 5.3** *Aqueous biphasic halide displacement reaction under moderate pressure in the absence of a catalyst*

in the absence of solvent, in the presence of liquid solvent, and at various pressures in $CO_2$-expanded toluene.

Results in Figure 5.4 show that in the absence of organic solvent the amount of by-products (benzyl alcohol and benzaldehyde) formed is to a very large extent. The presence of solvent appears to be very important in controlling the selectivity of the reaction towards the desired product and hence, reducing the formation of by-products. Subjecting the system to moderate pressures of $CO_2$ showed no conclusive evidence of improvements in the yield of the reaction. Pressures were applied between ambient pressure up to 70 bar $CO_2$. The yield of product (BzBr) remained fairly constant throughout most of the runs. At higher pressures, by-product formation is increased significantly and was favoured towards the formation of benzaldehyde as opposed to benzyl alcohol which was produced at ambient pressure conditions. This reduced the selectivity of the reaction.

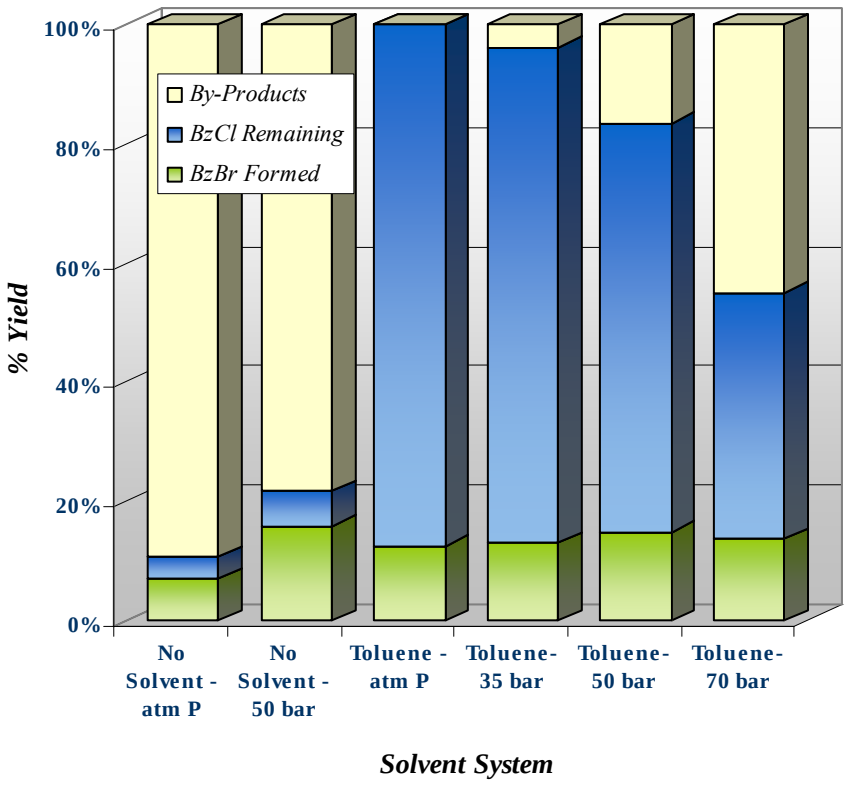


***Figure 5.4*** *Comparison of the yield of benzyl bromide in the presence and absence of a solvent*

### 5.2.5 By-Product Formation

The first two reactions carried out in the absence of organic solvent resulted in the production of mostly benzyl alcohol. The undiluted reaction substrate was forced to proceed by reacting only at the liquid-liquid interface due to the absence of toluene. Benzyl alcohol was formed on reaction with water which was present in the aqueous phase. Further reactions were carried out using toluene as a solvent, and these were monitored as a function of pressure. It was noted that when pressurised, benzalydehyde was produced as the by-product in increasing yields as pressure was increased. It is thought that the benzyldehyde was produced via a benzyl alcohol intermediate as seen in the phase transfer reaction at ambient pressure (Figure 5.5) Benzaldehyde is the simplest representative of the aromatic aldehydes. Currently, liquid phase chlorination and oxidation of toluene are among the most used processes. There are also a number of discontinued applications such as partial oxidation of benzyl alcohol, alkali treating of benzal chloride and reaction between benzene and carbon monoxide. Reaction conditions presented in this work show a feasible new route for the production of benzaldehyde if reaction parameters are studied and optimised further.

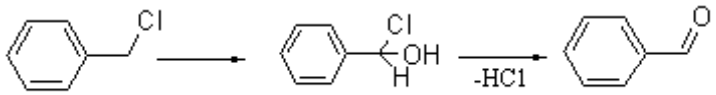


**Figure *5.5*** *Formation of benzaldeyde via a benzyl alcohol intermediate*

The phase transfer reaction was also carried out using methanol instead of water as the aqueous phase. Methanol and toluene as miscible at ambient pressure and temperature, but on addition of the substrates (benzyl chloride and potassium bromide) the solvents phase separate. It was hoped that by pressurising this system, the phases would be more partial to homogenise, and thus result in a reaction which occurred throughout the reaction mixture and not just at the reaction interface. Observation in the view cell (depicted in Section 2.2.8) determined that the phases remained immiscible. Improved yields of benzyl bromide were noted (increasing by 10 % in the absence of catalyst), however there was also a large amount of by-product (benzyl methyl ether) formed when pressure was applied.

### 5.2.6 Summary

Gas expanded biphasic systems were investigated as a method for replacing catalysts in phase transfer reactions. Initial results showed that percentage conversions varied only slightly from those under ambient pressure conditions. Visual observation showed a physical change in solvent property on dissolution of $CO_2$ resulting in the formation of a third $CO_2$-rich phase. A thorough analysis of the system was performed and various parameters aside from pressure effects were optimised in order to enhance reactivity. No significant improvement in miscibility of the organic and aqueous phases was noted. Physical parameters identified in Chapters Three and Four suggest that the solvent pairs chosen for this phase transfer study (toluene and water) would have been found to be unsuitable if the polarity of the two solvents on expansion was considered. It was initially hoped that gas expansion of the organic phase would improve miscibility and enhance product yields by improving mass transfer between the two phases. In a consideration of the change in polarity of toluene on expansion, results obtained by the dielectrometry method and the solvatochromism measurements indicate that it is likely that adding $CO_2$ to toluene has actually increased the polarity difference between the toluene and water phases, thus making them even less miscible.

In conclusion, further work remains to be carried out that builds on the characterisation of the properties of gas expanded liquids, particularly the differences in the properties of expanded solvents when various types of solutes are dissolved or suspended, in order to match the solvent system to the process requirements. Such work would use techniques such as solvatochromism and dielectrometry as previously discussed in Chapters 3 and 4 respectively. Furthermore, the data collated in the previous chapters can already be used to identify suitable immiscible/miscible solvent pairs, based upon their expanded solvent properties, and further work in this area is discussed later in this chapter.

## 5.3 Biodiesel Production

### 5.3.1 Introduction

Alternative new and renewable fuels have the potential to solve many of the current social problems and concerns, from air pollution and global warming to other environmental improvements and sustainability issues.[18] Biodiesel[19-23] refers to lower alkyl esters of long chain fatty acids, which are synthesised either by trans-esterification with lower alcohols or by esterification of fatty acids. Four primary methods are employed to make biodiesel, direct use and blending, microemulsions, thermal cracking (pyrolysis) and transesterification. Transesterification of vegetable oils and animal fats is the most common method. The transesterification reaction is affected by molar ratio of glycerides to alcohol, catalysts, reaction temperature, reaction time and free fatty acids and water content of oils or fats.

Despite having a myriad of advantages, biodiesel also has a few downsides. Producing biodiesel on a large scale requires considerable use of arable areas, and the uptake of large areas of land will have a considerable impact on the level of global food supply. Transportation and storage of biodiesel also requires special treatment. The properties of biodiesel make it undesirable for use at high concentrations. In its pure form, biodiesel is very viscous at low temperatures, which can cause problems for outdoor storage tanks in colder climates.

Over 350 oil-bearing crops have been identified, among which only sunflower,[22, 24, 25] safflower, soybean, cottonseed, rapeseed, and peanut oils are considered as potential alternative fuels for diesel engines.[26] Derived from a natural source, the esterification of biodiesel results in physical properties that can vary slightly, although most do not deviate greatly from the optimum fuel properties for diesel. A difference may also be observed between oils depending on the geographical location in which they have been grown and circumstances which have been derived from the weather or soil conditions.

A key problem associated with the use of pure vegetable oils as fuels, for diesel engines are caused by high fuel viscosity in compression ignition. The advantages of vegetable oils as diesel fuel[27] are:

- Readily available
- Renewable
- Higher heat content
- Lower sulfur content
- Lower aromatic content
- Biodegradable

### 5.3.2 Transesterification Reaction

The manufacturing procedure for biodiesel is much the same regardless of the feedstock used. Transesterification or alcoholysis is the displacement of alcohol from an ester in a process similar to hydrolysis, with the exception that alcohol is used instead of water.[28] This process has been widely used to reduce the high viscosity of triglycerides. The transesterification reaction is represented by the general equation as shown in Figure 5.6.

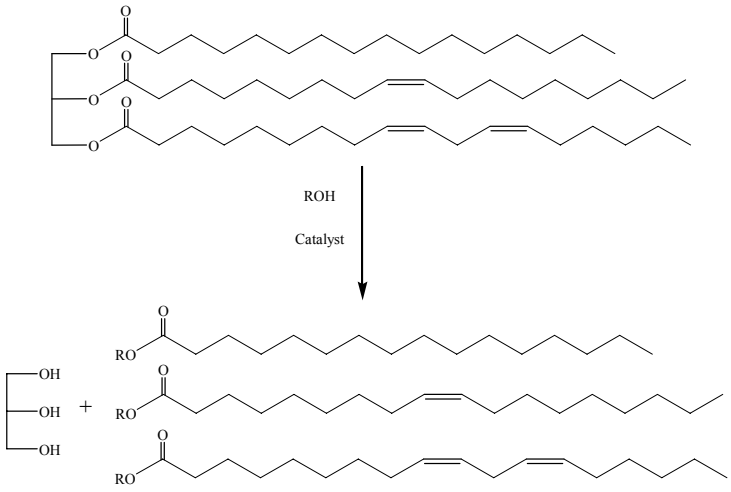


***Figure 5.6*** *Transesterification of triglycerides to alkyl esters of fatty acids and unwanted by-product glycerol.*

Transesterification of triglycerides produces fatty acid alkyl esters and glycerol. The glycerol layer settles down at the bottom of the reaction vessel. Diglycerides and monoglycerides are the intermediates in this process as depicted in Figure 5.7.

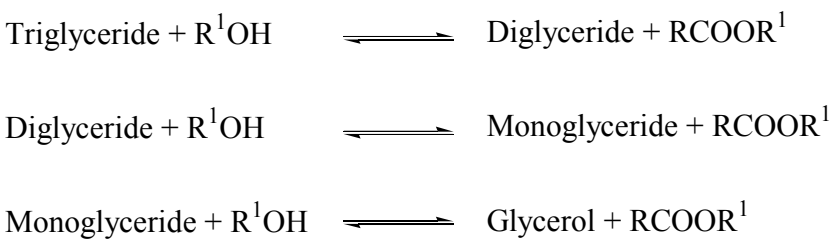


***Figure 5.7*** *General equation for the transesterification of triglycerides. The reaction is reversible so the equilibrium between the products and reactants must be forced to the formation of fatty acid esters. This can be easily done by choosing the appropriate ratio of initial reactants (excess of alcohol)*

The liberated fatty acid esters comprise of a mixture of C-18 species, such as stearic, linoleic, linolenic, and oleic acid; and C-16 derivatives such as palmitic acid in varying compositions which are dependent on the source.

Glycerol is a by-product and must be removed before biodiesel can be used as fuel, as the viscosity of the glycerol present in the mixture impedes the high pressure injection system of a modern diesel engine and may result in damage. Despite being an un-wanted by-product in the biodiesel process, glycerol has important value in many different industries. It is an important ingredient in innumerable pharmaceutical and cosmetic preparations because of its valuable emollient and soothing properties. In the food and beverage industry, glycerol serves as a humectant helping to retain moisture, in the preservation of foods.

Methanol and ethanol are the most frequently used alcohols, especially methanol because of its low cost and its physical and chemical advantages (polar and shortest chain alcohol). Neither are miscible with triglycerides at ambient temperature, and the reaction mixtures are usually mechanically stirred to enhance mass transfer. During the course of the reaction, emulsions usually form. In the case of methanolysis, the emulsions form quickly and are easily broken down to form a lower glycerol rich layer and upper methyl ester rich layer. In ethanolysis, these emulsions are more stable and can complicate the separation procedure and the subsequent purification of esters.[29] The emulsions result in part by formation of the intermediate monoglycerides and diglycerides, which have both polar hydroxyl groups and nonpolar hydrocarbon chains. Ethanol produces a more environmentally benign fuel. The Dangerous Properties of Industrial Materials[30] reports that;

*"The systemic effect of ethyl alcohol differs from that of methyl alcohol. Ethyl alcohol is rapidly oxidised in the body to carbon dioxide and water, and in contrast to methyl alcohol no cumulative effect occurs. Methyl alcohol ... once absorbed is only very slowly eliminated. ...in the body the products formed by its oxidation are formaldehyde and formic acid, both of which are toxic. Because of the slowness with which it is eliminated, methyl alcohol should be regarded as a cumulative poison."*

Despite its separation difficulties, ethanol is also the preferred alcohol in this process as it is derived from agricultural products and is renewable and biologically less objectionable in the environment. It can also be readily generated and purified by fermentation of vegetable matter and other biomass. Methanol on the other hand, is generally extracted from mineral oil processes.

### 5.3.3 Catalysts for triglyceride alcoholysis

The alcoholysis reaction can be catalysed by alkalis, acids, or enzymes. The alkalis include NaOH, KOH, carbonates and corresponding sodium and potassium alkoxides. Sulfuric acid, sulfonic acids and hydrochloric acid are usually used as acid catalysts. Lipases also can be used as biocatalysts. Alkali-catalysed transesterification is much faster than acid-catalysed transesterification and is most often used commercially. One of the main factors, which are very important at the beginning of alcoholysis, is how to improve mass transfer from the aqueous phase (ethanol) to the organic phase (triglyceride). This can be done by effective agitation or by the inclusion of an additional cosolvent which can influence the creation of the so-called pseudo-homogeneous phase.

Different mineral acids ($H_2SO_4$, $H_3PO_4$, HCl), as well as some organic acids (sulfonic acid), are usually used as catalysts for triglyceride alcoholysis. The reaction rate is very slow and desired conversions can take more than 70 hours to achieve. Acid-catalysed alcoholysis is generally employed in the case of vegetable oil containing more free fatty acids and water and, moreover, in the case of used vegetable oil as a feed for biodiesel production.[20, 31]

### 5.3.4 Supercritical Alcoholysis (SCA)

The transesterification of triglycerides by supercritical methanol, ethanol, propanol and butanol, has proved to be the most promising process. Supercritical conditions for alcohols are characterised with high density similar to the density of the liquid phase. The lower viscosity and diffusivity of supercritical compared to liquid alcohol, which are closer to these characteristics of alcohol in the gas phase are important parameters for creating good contact between the alcohol and the oil.

Methanol loses its polar behaviour under supercritical conditions which is also an advantage of SCA. Thus, the behaviour of supercritical methanol is comparable to the behaviour of a nonpolar solvent and it begins to act as a good medium and solvent in which the desired solubility of glyceride could be achieved. Supercritical methanol has also been used to develop a non-catalytic biodiesel production route that allows the design of a simple process and achievement of high yields because of simultaneous transesterification of triglycerides and methyl esterification of fatty acids.[32] Saka *et al*. investigated the transesterification of sunflower oil in sc methanol and supercritical ethanol at various temperatures (475 to 675 K).[33]

This work aims to establish if $CO_2$ at moderate pressures in liquid solvent could be used in its 'expanded' form to act as a solvent diluent to improve the performance of the reaction. The solubility of $CO_2$ would enable the polarity of the alcohol reagent to be reduced, similarly to that seen under supercritical conditions, yet still maintaining ambient temperature conditions and only exhibiting mild pressures. Soybean oil and Rapeseed oil were chosen as the feedstocks of study, because of their favourable cetane number and physical properties. The alcoholysis of soybean oil and rapeseed oil was compared at both ambient and pressurised conditions keeping all other parameters such as temperature, agitation, and reaction time constant.

### 5.3.5 Results and Discussion

Preliminary work carried out on the esterification reaction found that temperature had no detectable effect on the ultimate conversion to ester. However, at higher temperatures (< 100 °C) less time was required to reach maximum conversion. It was assumed that the expected cost of energy for heating would exceed the value of time saved by using higher temperatures. Room temperature was therefore considered to be the optimum temperature for conversion. A higher degree of conversion could be obtained if the oil and alcohol phases were homogenised. This would require

extremely vigorous agitation. Similarly to phase transfer catalysis, when the reaction mixture is monophasic, the conversion and time taken to reach maximum yield are independent of the stirring rate. The role of the $CO_2$ was to act as a mixing agent between oil and ethanol in order to carry out the reaction in a single phase reaction mixture.

On reaction completion, the biodiesel was carefully extracted. Excess alcohol and residual catalyst were washed from the ester with warm water. The ester phase was placed in a separating funnel, water was added gently into the top of the funnel. The excess alcohol and catalyst were removed by the water as it is percolated through the funnel. The washing procedure was repeated four to five times. During the process, some of the ester formed an emulsion with water and required a 24 hour settlement time before the layer could be analysed. The repercussions of not removing the catalyst rendered the biodiesel still catalytically active, and, on contact with water the esters would result in saponification. The presence of soap could consume the catalyst and reduce the catalytic efficiency, as well as causing an increase in viscosity, possibly leading to the formation of gels, resulting in difficulty when trying to achieve separation of glycerol on reaction completion.

Contamination of biodiesel with soaps (salts of the free fatty acid) leaves it viscous and can result in the formation of a precipitate of soap.[*] The values are calculated as a ratio of the peak area of ethyl caprate (internal standard) from GC data.

*Retention times:*

$R_t$ (ethyl caprate) = 11.38 min

$R_t$ (ethyl linolenate) = 18.39 min

$R_t$ (ethyl linoleate) = 2.00 min

$R_t$ (ethyl oleate) = 2.24 min

$R_t$ (ethyl stearate) = 2.28 min

Table 5.1 and Figure 5.8 compare the results of both the soybean oil and rapeseed oil alcoholysis at ambient pressure, and at 50 bar of $CO_2$.

[*] *If spilt on a wet fuel station forecourt, the soap will produce a slipping hazard, but the biggest problem with saponified biodiesel occurs if it enters an engine. The soaps in the fuel clog a high-pressure injector system and cause pump failure and engine damage.*

***Table 5.1*** *Data on formation of ethyl esters from biodiesel reaction in four different systems based on the ratio of ethyl ester to ethyl caprate*

| | **Ethyl Ester:Ethyl Caprate** | | | |
|---|---|---|---|---|
| | *Ethyl Linolenate* | *Ethyl Linoleate* | *Ethyl Oleate* | *Ethyl Stearate* |
| Rapeseed (1 bar) | 1.660 | 0.660 | 2.630 | 5.550 |
| Rapeseed (50 bar) | 0.518 | 0.666 | 2.611 | 0.277 |
| Soybean (1 bar) | 0.223 | 0.694 | 0.351 | 0.063 |
| Soybean (50 bar) | 0.285 | 1.119 | 0.500 | 0.095 |

Where:

$C_{20}H_{34}O_2$ Ethyl Linolenate (9,12,15–Octadecatrienoic acid)

$C_{20}H_{36}O_2$ Ethyl Linoleate ( 9,12-Octadecadienoic acid)

$C_{20}H_{38}O_2$ Ethyl Oleate ( 9–Octadecatrienoic acid)

$C_{20}H_{40}O_2$ Ethyl Stearate (Octadecanoate acid)

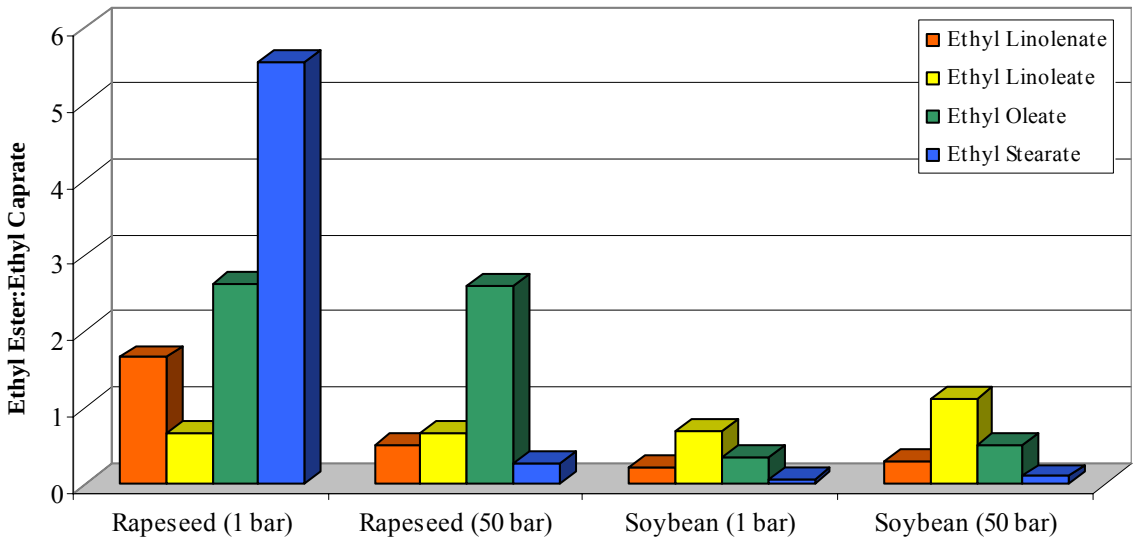


***Figure 5.8*** *Comparison of various biodiesel reactions in rapeseed oil and soybean oil at atmospheric pressure, and under gas expanded liquid (50 bar) conditions.*

Figure 5.8 shows that in rapeseed oil two of the ethyl esters, ethyl linolenate and ethyl stearate varied in product distribution quite appreciably when pressurised with $CO_2$. Yields of both these esters reduced significantly in the presence of $CO_2$. The remaining two esters, ethyl linoleate and ethyl oleate remained approximately the same. Soybean oil under gas expanded conditions, showed slightly better yields of all the ethyl esters with the most significant increase being that of the ethyl linoleate and ethyl oleate. The most noticeable effect of pressurisation was the large reduction in stearate production in the rapeseed oil. It is thought that on pressurisation the influence of $CO_2$ on the solubility of the reaction mixture results in insolubility of the saturated acid and hence hinders its formation during esterification. Pressurisation allows for some selective esterification, but the direction of selectivity required is very much dependent on the solubility of the products in expanded systems. Solubility is favoured towards more nonpolar substituents as expected. This work illustrates the difference in solvent behaviour when a system is expanded with $CO_2$. Although gas expansion does not provide a viable route for the production for biodiesel, this research does show that product distributions in the ethanolysis reaction can be altered depending on solute solubilities in the solvent of choice.

## 5.4 Solute Solubility Determination

Solubility data provide an insight into how well a fluid performs as a solvent for a particular solute which is of key importance in process design. The solubility of compounds in sc fluids has been the most extensively investigated area of sc fluid research. Solubility in supercritical fluids is mainly determined by the chemical functionality of the solute, the nature of the sc fluid solvent being used, and the operating conditions. Different molecular interactions govern the solubility and extractability of a compound in a SCF (solute-solvent interactions versus solute-matrix or solute-solute interactions). Solubility data of a solute in a solvent will give an indication of the extractability of that compound in that solvent.

### 5.4.1 Solubility Methods

Close to the critical point, the physical properties of the fluid change considerably and a significant difference in the solubility of substances is noted. Supercritical fluid extraction (SFE) is a procedure by which the solvent power of a supercritical fluid is utilised in order to induce separation at temperatures and pressures near the solvents critical point. Reported solubilities for nonpolar solids and liquids in sc$CO_2$ range between 0.1 to 10 mol %.[34] As well as $CO_2$, ethylene and ethane, SCF solvents studied in the literature include xenon (less polar/polarisable solvent than carbon dioxide),[35] toluene,[36] ammonia,[37] and water.[38] Carbon dioxide is one of the most commonly used gases in supercritical fluid extraction. It is an easy gas to handle, it is inert, nontoxic and nonflammable, and it has a convenient critical temperature.

An ideal extraction method should be rapid, simple and inexpensive to perform. It should yield quantitative recovery of the target analytes without loss or degradation and the sample obtained should be immediately ready for analysis without additional concentration or fractionation steps. No additional laboratory wastes should be generated. Liquid solvent extractions fail to meet a number of these goals but SFE has emerged as a promising tool to overcome these difficulties. The major problem encountered with sc $CO_2$ and other commonly used sc fluids, such as ethane, is that they are nonpolar, which precludes the dissolution of a number of polar solutes.

### 5.4.2 Solubility Investigations in Supercritical Systems

There is a great incentive to improve polarity, and it has been found that the addition of a small amount of suitable cosolvent can greatly enhance the solvent power of sc $CO_2$. Kurnik and Reid[39] demonstrated that the solubility of a solid in a sc solvent can be enhanced in some instances by the presence of a cosolvent. The concept of adding cosolvent to a SCF first received attention many years ago however, the solubility measurements of solids in SCFs with cosolvents is still a growing area.[40]

Schmitt and Reid[41] have determined the solubility of phenanthrene and benzoic acid in supercritical carbon dioxide and in supercritical ethane using benzene, cyclohexane, acetone or methylene chloride as cosolvents. They noted a significant enhancement in the solubility of the triphasic system, benzoic acid - ethane – acetone, but no significant observations were made for any of the other systems studied. IR data confirmed the formation of a complex between benzoic acid and acetone but not for the other solute-cosolvent mixtures. Acetone served as an entrainer for benzoic acid in supercritical ethane but not in supercritical carbon dioxide, the author reported that this indicated the importance on the choice of supercritical solvent used. Walsh *et al*.[42] studied the chemical functionality of the two carbonyl oxygens of carbon dioxide that compete with other hydrogen bond acceptors for the hydrogen bond donors. They also investigated the comparative concentration of carbon dioxide and cosolvent. The cosolvent was shown to have an important role in determining the selectivity for a component in a mixture of solutes.[43]

For the majority of systems, the resultant increase in solvent power of the SCF when a cosolvent is added is due to an increase in the density of the solvent mixture. This increased solubility is comparable to that which can be achieved with the pure solvent through variation of temperature and pressure. Density variation is not the only reason for large enhancements of solubility due to the addition of a cosolvent. Depending on the solute, this can also be due to the chemical interaction between the solute and the cosolvent. It is known that solubility may increase by a factor of three to seven by the addition of a small amount of polar solvent for systems that form strong hydrogen bonds.[44] The most frequently used polar cosolvents include methanol and acetone.

In Chapters three and four, the tunable properties achievable by expanding liquid solvents with moderate pressures of $CO_2$ gas have been demonstrated. These systems differ to cosolvent modified supercritical fluids in the sense that a gas expanded liquid is a liquid containing a dissolved gas (usually resulting in volume expansion of the liquid solvent), whereas a cosolvent modified supercritical fluid is mostly a gas containing a small amount of a liquid entrainer exposed to high pressures and temperature to maintain the supercritical conditions. One of the main disadvantages associated with cosolvent modified sc systems is the resultant increase in the critical pressure of the mixture from adding co-solvent, and this has limiting effects on processing variables. The advantage of using gas expanded liquids over SCFs is the ability to continue to tune physical properties when the possible combinations of solvent, expanding gas, and/or cosolvent are taken into consideration. GXLs are able to achieve a wider spectrum of solvent properties extending to the polar solvent region allowing for the solubility of polar solutes and yet still operating at only moderate pressure of expanding gas.

This work reports the first measured solubilities of organic solutes in gas expanded ethanol and gas expanded dimethyl sulfoxide determined using the dielectrometry method. Solubilities for the same solutes were also determined in liquid $CO_2$, $scCO_2$, and $scCO_2$ with ethanol as an entrainer. Solvent systems of differing polarity were chosen to compare the suitability of GXLs in replacing current $CO_2$-based solvents. The higher polarity of the two gas expanded solvents (ethanol and DMSO) resulted in higher solubilities of both polar and nonpolar solutes than in supercritical $CO_2$, this makes them more attractive replacement solvents for use in current applications involving polar compounds such as extraction techniques and as solvents in chemical reactions.

### 5.4.3 Results and Discussion

The solubilities of salicylic acid, toluic acid and naphthalene were measured in liquid $CO_2$, liquid phase ethanol, gas expanded ethanol, and gas expanded DMSO at room temperature (except for sc $CO_2$ which was measured at 323 K, and 120 bar). The cell shown in Figure 2.3 was used to carry out solubility measurements. Excess solute was loaded into the reaction vessel and placed between the two metal sieves. The capacitance was measured as described in section 2.3.2 in five different solvent systems. The solubility of solid solutes in a fluid is found by converting capacitance

values to relative permittivity values, and by using the Clausius-Mossotti model outlined below.

The theoretical approach for the calculation of solubility used by Hourri and co-workers was modified slightly to incorporate the use of polar solutes.

For a polar solute the first dielectric virial coefficient is found to be[45]

$$A_e^{\ s} = \frac{4\pi Na}{3}\left(\alpha + \frac{\mu^2}{3k_BT}\right) \qquad \textbf{(5.4)}$$

where $\boldsymbol{N_a}$ is Avogadros number and $\boldsymbol{\alpha}$ is the molecular polarisability, $\boldsymbol{\mu}$ is the permanent dipole moment, $\boldsymbol{k_B}$ is the Boltzman constant and $\boldsymbol{T}$ is the temperature in Kelvin. Data for $\boldsymbol{\mu}$ was approximated using Spartan Pro[46] molecular modelling computer program.

For a nonpolar solute the first dielectric virial coefficient is given by[47]

$$A_e^{\ s} = \frac{4\pi Na}{3}\alpha \qquad \textbf{(5.5)}$$

Equation 2.4 then gives the working relation for the solubility determination, which is

$$\rho^s = \frac{CM' - CM''}{A_e^{\ s}} \qquad \textbf{(5.6)}$$

where,

$$CM = \frac{(\varepsilon_r - 1)}{(\varepsilon_r + 2)} \qquad \textit{Clausius-Mossotti function} \ \textbf{(5.7)}$$

and $\varepsilon_r$ is the relative permittivity. The primed quantities indicate the saturated solvent used, the double primed quantities belong to the solvent before the addition of solute.

The capacitance values used in Equation 2.1 for the calculation of the relative permittivity were taken from an average of five replicate readings. The readings were found to vary by no more than ± 0.005 pF. The calculated relative permittivity values were found to vary by no more than ± 0.03 resulting in an error maximum of ± 2 %. The molecular polarisabilities used in Equation 5.5 to calculate the first dielectric virial coefficient were taken from the literature[16] or calculated via an additive method that was introduced by Le Fevre.[48]

The uncertainty in the molecular polarisability value is unknown but if a theoretical maximum uncertainty of 5 % is assumed then the mole fraction solubility is found to fluctuate by no more than ± 0.5 %. For polar solutes, the molecular polarisability[34,35] and permanent dipole moment values[49] are needed to calculate the first dielectric virial coefficient from equation 5.5. In this equation the molecular polarisability is found to be insignificant and the dipole moment value dominates the first dielectric virial coefficient. If a theoretical 5 % uncertainty is taken in both these properties the error in the mole fraction solubility is found to increase to ± 6 %. Actual uncertainties are likely to be less but ± 0.5 % and ± 6 % must be taken as the maximum error limits for the nonpolar and polar solutes respectively. The molecular polarisability, dipole moment and first dielectric virial coefficient values for each of the solutes used in this work are listed in the Appendix in Table 9.

The dielectric constants for the gas expanded solvents are significantly higher than that for liquid $CO_2$, or supercritical $CO_2$, indicating that these are the more polar solvents which would suggest that polar solutes should have a better solubility in the expanded solvents than in supercritical or liquid $CO_2$.

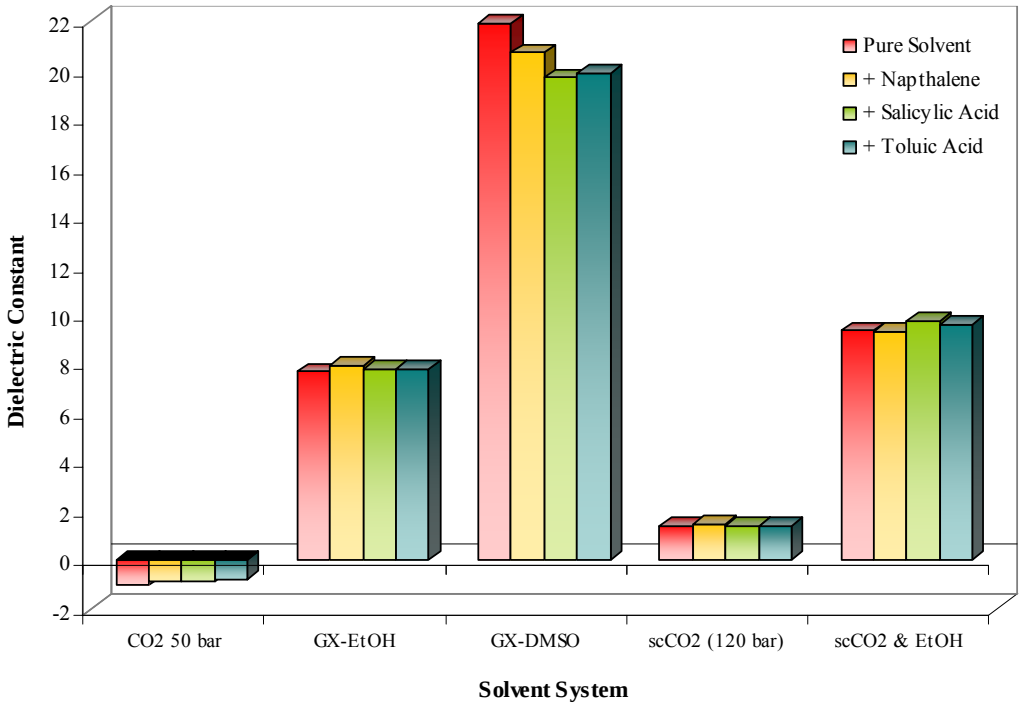


***Figure 5.9*** *Solubility comparison of naphthalene, salicylic acid, and toluic acid in liquid $CO_2$, gas expanded ethanol, gas expanded DMSO, $scCO_2$, and $scCO_2$ with ethanol as cosolvent*

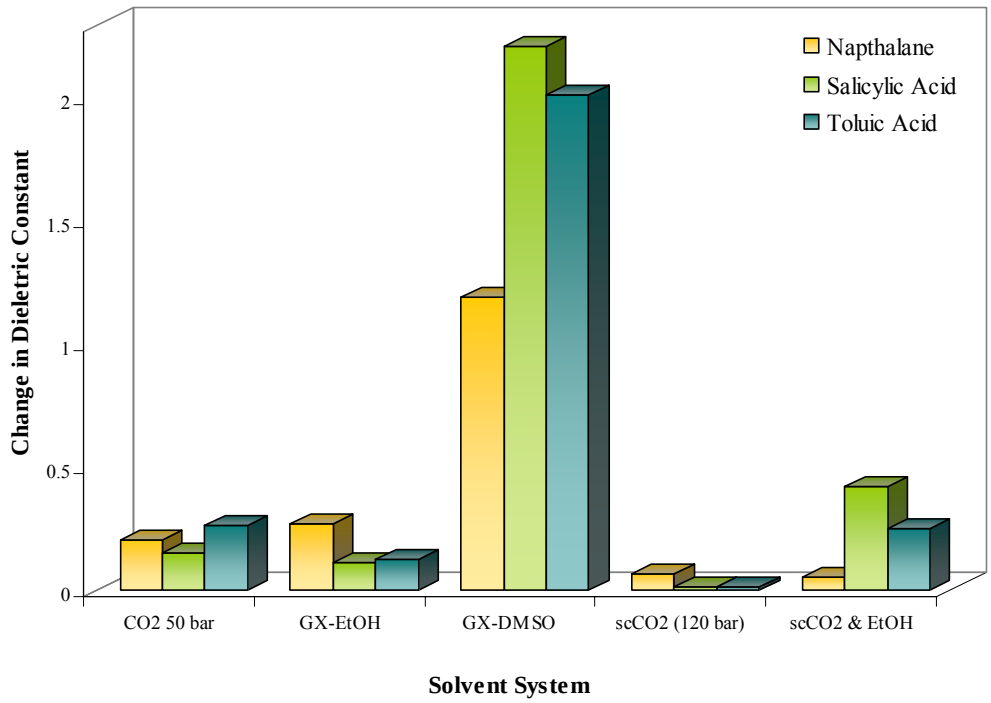


***Figure 5.10*** *Comparison of the change in dielectric constant of each solvent system when a solute is added (in excess to allow saturation)*

Figure 5.9 compares the polarity as indicated by the dielectric measurement for the pure solvent, and the saturated solvent on addition of the solute. All of the solutes showed a certain degree of solubility in each solvent system studied, and a plot of the change in dielectric constant form the pure to the saturated system (Figure 5.10) shows that a greater degree of solubility enhancement was seen in both of the gas expanded solvents, ethanol and DMSO. The more polar expanded solvents showed a greater degree of change when saturated with toluic acid. Conversely, liquid $CO_2$ performed as a slightly better solvent for the solutes studied than sc $CO_2$ and sc $CO_2$ with ethanol as cosolvent. Table 5.2 below shows the values for mole fraction solubility of each solute in the five different solvent systems studied. In Figure 5.11 the solubility of the solutes as a function of mole fraction solubility is plotted. Results for liquid $CO_2$ have been omitted due to limitations with the equipment, where it was noticed that low dielectric materials generated large numerical discrepancies which followed through in the mole fraction calculations.

***Table 5.2*** *Mole fraction solubilities of naphthalene, salicylic, and toluic acid in various pressurised solvent conditions*

| ***Where Ps = (CM'-CM''/A)*** | | | |
|---|---|---|---|
| **Solvent** | **Naphthalene** | **Salicyclic Acid** | **Toluic Acid** |
| **$CO_2$ 50 bar**[†] | 14.002 | 2.617 | 5.990 |
| **GX-EtOH** | 0.203 | 0.020 | 0.032 |
| **GX-DMSO** | 0.158 | 0.073 | 0.096 |
| **sc$CO_2$ (120 bar)** | 0.377 | 0.016 | 0.023 |
| **sc$CO_2$ & EtOH** | 0.028 | 0.058 | 0.050 |

[†] Mole fraction values for compressed $CO_2$ are clearly wrong and from this point onwards this solvent will not be used in any further comparisons.

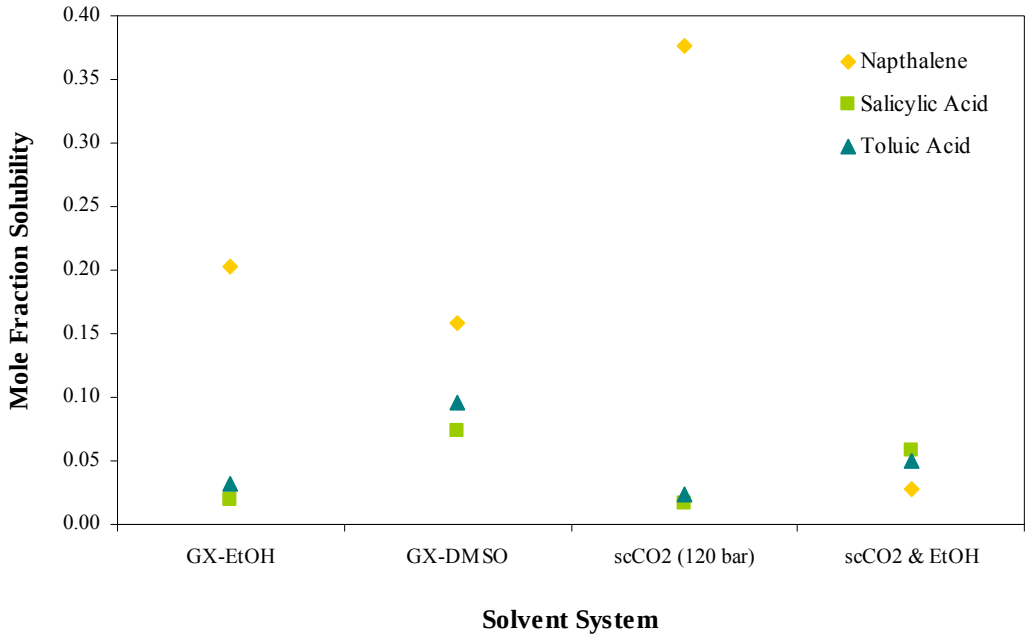


***Figure 5.11*** *Solubilities of naphthalene, salicylic, and toluic acid in gas expanded and supercritical solvent systems*

Both of the supercritical solvent systems studied behaved as expected. The pure sc $CO_2$ showed greater mole fraction solubility towards the nonpolar solute naphthalene, and less so to toluic acid, and even less towards salicylic acid which was the most polar solute investigated. The ethanol-modified sc $CO_2$ behaved slightly differently, and observed an increase in solubility towards salicylic acid, followed by toluic acid. Poorer solubility in sc$CO_2$ with ethanol was noticed for naphthalene. This was as expected as the addition of ethanol increases the overall polarity/polarisability of the solvent changing its physical properties such that it obeys the rules of 'like dissolves like' and therefore acts as a better solvent towards more polar solutes, and a poorer solvent for nonpolar solutes.

The dielectrometry method studied in Chapter 3 has been used for the determination of solute solubility studies of nonpolar naphthalene, toluic acid, and polar salicylic acid in various solvent systems of differing polarity. For the first time, solubility data for these solutes have been measured in gas expanded systems, and the results have been compared and contrasted with the behaviour of these solutes in supercritical and liquid $CO_2$. Gas expanded liquids have shown a great potential for tunability as determined in Chapters 3 and 4, and the present study on solute solubility has shown their potential as replacement solvents for processes which currently

undergo supercritical extraction. $CO_2$ expanded DMSO is the most versatile solvent in terms of its ability to solvate nonpolar and polar solutes, and supercritical $CO_2$ is the worst solvent in this study as it was only suitable for nonpolar solutes. Although the mechanism of the solubility enhancement and the selectivity improvement by a cosolvent is very complex, the interactions between the solutes and cosolvents play an important role when both polar solutes and polar cosolvents are involved (and nonpolar solutes with nonpolar solvents).[42, 50, 51] This leads to significant increases in both the solubility and the selectivity. This gives GXLs a practical advantage over comparable supercritical systems in terms of specialised equipment and the outlay associated with it. In terms of solvent power and transportability when compared to gases and liquids, GXLs can overcome solubility limitations that are normally observed in supercritical fluids due to their preference towards nonpolar solutes.

## 5.5 Phase Separation in Pressurised Systems

High pressure $CO_2$ extraction from liquid solutions is a growing area of research in spite of process difficulties that remain to be solved. It has the possibility to operate as a continuous automated process with much lower operating costs than that required from the extraction of solids. Supercritical fluid extraction has received much attention for its potential for laying the foundation for processes that would make better alternatives to energy-intensive techniques such as distillation. Supercritical or near-critical fluids have been proven successful as suitable solvents for the extraction of organic compounds from aqueous solutions. The chemical nature of high pressure solvents may rule-out the need for separations involving distillation or extraction with organic solvents.

From the late 1970's, a number of investigators have worked on supercritical fluid extraction of ethanol from fermentation broths to obtain "dry" ethanol, for use as fuel in motors. Although this application has now been abandoned, a plethora of information on the phase equilibria of the $CO_2$-ethanol-water system has resulted from its publication. High pressure techniques used for the extraction of ethanol from the fermentation of aqueous solutions have several attractive aspects as recovery processes for ethanol, and have been investigated by many researchers.

The dehydration of ethanol using supercritical $CO_2$ has been extensively deliberated upon, since it is non-flammable and nontoxic, and allows ambient-temperature operation to be performed. The $CO_2$ solvent extraction method can be optimised for ethanol selectivity by determining the most favorable temperature, pressure and entrainer. Nagahama *et al.,*[52] and Brignole and co-workers[53] have investigated the use of $CO_2$ as a solvent and have reported that the azeotropic concentration of ethanol-water could be broken using $CO_2$ solvent at 313 K and 3.9 to 5.8 MPa, 333 K and 10 MPa, and liquid $CO_2$ (293 K) respectively. Several studies on the phase behaviour of the carbon dioxide-ethanol-water systems at high pressures have been reported in the literature. Baker and Anderson[54] have shown that ethanol extraction with compressed $CO_2$ does not result in alcohol concentrations that are greater than that corresponding to the ethanol-water azeotrope.

Multiphase equilibria for the carbon dioxide-alcohol-water system have been reported. Yoon *et al*[55] measured the two and three phase equilibria for the carbon dioxide-methanol-water system. Efremova and Shvartz[56, 57] investigated the liquid-liquid and gas-liquid critical end points for the carbon dioxide-methanol (and

ethanol)-water systems. Lim and Lee have determined the tie-lines in the two phase region and three phase equilibrium compositions at temperatures close to the critical point of carbon dioxide also for the carbon dioxide-ethanol-water system.[58]

### 5.5.1 Phase Equilibria in $CO_2$-based systems

The use of solvents in chemical industries poses a threat to our ecosystems due to their high volatility and toxic nature. 'Benign' replacement solvents are currently being sought to curtail problems inherent with the release of solvents into the environment. Carbon dioxide based expanded solvents have already started to show 'promise' as alternative media for performing catalytic reactions such as oxidations,[59] hydroformylations,[60, 61] and solid-acid catalysed reactions.[62] So far, researchers have concentrated on determining transport properties, such as that by Sassiat *et al*.[63] who reported diffusion coefficients for benzene in $CO_2$-expanded methanol showing a four and five fold increase on expansion with $CO_2$. Similar expansions have been experienced by Kho *et al*.[64] who noticed a fourfold decrease in solvent viscosities of $CO_2$ expanded fluorinated solvents when $CO_2$ was added. Laird *et al*.[65] have reviewed work on the calculation of phase equilibria and transport properties of GXLs using molecular simulation methods. They determined Monte Carlo simulation and PR-EOS calculations resulting from the volume expansion properties, and pressure compositions and density diagrams in GXL systems studied.

Chapters three and four have shown that expansion of an organic solvent by $CO_2$ can be used to tune liquid density, solubility strength, and both local and bulk polarity properties. In order to optimise the use of $CO_2$ for applications in industry it is useful to determine knowledge of their solvent compatibility in particularly for multi-component mixtures. Experimental data on carbon dioxide expanded liquids are now available in the literature[66-68] but data in general is still quite sparse. The limiting case of equilibrium between two components (binary systems) presents a suitable starting point for determining multi-component phase behaviour.

This work reports liquid-liquid equilibria behaviour for 120 binary solvent systems at room temperature comparing their phase behaviour at ambient pressure and gas expanded conditions. Gas expansion can be used to induce miscibility at ambient temperatures for solvent combinations that are biphasic at standard pressure as well as being used in anti-solvent applications for precipitation studies. It is hoped that these

data will assist in providing a new route to enhance reaction rates, and facilitate extraction and separation methods.

### 5.5.2 Results and Discussion

The gas expanded liquid-liquid phase behaviour of 120 binary solvent systems was determined at room temperature and 50 bar of $CO_2$ in a high pressure view cell. The results are shown in Figures 5.12 and 5.13, where 15 different organic solvents were compared for miscibility/immiscibility with each other at both ambient and pressurised conditions. The solvents chosen for this study were based on data obtained for expanded solvents screened in Chapters 3 and 4.

The addition of $CO_2$ will have several effects on the system being studied:

- Change density
- Decrease relative permittivity
- Decrease the polarisability of the solvent
- Decrease the packing density and affect the entropy and free volume
- Change volume expansion ratio's depending on $CO_2$ solubility

The aim of this work is to determine what causes the mixed liquids to change their phase behaviour.

The data is colour-coded for ease of viewing. For both ambient and pressurised conditions, a 'white' box reveals binary solvent systems which are miscible, a blue box represents solvent combinations which are immiscible, and the grey boxes in the second scheme represent systems which were miscible at a fixed volume of liquid solvent, but could be made 'immiscible' if either the volume ratio of the two components was altered (i.e. a 2:1, or 3:1 ratio) or if the volume of liquid solvent added was changed. For example, in the first scheme (Figure 5.12) the red star shows that under ambient conditions 1, 2 dichloroethane is miscible with propan-1-ol, on pressurisation (Figure 5.13) a blue box indicates that the addition of $CO_2$ results in phase separation of the two solvents. The yellow star shows that acetone and acetonitrile are miscible under ambient pressure conditions, and remain miscible even when pressurised. The green star in Figure 5.12 represents the miscibility between

cyclohexane and methanol under ambient conditions, and when pressurised these solvents remain miscible. However, when the volume ratio of liquid-liquid binary solvent in the cell was increased and the system then pressurised, phase separation was induced. At this stage it was not clear as to the extent of 'immiscibility' – as it was believed that visual observation of phase separation was not a clear indication of phase splitting, and equipment limitations meant that we were unable to determine the actual composition of each phase. A 'dye' was used to clarify any phase changes, as can be seen with the cyclohexane-ethanol case in Figure 5.14.

In Figure 5.14, picture 1 shows the miscibility of cyclohexane and ethanol at 50 bar of $CO_2$ under experimental conditions (1.0 mL volume of solvent is used in a 9 mL volume vessel). Picture 2 shows the change in behaviour when the volume of initial liquid solvent is increased to 1.5 mL, and picture 3 shows what appears to be complete phase immiscibility when the solvent volume is increased further more to 2 mL. The 'dye' used to distinguish between the two phases in this case is phenol blue. Earlier work in Chapter 3 showed how the polarity of a solvent can be determined visually by noting the colour of the dye in the solvent of choice. Here we can see that in the case for Phenol Blue, the top phase is less polar than the bottom phase (Phenol Blue becomes more purple towards the nonpolar solvents).

"*Like dissolves like*" is usually the basic rule followed when determining which solvents will phase separate, and which will mix. This means that in order for a solvent to dissolve another substance the intermolecular forces which hold that substance together as a liquid or a solid must be broken. Intermolecular forces between molecules of the solvent must therefore be interrupted in order to accommodate the solute molecules. The ability of different combinations of solvent pairs to enable biphasic operation can be estimated using the principle of "like dissolves like" in with the help of diagrams as shown in Figure 5.15.[69]

Miscibility of liquid solvents is controlled by the enthalpy of mixing, and in order for solvents to mix, the enthalpy of mixing is predominantly negative as generally the enthalpy of mixing is small. This arises from interaction between unlike solvent molecules, and solvent systems which are immiscible are ones where very polar solvents are combined with non-polarisable molecules.

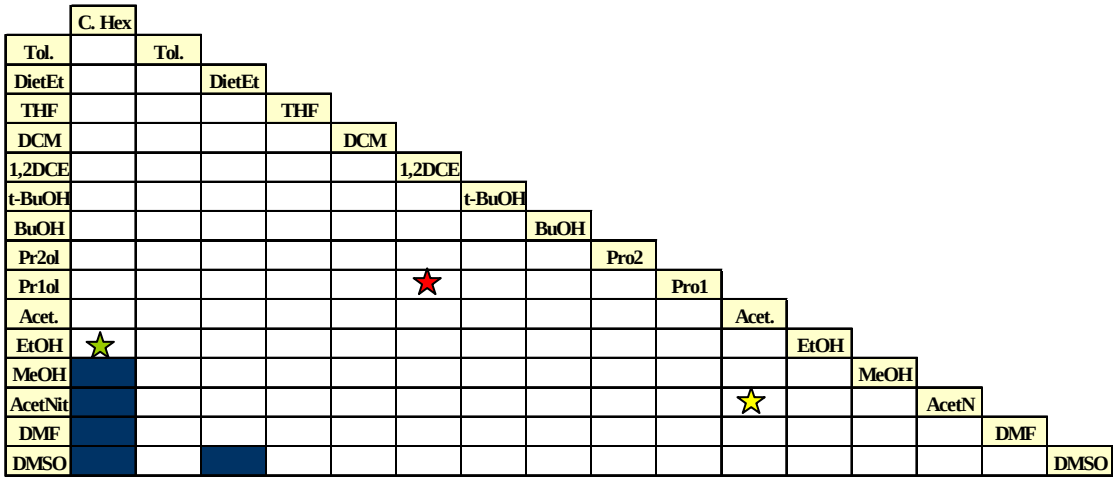


***Figure 5.12*** *Phase behaviour results for binary solvent systems at ambient temperature and pressure. Where a white box represents solvents that are 'miscible', and a blue box represents solvents that are 'immiscible'*

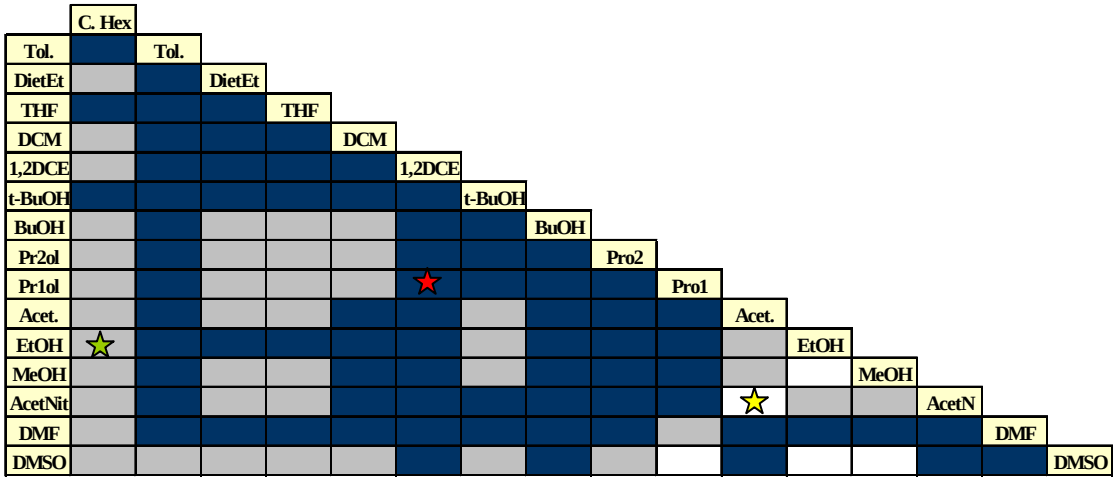


***Figure 5.13*** *Phase behaviour results for binary solvent systems at ambient temperature and 50 bar $CO_2$. The additional 'grey' boxes reveal solvent systems which were initially shown to be miscible when pressurised with $CO_2$, but can be made 'immiscible' if the ratio the two solvents is altered*

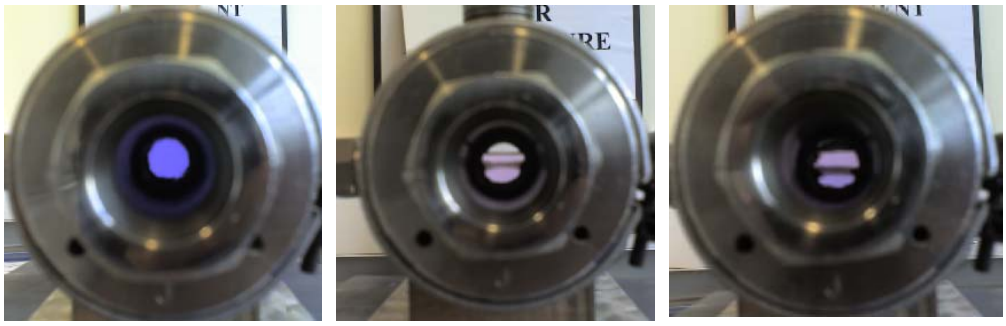

1 2 3

***Figure 5.14*** *The series of pictures taken represent changes in phase behaviour of the binary system cyclohexane-ethanol upon expansion*

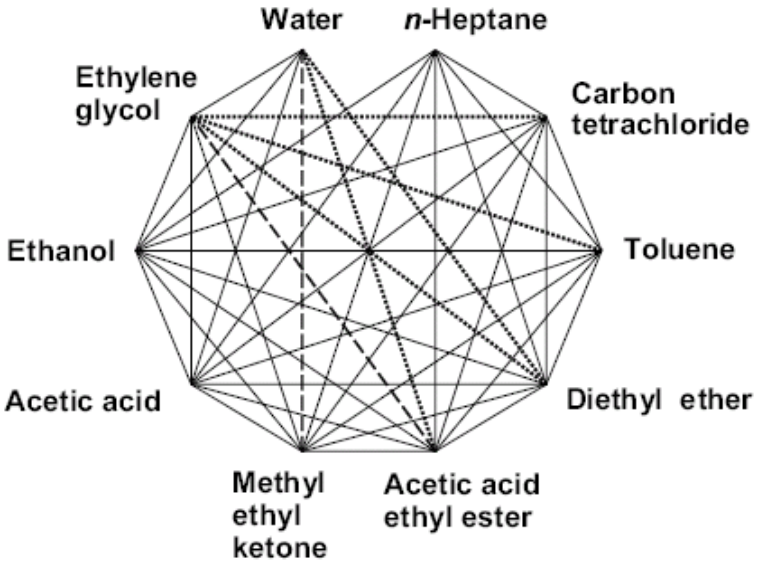


***Figure 5.15*** *Miscibility of organic solvents: —— miscible in all proportions; – – limited miscibility; ..... little miscibility; no line: immiscible*[69]

Results from Figures 5.12 and 5.13, show that under gas expanded conditions it is possible to split almost all of the binary systems studied (with five exceptions). There is no single parameter such as polarity, density or $CO_2$ solubility which determines how binary expanded solvents behave. Taking an example of each it is possible to find an exception to what the predicted result may be. For the case of cyclohexane-DMSO, under ambient pressure conditions, both solvents are at opposite ends of the π* polarity scale from the solvents studied where cyclohexane has a π* of 0.0 (nonpolar), and DMSO has π* of 1.0 (polar). On pressurisation, it would be expected that $CO_2$ would be preferentially more soluble in cyclohexane (due to similarities in polarity), than in DMSO. This would decrease the polarity of cyclohexane when expanded (making it even more nonpolar), and increase the polarity difference between cyclohexane and DMSO even more. If the rule of thumb 'like dissolved like' is to be believed, then a switch in phase behaviour from immiscible to miscible for this system on expansion is very 'out of character'. Cyclohexane and DMSO are at opposite ends of the polarity scale (Kamlet & Taft's π*-scale of polarisabilities) and so you would not expect the two solvents to be miscible. The results from the phase behaviour observations from this study are shown in Figure 5.16.

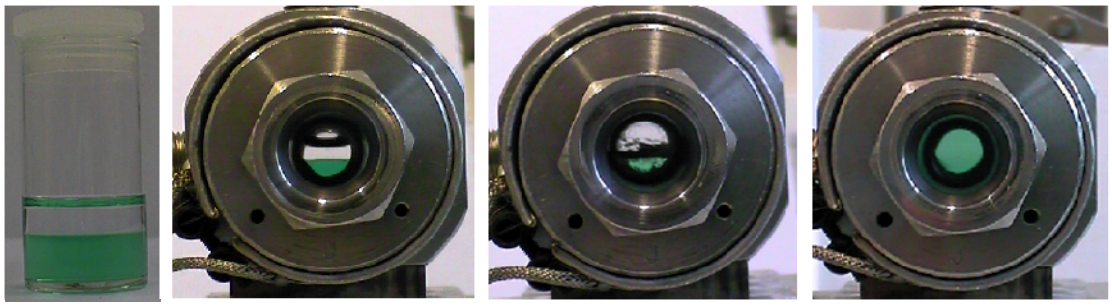

***Figure 5.16*** *Phase behaviour of cyclohexane-DMSO binary solvent system. Under ambient pressure (in sample vial, and view cell picture 1), during pressurisation, and after reaching an equilibrated state*

Using data determined in Chapter 4, it is possible that the calculated solubility of $CO_2$ in cyclohexane may be to such a large extent that for some cases (in particularly this one), $CO_2$ behaves as the major solvent component, and cyclohexane acts more like a 'solute', thus inducing miscibility with DMSO. Similar polarity based systems were also tested for phase miscibility, including cyclohexane-glycerol-$CO_2$, and

cyclohexane-ethylene glycol-$CO_2$, but neither of which resulted in a phase change to form a single phase mixed system.

To determine which solvents will split upon $CO_2$ expansion it is necessary to consider the thermodynamics of mixing of why the two miscible solvents would phase separate. The enthalpy of mixing of two solvents must be endothermic at ambient pressure and it is likely that the mixing of most solvents will be dominated by enthalpic considerations. It is unlikely that $CO_2$ expansion will lead to a large endothermic process to drive the separation of the two phases, therefore, it seems logical that the increase in entropy obtained by expanding the two components resulted in phase separation. Systems that were immiscible at ambient pressure but miscible when pressurised clearly have $CO_2$ acting as a cosolvent.

The majority of solvents are miscible under ambient pressure conditions. Under these conditions, without $CO_2$, solvent-solvent interactions are strong and so the enthalpy of mixing is exothermic, if the entropy change is small and slightly negative then the solvents will remain miscible. Increased order within the solvent system on addition of $CO_2$ could be the source of phase splitting on expansion. The solvents which do not phase separate all have an alcohol component, and it is possible to relate this to the distinguished behaviour of alcohol-based systems as seen in previous chapters as a result of the inability to break through their strong hydrogen bonds.

To elucidate the cause of the phase behaviour upon pressurisation the densities of the mixed fluids were determined at ambient pressure. Figure 5.17 shows the density of the solvents that mix at ambient pressure. For most solvent mixtures there is only a very small positive change in density when the solvents are mixed compared to the density of the individual components. This suggests that the entropy of mixing is small and generally slightly negative, proving that the entropy must dominate miscibility.

| | C Hex | | | | | | | | | | | | |
|---|---|---|---|---|---|---|---|---|---|---|---|---|---|
| **Tol** | 0.811 | **Tol** | | | | | | | | | | | |
| **Ether** | 0.738 | 0.789 | **Ether** | | | | | | | | | | |
| **THF** | 0.828 | 0.871 | 0.799 | **THF** | | | | | | | | | |
| **DCM** | 1.048 | 1.090 | 1.012 | 1.035 | **DCM** | | | | | | | | |
| **t-BuOH** | 0.780 | 0.826 | 0.751 | 0.834 | 0.889 | **t-BuOH** | | | | | | | |
| **BuOH** | 0.791 | 0.835 | 0.762 | 0.847 | 1.066 | 0.800 | **BuOH** | | | | | | |
| **Pr2ol** | 0.779 | 0.822 | 0.749 | 0.833 | 1.053 | 0.787 | 0.800 | **Pr2ol** | | | | | |
| **Acet** | 0.780 | 0.827 | 0.752 | 0.836 | 1.055 | 0.789 | 0.801 | 0.789 | **Acet** | | | | |
| **EtOH** | 0.783 | 0.822 | 0.750 | 0.833 | 1.053 | 0.787 | 0.797 | 0.784 | 0.788 | **EtOH** | | | |
| **MeOH** | | 0.823 | 0.749 | 0.833 | 1.053 | 0.787 | 0.798 | 0.786 | 0.789 | | **MeOH** | | |
| **MeCN** | | 0.818 | 0.744 | 0.834 | 1.049 | 0.783 | 0.793 | 0.781 | | 0.781 | 0.780 | **MeCN** | |
| **DMF** | | 0.904 | 0.831 | 0.916 | 1.135 | 0.869 | 0.879 | 0.868 | 0.871 | 0.868 | 0.869 | 0.862 | **DMF** |
| **DMSO** | | 0.985 | | 0.992 | 1.210 | 0.943 | 0.954 | 0.942 | 0.945 | | | 0.939 | 1.022 |

**Figure 5.17** Mixed density values for solvent pairs that are miscible at ambient pressure which then phase separate on expansion with $CO_2$. The green boxes represent solvent pairs that are either immiscible at ambient pressure, or solvent pairs which do not change phase behaviour on expansion.

It has been shown in Chapter 4 that pressurisation with $CO_2$ at 50 bar results in an increase in free volume for most solvents suggesting that the entropy of the pressurised systems is more positive which would favour phase separation. Without significant thermodynamic data a detailed analysis of these systems is impossible, but more evidence can be drawn from the systems that remain miscible upon pressurisation. Table 5.3 shows the measured and calculated (determined by the average density of the individual components) density values for the mixed solvent systems at ambient pressure and at 50 bar pressure of $CO_2$. It can clearly be seen that these systems have a considerably larger than expected density at 50 bar $CO_2$ pressure. This means that the entropy of the pressurised systems must be strongly negative. It is presumed that the enthalpy of mixing must be strongly negative otherwise the systems would phase separate. It must therefore be inferred that the systems that split on pressurisation must have a relatively small enthalpy of mixing at ambient pressure.

***Table 5.3*** *Density measurements of four mixed solvent pairs (1:1 ratio) at ambient pressure, and when pressurised with $CO_2$ at 50 bar. 'Expected' densities are also included; these have been determined by taking an average of the density values for the pure components. Expected densities for the expanded systems are taken from an average of the expanded density values determined for expanded solvents in Chapter 4*

| | | **Density at Ambient Pressure (g cm$^{-3}$)** | | **Density at 50 bar $CO_2$ (g cm$^{-3}$)** | |
|---|---|---|---|---|---|
| **Solvent Pair** | | *expected* | *actual* | *expected* | *actual* |
| **EtOH** | **MeOH** | 0.788 | 0.787 | 0.811 | 0.847 |
| **DMSO** | **EtOH** | 0.941 | 0.950 | 0.957 | 0.973 |
| **DMSO** | **MeOH** | 0.943 | 0.958 | 0.946 | 0.976 |
| **Acetone** | **MeCN** | 0.782 | 0.782 | 0.858 | 0.879 |

Chapters three and four have shown the simplistic nature of GXLs by determining their physical parameters, however, initial studies of phase behaviour in binary

mixtures have come up with some interesting results, and it is clear to see that expanded solvents can become very complex when additional cosolvents are added. It is possible to see from Figure 5.13 and Figure 5.14 that GXLs can act as both pro- and anti solvents, and can therefore can be used to induce miscibility (for example PTC applications), or be used in phase separations studies such as the precipitation of solids, in extractions, separations and to replace distillation methods.

This work has assessed the change in phase behaviour of mixed binary solvents on expansion with 50 bar of $CO_2$ at ambient temperature. It was noted that 115 of the 120 system studies showed the ability to undergo phase inversion when pressurised. Phase separation was observed by the addition of a negligible amount of 'dye' to show the difference in polarity between the two separate phases. Secondary studies of those solvents which did not show any change in phase behaviour showed that if experimental conditions were optimised and volume ratio's of the components were altered, then conditions could be achieved where phase behaviour could be inverted such as that seen earlier with the case of cyclohexane-ethanol-$CO_2$.

Gas expanded liquids have many advantages over conventional liquid solvents. Chemically, they have a variable relative permittivity, preferential solvation towards polar species, and improved diffusion rates. Processes can therefore achieve facile separation of products, have a lower viscosity, adjustable solvent power and density, and yet still be inexpensive. Most importantly, the health and safety aspect includes use of a gas that is noncarcinogenic, non toxic and non flammable, environmentally leading to a reduction in the amount of solvent used.

## 5.6 References


1. P. G. Jessop, T. Ikariya and R. Noyori, *Chemical Reviews*, 1999, **99**, 475-493.
2. P. G. Jessop, C. A. Eckert, C. L. Liotta, R. J. Bonilla, J. S. Brown, R. A. Brown, P. Pollet, C. A. Thomas, C. Wheeler and D. Wynne, *Clean Solvents*, 2002, **819**, 97-112.
3. W. Leitner and P. G. Jessop, *Chemical synthesis using supercritical fluids*, Wiley-VCH, Weinheim ; New York, 1999.
4. C. D. Ablan, J. P. Hallett, K. N. West, R. S. Jones, C. A. Eckert, C. L. Liotta and P. G. Jessop, *Chemical Communications*, 2003, 2972-2973.
5. C. M. Starks, *Journal of the American Chemical Society*, 1971, **93**, 195.
6. D. Albanese, D. Landini, A. Maia and M. Pensa, *Journal of Molecular Catalysis A - Chemical*, 1999, **150**, 113.
7. M. J. Burk, S. Feng, M. F. Gross and W. Tumas, *Journal of the American Chemical Society*, 1995, **117**, 8277.
8. B. Zaidman, Y. Sasson and R. Neumann, *Industrial & Engineering Chemistry Product Research and Development*, 1985, **24**, 390-393.
9. C. M. Starks, C. L. Liotta and M. Halpern, *Phase-transfer catalysis : fundamentals, applications, and industrial perspectives*, Chapman & Hall, New York, 1994.
10. D. Landini, *Journal of the Chemical Society, Chemical Communications*, 1974, 879.
11. C. Reichardt, *Solvents and Solvent effects in Organic Chemistry (3rd Edition)*, Wiley-VCH, 2003.
12. E. V. Dehmlow, R. Richter and A. B. Zhivich, *Journal of Chemical Research-S*, 1993, 504-505.
13. W. Keim, F. H. Kowaldt, R. Goddard and C. Kruger, *Angewandte Chemie-International Edition in English*, 1978, **17**, 466-467.
14. F. Joo and A. Katho, *Journal of Molecular Catalysis a-Chemical*, 1997, **116**, 3-26.
15. E. de Wolf, G. van Koten and B. J. Deelman, *Chemical Society Reviews*, 1999, **28**, 37-41.
16. D. R. Lide, ed., *CRC Handbook of Chemistry and Physics*, 84th edn., Boca Raton, 2003.

17. M. Wei, G. T. Musie, D. H. Busch and B. Subramaniam, *Journal of the American Chemical Society*, 2002, **124**, 2513-2517.
18. H. L. M. a. L. B. Laveb, *Progress in Energy and Combustion Science*, 2003, **29**, 1-69.
19. S. Saka and D. Kusdiana, *Fuel*, 2001, **80**, 225-231.
20. H. Fukuda, A. Kondo and H. Noda, *Journal of Bioscience and Bioengineering*, 2001, **92**, 405-416.
21. S. Espinosa, S. Diaz and E. A. Brignole, *Industrial & Engineering Chemistry Research*, 2002, **41**, 1516-1527.
22. M. A. Jackson and J. W. King, *Journal of the American Oil Chemists Society*, 1997, **74**, 103-106.
23. G. Vicente, M. Martinez, J. Aracil and A. Esteban, *Industrial & Engineering Chemistry Research*, 2005, **44**, 5447-5454.
24. P. M. Ndiaye, E. Franceschi, D. Oliveira, C. Dariva, F. W. Tavares and J. V. Oliveira, *Journal of Supercritical Fluids*, 2006, **37**, 29-37.
25. W. Du, Y. Y. Xu, D. H. Liu and J. Zeng, *Journal of Molecular Catalysis B-Enzymatic*, 2004, **30**, 125-129.
26. R. W. Pryor, M. A. Hanna, J. L. Schinstock and L. L. Bashford, *Transactions of the Asae*, 1983, **26**, 333-337.
27. A. Demirbas, *Energy Conversion and Management*, 2003, **44**, 2093-2109.
28. A. Srivastava and R. Prasad, *Renewable & Sustainable Energy Reviews*, 2000, **4**, 111-133.
29. W. Y. Zhou, S. K. Konar and D. G. B. Boocock, *Journal of the American Oil Chemists Society*, 2003, **80**, 367-371.
30. N. I. Sax, *Dangerous Properties of Industrial Materials (4th Edition)*, Van Nostrand Reinhold, New York, U.S., 1975.
31. Y. Zhang, M. A. Dube, D. D. McLean and M. Kates, *Bioresource Technology*, 2003, **89**, 1-16.
32. A. Demirbas, *Energy Sources*, 2002, **24**, 835-841.
33. D. Kusdiana and S. Saka, *Fuel*, 2001, **80**, 693-698.
34. K. D. Bartle, A. A. Clifford, S. A. Jafar and G. F. Shilstone, *Journal of Physical and Chemical Reference Data*, 1991, **20**, 713-756.
35. R. D. Smith, S. L. Frye, C. R. Yonker and R. W. Gale, *Journal of Physical Chemistry*, 1987, **91**, 3059.

36. D. F. Williams, *Chemical Engineering Science*, 1981, **36**, 1769-1788.
37. C. R. Yonker and R. D. Smith, *Fluid Phase Equilibria*, 1985, **22**, 175.
38. M. Uematsu and E. U. Franck, *Journal of Physical and Chemical Reference Data*, 1980, **9**, 1291-1306.
39. R. T. Kurnik and R. C. Reid, *Fluid Phase Equilibria*, 1982, **8**, 93-105.
40. D. K. Joshi and J. M. Prausnitz, *American Institute of Chemical Engineers*, 1984, **30**, 522-525.
41. W. J. Schmitt and R. C. Reid, *Fluid Phase Equilibria*, 1986, **32**, 77-99.
42. J. M. Walsh, G. D. Ikonomou and M. D. Donohue, *Fluid Phase Equilibria*, 1987, **33**, 295-314.
43. J. M. Dobbs and K. P. Johnston, *Industrial & Engineering Chemistry Research*, 1987, **26**, 1476-1482.
44. J. M. Dobbs, J. M. Wong, R. J. Lahiere and K. P. Johnston, *Industrial & Engineering Chemistry Research*, 1987, **26**, 56-65.
45. G. Anitescu and L. L. Tavlarides, *Journal of Supercritical Fluids*, 1997, **10**, 175-189.
46. W. I. Irvine, *Spartan Pro*, CA, USA.
47. E. H. Buechner, *Zeitschrift fur Physikalische Chemie* 1906, **54**, 665.
48. R. J. W. L. Fevre, *Advances in Physical Organic Chemistry*, 1965, **3**, 1.
49. A. L. McClellan, *Tables of Dipole Moments*, Freeman, San Francisco, 1963.
50. Y. Koga, Y. Iwai, Y. Hata, M. Yamamoto and Y. Arai, *Fluid Phase Equilibria*, 1996, **125**, 115-128.
51. R. M. Lemert and K. P. Johnston, *Industrial & Engineering Chemistry Research*, 1991, **30**, 1222-1231.
52. T. Suzuki, N. Tsuge and K. Nagahama, *Fluid Phase Equilibria*, 1991, **67**, 213-226.
53. G. D. Bothun, B. L. Knutson, H. J. Strobel, S. E. Nokes, E. A. Brignole and S. Diaz, *Journal of Supercritical Fluids*, 2003, **25**, 119-134.
54. L. C. W. Baker and T. F. Anderson, *Journal of the American Chemical Society*, 1957, **79**, 2071.
55. J. H. Yoon, *Industrial & Engineering Chemistry Research*, 1993, **32**, 2881-2887.
56. A. V. Shvarts and G. D. Efremova, *Russian Journal of Physical Chemistry,Ussr*, 1969, **43**, 968.

57. A. V. Shvarts and G. D. Efremova, *Russian Journal of Physical Chemistry,Ussr*, 1970, **44**, 614.
58. J. S. Lim and Y. Y. Lee, *Journal of Supercritical Fluids*, 1994, **7**, 219.
59. M. Wei, G. T. Musie, D. H. Busch and B. Subramaniam, *Green Chemistry*, 2004, **6**, 387-393.
60. H. Jin and B. Subramaniam, *Chemical Engineering Science*, 2004, **59**, 4887-4893.
61. H. Jin, B. Subramaniam, A. Ghosh and J. Tunge, *American Institute of Chemical Engineers Journal*, 2006, **52**, 2575-2581.
62. C. J. Lyon, V. S. R. Sarsani and B. Subramaniam, *Industrial & Engineering Chemistry Research*, 2004, **43**, 4809-4814.
63. P. R. Sassiat, *Analytical Chemistry*, 1987, **59**, 1164-1170.
64. Y. W. Kho, D. C. Conrad and B. L. Knutson, *Fluid Phase Equilibria*, 2003, **206**, 179-193.
65. Y. Houndonougbo, K. Kuczera, B. Subramaniam and B. B. Laird, *Molecular Simulation*, 2007, **33**, 861-869.
66. A. Kordikowski, A. P. Schenk, R. M. VanNielen and C. J. Peters, *Journal of Supercritical Fluids*, 1995, **8**, 205-216.
67. A. Bamberger, *Journal of Supercritical Fluids*, 2000, **17**, 97-110.
68. C. M. J. Chang, C. Y. Day and C. Y. Chen, *Journal of the Chinese Institute of Chemical Engineers*, 1996, **27**, 243-249.
69. G. Duve, O. Fuchs and H. Overbeck, *Losemittel Hoeschst (6th Edition)*, Hoescht AG, Frankfurt, 1976.

# CHAPTER 6

## Summary and Future Work

---



---

## 6.1 Summary

The use of $CO_2$ as an alternative to traditional organic solvents has been an extensive area of research over the last several decades with research focusing mainly on supercritical applications. Gas eXpanded Liquids (GXLs) combine the advantages of liquid $CO_2$ and cosolvents. Much like its supercritical counterpart, the solvent power of GXLs can be tuned by varying the liquid phase concentration as a function of pressure. Operating pressures for GXLs are typically between 3 to 8 MPa, and hence much lower than those required for supercritical conditions, thus giving GXLs a practical advantage.

The character and content of a solvent are what determine the solvation behaviour of expanded liquids over a given compound. $CO_2$ expanded media have been shown to generate a range of tunable physical properties for which they can be used to generate a continuum of alternative solvent media with variable solvent power, as a function of pressure (extent of expansion), or their composition, thus offering a multitude of opportunities for industrial applications.

Gas expansion of various solvents has given rise to a wide range of solvent properties for which physical parameters have now been established. Key changes in physical properties of a range of solvents when expanded under moderate pressures of $CO_2$ at ambient temperature have been determined. Applications of GXLs have also been studied for implementation in reactions, extractions and separation processes.

### 6.1.1 Solvatochromism

Spectroscopic measurements of a range of binary mixtures of organic solvent with carbon dioxide have been recorded to calculate solvatochromic parameters for gas expanded liquids. This work has investigated the dipolarity/polarisability and hydrogen bond donating acidity in terms of Kamlet-Taft solvatochromism parameters. $\pi^*$ and $\alpha$ in 15 solvents ranging from nonpolar cyclohexane to polar DMSO have been determined at ambient temperature (298 K) and at 50 bar pressures of $CO_2$. Data obtained for gas expanded solvents showed a significant change in polarity upon addition of $CO_2$, modifying the properties of traditional organic solvents. It is possible to devise alternative solvents mixture using $CO_2$ expansion that could replace either more expensive or toxic solvents. Determination of Kamlet and Taft parameters have shown that it is possible to provide a solvent strength scale that facilitates

comparisons between $CO_2$ expanded traditional solvents and their unexpanded equivalents. Although solvatochromic data are not completely appropriate for the determination of solvent power or absolute solubilities, they have shown promise of providing an insight into the local solvent surroundings in both single solvents (liquid solvents) and binary mixtures (expanded solvents).

### 6.1.2 Physical Properties

This work assesses the validity of a quick, simple, and precise in situ technique for determining the dielectric constant of GXLs. Density, dielectric constant data, and $CO_2$ solubilities at 25 ºC and 50 bar pressure for a range of $CO_2$-expanded solvents are reported here for the first time. The dissolution of $CO_2$ into liquid organic solvents to generate expanded liquids has shown result in significant changes in the dielectric polarity of a solvent medium. The bulk polarity of all solvents changed quite significantly. This in some cases has allowed an instant shift in polarity from polar to non-polar media simply by adding moderate pressures of $CO_2$.

Density values for the expanded solvents were found to be similar to those of the unexpanded solvents. However, the presence of the gaseous component results in solvation and transport properties that are intermediate between that of a dense gas and a pure liquid, thereby enhancing their mass transport ability. Finally, correlation between the change in molar free volume upon expansion and the Hildebrand solubility parameter showed that the expansion of molecular solvents is controlled by the thermodynamics of cavity formation.

### 6.1.3 Applications of GXLs

Biphasic reaction chemistry, selectivity, solubility and phase behaviour were all probed as potential applications for gas expanded solvents. Initial experimentation in each area found promising results for the use of expanded solvents in synthetic chemistry. Gas expanded biphasic systems were investigated as a method for eliminating the need for catalysts in phase transfer reactions. The nucleophilic displacement reaction of benzyl chloride to benzyl bromide was studied. Initial results showed that percentage conversions varied only slightly from those under ambient pressure conditions. However, reaction conditions presented in this work resulted in finding a feasible new route for the production of benzaldehyde.

The use of GXLs as potential solvents for use in the biodiesel reaction showed that pressurisation allowed for some selective esterification, but the direction of selectivity required is very much dependent on the solubility of the products in expanded systems. Solubility was favoured towards more nonpolar substituents as expected.

The dielectrometry method studied in Chapter 3 has been used for the determination of solute solubility studies of non-polar naphthalene, toluic acid, and polar salicylic acid to be determined in various solvent systems of differing polarity. For the first time, solubility data for these solutes have been measure in gas expanded systems, and the results have been compared and contrasted with the behaviour of these solutes in supercritical and liquid $CO_2$. $CO_2$ expanded DMSO was the most versatile solvent in terms of its ability to solvate nonpolar and polar solutes. Supercritical $CO_2$ was the worst solvent in this study as it was only suitable for nonpolar solutes. This gives GXLs a practical advantage over comparable supercritical systems in terms of specialised equipment and the outlay associated with it. In terms of solvent power and transportability when compared to gases and liquids, GXLs can overcome solubility limitations that are normally observed in supercritical fluids due to their favorability towards nonpolar solutes.

The final application studied has assessed the change in phase behaviour of mixed binary solvents on expansion with 50 bar of $CO_2$ at ambient temperature. It was noted that 115 of the 120 system studies showed the ability to undergo phase inversion when pressurised. It was postulated that the miscibility of liquid solvents is controlled by the enthalpy of mixing, and in order for solvents to mix the enthalpy of mixing must have been predominantly negative as generally the enthalpy of mixing is small. This arises from interaction between unlike solvent molecules, and solvent systems which are immiscible were ones where very polar solvents were combined with non-polarisable molecules. It was concluded that to determine why certain solvents split upon $CO_2$ expansion it would be necessary to consider the thermodynamics of mixing to understand why the two miscible solvents would phase separate, but without significant thermodynamic data a detailed analysis of these systems is impossible.

## 6.2 Future Work

Despite having been around for over a decade, GXLs are still in their infancy. The character and content of a solvent are what determine the solvation behaviour of expanded liquids over a given compound. $CO_2$ expanded media have shown to generate a range of tunable physical properties for which they can be used to generate a continuum of alternative solvent media with variable solvent power, as a function of pressure (extent of expansion), or their composition, thus offering a multitude of opportunities for industrial applications.

Knowledge of the ability for a $CO_2$ expanded liquid to act as a solvent for a particular solute is essential in process design. Chapter three and four have reported the determination of key physical properties for gas expanded liquids to understand what happens in expanded solvents at a molecular level. There is only one more key physical parameter which could give an insight as to the behaviour of gas expanded liquids, and that is viscosity. An area for future consideration is to measure the viscosity of expanded fluids. Recent work carried out by Abbott *et al*. has seen the use of a novel technique which uses a piezoelectric quartz crystal as a viscometer. The method would work well for expanded liquids as it is simple, inexpensive, and allows for direct in situ measurements.

The solutes used for the solubility determinations in Chapter five have shown characteristics that make $CO_2$-based solvents promising solvents for use in applications. Solubility data in the literature for gas expanded systems is still relatively few. These data must be extended to cover a wider range of solutes, and expanded solvents. Galicia-Luna *et al*.[1] report a new method of determining solubility and saturation density simultaneously, which could be used for further investigations into solute/solvent combinations. Compressed densities of a pressurised fluid (containing a dissolved solid) are obtained far and close to the solid solubility limits without any sampling and expensive analysis equipments. Once a reliable method has been established, and more data has been collated on solute behaviour, then it is possible that these solvents will be seen as possible replacements to both liquid and supercritical solvents.

Reaction kinetics can also be measured by application of the dielectrometry technique. This method can be used to determine rate constants of reactions such as Friedel Crafts or Diels Alder reactions in expanded fluids. The effect on the reaction

selectivity and rate to changes in the reagent/catalyst concentration, time, temperature and pressure can also be addressed.

One of the most important observations which resulted from this research was that miscible solvents could be split via the application of modest $CO_2$ pressure. This has clear application in biphasic catalysis and solvent separation. An understanding of the causes of solvent separation is therefore of paramount importance. It is clear from the results in Chapter 5 that the separation is related to the thermodynamics of the solvent-solute interactions and it is therefore important to quantify these for both the mixed solvents at ambient pressure and the individual solvents at 50 bar $CO_2$. Once these data are obtained a model for the separation of solvents can be devised.

## Reference

1. A. Zúñiga-Moreno, L. A. Galicia-Luna and L. E. Camacho-Camacho, *Fluid Phase Equilibria*, 2005, **234**, 151.

# APPENDIX

| Solvent | $\lambda_{max}$ Phenol Blue at Ambient Pressure | | | | | Average |
|---|---|---|---|---|---|---|
| **C. Hex** | 550.3 | 550.3 | 550.3 | 550.2 | 550.3 | 550.3 |
| **Toluene** | 573.6 | 573.6 | 573.6 | 573.6 | 573.6 | 573.6 |
| **Ether** | 561.3 | 561.3 | 561.3 | 561.3 | 561.3 | 561.3 |
| **THF** | 576.6 | 576.6 | 576.6 | 576.6 | 576.6 | 576.6 |
| **DCM** | 591.1 | 591.1 | 591.1 | 591.1 | 591.1 | 591.1 |
| ***t*-BuOH** | 590.9 | 590.9 | 590.9 | 590.9 | 590.9 | 590.9 |
| **Butanol** | 601.3 | 601.3 | 601.3 | 601.3 | 601.3 | 601.3 |
| **Prop2** | 597.9 | 597.9 | 597.9 | 597.9 | 597.9 | 597.9 |
| **Acetone** | 582.1 | 582.1 | 582.1 | 582.1 | 582.1 | 582.1 |
| **EtOH** | 603.1 | 603.1 | 603.1 | 603.1 | 603.1 | 603.1 |
| **MeOH** | 609.3 | 609.3 | 609.3 | 609.3 | 609.3 | 609.3 |
| **MeCN** | 585.3 | 585.3 | 585.3 | 585.3 | 585.3 | 585.3 |
| **DMF** | 592.7 | 592.7 | 592.7 | 592.7 | 592.7 | 592.7 |
| **DMSO** | 604.1 | 604 | 604.1 | 604 | 604 | 604.0 |
| **Prop1** | 601.7 | 601.7 | 601.7 | 601.7 | 601.7 | 601.7 |

Table 1. $\lambda_{max}$ measurements for solvents at ambient pressure and temperature using Phenol Blue as a solvatochromic probe. The wavelength of each absorbance maximum was calculated from the average of five spectra**.**

| Solvent | $\lambda_{max}$ Phenol Blue at 50 bar $CO_2$ | | | | | Average |
|---|---|---|---|---|---|---|
| **C. Hex** | 545.0 | 545.0 | 545.4 | 545.0 | 545.0 | 545.1 |
| **Toluene** | 556.3 | 556.2 | 556.1 | 556.0 | 556.1 | 556.1 |
| **Ether** | 549.7 | 549.7 | 549.7 | 549.7 | 549.7 | 549.7 |
| **THF** | 565.5 | 565.5 | 565.5 | 565.5 | 565.5 | 565.5 |
| **DCM** | 571.5 | 571.5 | 571.6 | 571.6 | 571.6 | 571.6 |
| ***t*-BuOH** | 588.3 | 588.3 | 588.3 | 588.4 | 588.3 | 588.3 |
| **Butanol** | 593.4 | 593.4 | 593.4 | 593.4 | 593.4 | 593.4 |
| **Prop2** | 585.6 | 585.7 | 585.6 | 585.6 | 585.6 | 585.6 |
| **Acetone** | 570.4 | 570.4 | 570.4 | 570.4 | 570.4 | 570.4 |
| **EtOH** | 580.8 | 580.8 | 580.8 | 580.8 | 580.8 | 580.8 |
| **MeOH** | 587.6 | 587.6 | 587.6 | 587.5 | 587.6 | 587.6 |
| **MeCN** | 575.8 | 575.8 | 575.8 | 575.7 | 575.8 | 575.8 |
| **DMF** | 591.6 | 591.7 | 591.6 | 591.6 | 591.6 | 591.6 |
| **DMSO** | 597.1 | 597.1 | 597.2 | 597.2 | 597.1 | 597.1 |
| **Prop1** | 584.4 | 584.4 | 584.4 | 584.4 | 584.4 | 584.4 |

Table 2. $\lambda_{max}$ measurements for solvents at 50 bar $CO_2$ and ambient temperature using Phenol Blue as a solvatochromic probe. The wavelength of each absorbance maximum was calculated from the average of five spectra.

| Solvent | $\lambda_{max}$ Nile Red at Ambient Pressure | | | | | Average |
|---|---|---|---|---|---|---|
| **C. Hex** | 501.4 | 501.4 | 501.4 | 501.4 | 501.4 | 501.4 |
| **Toluene** | 522.9 | 522.9 | 522.9 | 522.9 | 522.9 | 522.9 |
| **Ether** | 511.9 | 512.1 | 512.1 | 512.1 | 512.1 | 512.1 |
| **THF** | 525.0 | 525.0 | 525.0 | 525.0 | 525.0 | 525.0 |
| **DCM** | 537.2 | 537.2 | 537.2 | 537.2 | 537.2 | 537.2 |
| ***t*-BuOH** | 537.1 | 537.1 | 537.1 | 537.1 | 537.1 | 537.1 |
| **Butanol** | 545.2 | 545.2 | 545.2 | 545.2 | 545.2 | 545.2 |
| **Prop2** | 543.8 | 543.8 | 543.8 | 543.8 | 543.8 | 543.8 |
| **Acetone** | 532.0 | 532.0 | 532.0 | 532.0 | 532.0 | 532.0 |
| **EtOH** | 548.8 | 548.8 | 548.8 | 548.8 | 548.8 | 548.8 |
| **MeOH** | 554.1 | 554.1 | 554.1 | 554.1 | 554.1 | 554.1 |
| **MeCN** | 534.0 | 534.0 | 534.0 | 534.0 | 534.0 | 534.0 |
| **DMF** | 541.7 | 541.7 | 541.7 | 541.7 | 541.7 | 541.7 |
| **DMSO** | 548.8 | 548.8 | 548.8 | 548.8 | 548.8 | 548.8 |
| **Prop1** | 546.9 | 546.9 | 546.9 | 546.9 | 546.9 | 546.9 |

Table 3. $\lambda_{max}$ measurements for solvents at ambient pressure and temperature using Nile Red as a solvatochromic probe. The wavelength of each absorbance maximum was calculated from the average of five spectra.

| Solvent | $\lambda_{max}$ Nile Red at 50 bar $CO_2$ | | | | | Average |
|---|---|---|---|---|---|---|
| **C. Hex** | 497.5 | 497.3 | 497.5 | 497.6 | 497.5 | 497.5 |
| **Toluene** | 508.8 | 508.8 | 508.8 | 508.9 | 508.8 | 508.8 |
| **Ether** | 502.7 | 502.7 | 502.7 | 502.7 | 502.7 | 502.7 |
| **THF** | 517.3 | 517.5 | 517.5 | 517.5 | 517.5 | 517.5 |
| **DCM** | 523.2 | 523.2 | 523.4 | 523.2 | 523.2 | 523.2 |
| ***t*-BuOH** | 533.7 | 533.7 | 533.8 | 533.8 | 533.8 | 533.8 |
| **Butanol** | 540.3 | 540.3 | 540.4 | 540.4 | 540.3 | 540.3 |
| **Prop2** | 531.7 | 531.7 | 531.7 | 531.7 | 531.7 | 531.7 |
| **Acetone** | 519.2 | 519.2 | 519.2 | 519.2 | 519.2 | 519.2 |
| **EtOH** | 527.1 | 526.9 | 526.9 | 526.9 | 526.9 | 526.9 |
| **MeOH** | 534.2 | 534.2 | 534.0 | 534.2 | 534.2 | 534.2 |
| **MeCN** | 523.5 | 523.5 | 523.5 | 523.6 | 523.5 | 523.5 |
| **DMF** | 539.7 | 539.7 | 539.7 | 539.8 | 539.7 | 539.7 |
| **DMSO** | 544.5 | 544.5 | 544.6 | 544.6 | 544.6 | 544.6 |
| **Prop1** | 531.1 | 531.1 | 531.2 | 531.0 | 531.1 | 531.1 |

Table 4. $\lambda_{max}$ measurements for solvents at 50 bar $CO_2$ and ambient temperature using Nile Red as a solvatochromic probe. The wavelength of each absorbance maximum was calculated from the average of five spectra.

| Solvent | Capacitance at Ambient Pressure | | | | | Average |
|---|---|---|---|---|---|---|
| **C. Hex** | 9.280E-12 | 9.286E-12 | 9.275E-12 | 9.283E-12 | 9.277E-12 | 9.280E-12 |
| **Toluene** | 1.206E-11 | 1.206E-11 | 1.207E-11 | 1.207E-11 | 1.206E-11 | 1.206E-11 |
| **Ether** | 1.703E-11 | 1.703E-11 | 1.703E-11 | 1.703E-11 | 1.703E-11 | 1.703E-11 |
| **THF** | 2.426E-11 | 2.425E-11 | 2.433E-11 | 2.413E-11 | 2.424E-11 | 2.424E-11 |
| **DCM** | 2.528E-11 | 2.522E-11 | 2.539E-11 | 2.550E-11 | 2.535E-11 | 2.535E-11 |
| ***t*-BuOH** | 3.987E-11 | 3.994E-11 | 3.997E-11 | 4.003E-11 | 4.003E-11 | 3.997E-11 |
| **Butanol** | 5.405E-11 | 5.405E-11 | 5.404E-11 | 5.404E-11 | 5.405E-11 | 5.405E-11 |
| **Prop2** | 5.893E-11 | 5.895E-11 | 5.893E-11 | 5.892E-11 | 5.893E-11 | 5.893E-11 |
| **Acetone** | 5.942E-11 | 5.931E-11 | 5.952E-11 | 5.944E-11 | 5.932E-11 | 5.940E-11 |
| **EtOH** | 7.265E-11 | 7.264E-11 | 7.267E-11 | 7.268E-11 | 7.268E-11 | 7.266E-11 |
| **MeOH** | 9.366E-11 | 9.367E-11 | 9.368E-11 | 9.372E-11 | 9.361E-11 | 9.367E-11 |
| **MeCN** | 9.981E-11 | 9.977E-11 | 9.984E-11 | 9.989E-11 | 9.993E-11 | 9.985E-11 |
| **DMF** | 1.082E-10 | 1.083E-10 | 1.082E-10 | 1.082E-10 | 1.081E-10 | 1.082E-10 |
| **DMSO** | 1.362E-10 | 1.362E-10 | 1.362E-10 | 1.362E-10 | 1.362E-10 | 1.362E-10 |
| **Prop1** | 6.057E-11 | 6.051E-11 | 6.056E-11 | 6.055E-11 | 6.059E-11 | 6.056E-11 |

Table 5. Capacitance measurements for solvents at ambient temperature and pressure, the average capacitance from five separate readings was used to calculate values for Relative Permittivity.

| Solvent | Capacitance at 50 bar $CO_2$ | | | | | Average |
|---|---|---|---|---|---|---|
| **C. Hex** | 7.540E-12 | 7.568E-12 | 7.544E-12 | 7.531E-12 | 7.545E-12 | 7.545E-12 |
| **Toluene** | 8.803E-12 | 8.814E-12 | 8.816E-12 | 8.821E-12 | 8.818E-12 | 8.815E-12 |
| **Ether** | 1.071E-11 | 1.071E-11 | 1.073E-11 | 1.074E-11 | 1.074E-11 | 1.073E-11 |
| **THF** | 1.317E-11 | 1.313E-11 | 1.316E-11 | 1.319E-11 | 1.318E-11 | 1.317E-11 |
| **DCM** | 1.387E-11 | 1.370E-11 | 1.371E-11 | 1.378E-11 | 1.377E-11 | 1.377E-11 |
| ***t*-BuOH** | 3.160E-11 | 3.171E-11 | 3.168E-11 | 3.168E-11 | 3.167E-11 | 3.167E-11 |
| **Butanol** | 3.485E-11 | 3.492E-11 | 3.500E-11 | 3.479E-11 | 3.488E-11 | 3.489E-11 |
| **Prop2** | 3.713E-11 | 3.701E-11 | 3.701E-11 | 3.705E-11 | 3.716E-11 | 3.707E-11 |
| **Acetone** | 2.587E-11 | 2.596E-11 | 2.571E-11 | 2.593E-11 | 2.597E-11 | 2.589E-11 |
| **EtOH** | 2.760E-11 | 2.762E-11 | 2.773E-11 | 2.774E-11 | 2.758E-11 | 2.766E-11 |
| **MeOH** | 3.516E-11 | 3.516E-11 | 3.516E-11 | 3.516E-11 | 3.516E-11 | 3.516E-11 |
| **MeCN** | 4.084E-11 | 4.091E-11 | 4.103E-11 | 4.091E-11 | 4.106E-11 | 4.095E-11 |
| **DMF** | 5.017E-11 | 5.002E-11 | 5.014E-11 | 5.019E-11 | 5.001E-11 | 5.010E-11 |
| **DMSO** | 5.996E-11 | 5.994E-11 | 5.999E-11 | 5.991E-11 | 6.003E-11 | 5.997E-11 |
| **Prop1** | 3.848E-11 | 3.852E-11 | 3.860E-11 | 3.851E-11 | 3.858E-11 | 3.854E-11 |

Table 6. Capacitance measurements for solvents at ambient temperature and 50 bar pressure of $CO_2$, the average capacitance from five separate readings was used to calculate values for Relative Permittivity.

| Solvent | Period of Oscillation at Ambient Pressure | | | Average |
|---|---|---|---|---|
| **C.Hex** | 4040.14 | 4040.23 | 4040.45 | 4040.27 |
| **Tol** | 4056.69 | 4056.52 | 4056.79 | 4056.67 |
| **Ether** | 4027.23 | 4027.06 | 4026.75 | 4027.01 |
| **THF** | 4060.94 | 4060.74 | 4060.92 | 4060.87 |
| **DCM** | 4148.25 | 4148.26 | 4148.29 | 4148.27 |
| **t-BuOH** | 4042.29 | 4042.01 | 4042.05 | 4042.12 |
| **BuOH** | 4046.53 | 4046.57 | 4046.64 | 4046.58 |
| **Prop2** | 4041.51 | 4041.32 | 4041.82 | 4041.55 |
| **Acet** | 4042.63 | 4042.27 | 4042.46 | 4042.45 |
| **EtOH** | 4041.22 | 4041.13 | 4041.51 | 4041.29 |
| **MeOH** | 4041.55 | 4041.55 | 4041.82 | 4041.64 |
| **MeCN** | 4039.53 | 4039.77 | 4039.80 | 4039.70 |
| **DMF** | 4074.41 | 4074.52 | 4074.28 | 4074.40 |
| **DMSO** | 4104.03 | 4104.17 | 4104.36 | 4104.19 |
| **Prop2** | 4043.44 | 4043.28 | 4043.65 | 4043.46 |

Table 7. Period of Oscillation measurements for solvents at ambient temperature and pressure, the average value from three separate readings was used to calculate values for density.

| Solvent | Period of Oscillation at 50 bar $CO_2$ | | | Average |
|---|---|---|---|---|
| **C.Hex** | 4044.18 | 4044.75 | 4044.41 | 4044.45 |
| **Tol** | 4061.72 | 4062.09 | 4061.88 | 4061.90 |
| **Ether** | 4043.12 | 4043.67 | 4043.58 | 4043.46 |
| **THF** | 4067.71 | 4068.23 | 4067.94 | 4067.96 |
| **DCM** | 4141.11 | 4141.72 | 4141.15 | 4141.33 |
| **t-BuOH** | 4044.40 | 4043.74 | 4043.93 | 4044.02 |
| **BuOH** | 4048.92 | 4048.81 | 4049.18 | 4048.97 |
| **Prop2** | 4043.77 | 4043.79 | 4043.40 | 4043.65 |
| **Acet** | 4056.29 | 4055.91 | 4055.63 | 4055.94 |
| **EtOH** | 4049.36 | 4049.21 | 4049.28 | 4049.28 |
| **MeOH** | 4044.34 | 4044.83 | 4044.91 | 4044.69 |
| **MeCN** | 4056.88 | 4056.62 | 4057.16 | 4056.89 |
| **DMF** | 4077.72 | 4077.69 | 4077.86 | 4077.76 |
| **DMSO** | 4103.03 | 4103.24 | 4103.45 | 4103.24 |
| **Prop2** | 4051.89 | 4051.99 | 4051.96 | 4051.95 |

Table 8. Period of Oscillation measurements for solvents at 50 bar pressure of $CO_2$, the average value from three separate readings was used to calculate values for density.

| **Solutes** | **$\alpha$ x $10^{39}$ ($J^{-1} C^2 m^2$)** | **$\mu$ x $10^{30}$ (C m)** | **$A_e^s$ ($dm^3 mol^{-1}$)** |
|---|---|---|---|
| *o*-hydroxybenzoic acid | 1.37 | 8.839 | 0.155474 |
| *p*-toluic acid | 1.68 | 6.671 | 0.108998 |
| Naphthalene | 1.83 | 0 | 0.041586 |

Table 9. Molecular polarisability, dipole moment, and first dielectric virial coefficients for the solutes used in the solubility studies.